TEMPORAL AND SPATIAL DISTRIBUTION OF GREENHOUSE GASES IN CENTRAL KENYA

BY

JOHN KIPKEMOI ROTICH

I56/72733/2008

A Dissertation submitted in partial fulfillment of the requirements for the degree of Master of Science in Meteorology,
University of Nairobi

DEPARTMENT OF METEOROLOGY

SCHOOL OF PHYSICAL SCIENCES,

UNIVERSITY OF NAIROBI

AUGUST 2013

DECLARATION

I hereby declare that this dissertation is my original work and has not been presented for a degree in any university.

Signed ---------- Date ----------

John Kipkemoi Rotich,
I56/72733/08

This dissertation has been submitted for examination with our approval as university supervisors;

Signed ---------- Date ----------

Prof. N. J. Muthama
Department of Meteorology
University of Nairobi

Signed ---------- Date ----------

Dr. R. E. Okoola
Department of Meteorology
University of Nairobi

DEDICATION

This dissertation is dedicated to my Mother, who has shown great determination in the midst of many odds. Her humility and courage has given me much inspiration. May she gain extra strength and cheerfulness.

ABSTRACT

The increasing concentration of greenhouse gases brought about by human activities has been thrown into sharp focus by the adverse effects of climate change on the environment. As part of the important steps to achieving a healthy environment, a study of the fluxes and transport into the country of these gases is necessary. The objective of this study is to assess the concentrations of greenhouse gases in Central Kenya. An investigation was carried out to establish their spatial and temporal distributions, transport and the source regions. The impact of the surrounding area on the background monitoring station of Mount Kenya was also investigated. The study period was from the year 2002 to 2010 and the major greenhouse gases considered were Carbon Dioxide, Methane and Ozone.

The data sets used were from the Kenya Meteorological Department for the ozone and rainfall data sets, the global meteorological reanalysis data sets from the National Center for Environmental Prediction- National Center for Atmospheric Research (NCEP- NCAR), and the greenhouse gases data were from the Greenhouse Observing satellite (GOSAT) and the Air resources Laboratory (ARL) of the National Oceanic and Atmospheric Administration of the USA. Air filled flasks from the Mt Kenya GAW Station were analysed for greenhouse gases from December 2003 to November 2011 at the ARL.

Statistical and graphical methods were used to assess the spatial and temporal distributions of the greenhouse gases in Central Kenya and to investigate for any correlations or trends. The Hybrid Single - Particle Lagrangian Integrated Trajectory (HYSPLIT) model generated trajectories were used to investigate the transport of the greenhouse gases into the region. The Grids Analysis and Display System (GrADS) was deployed to display the spatial distribution of the greenhouse gases as observed by GOSAT over the country. Another tool, ArcView GIS, was used to show the spatial distributions of the fluxes of Carbon dioxide from fossil fuel and the biosphere.

This study confirmed that there are six different pathways of air transport into the country. These are from the North, North East from Saudi Arabia through Somalia, from India and Pakistan, East from the Indian Ocean, South East from the South West Indian Ocean and Madagascar and from the West. Another significant circulation is the recirculation within the country, especially in the months of July and August. High Ozone is injected into the

country from the North - East from the Arabian Peninsula. Much lower values were recorded with the maritime air but the recirculation in the country showed a more uniform and higher concentration than the maritime air. The trend analysis showed an increasing trend in July and August though not yet statistically significant. A contrast was found in the diurnal variation of tropospheric Ozone over Mt Kenya and at Nairobi. There is a night maximum in Mt Kenya and a minimum in the afternoon. The converse is true for Nairobi where an afternoon maximum occurs; possibly due to a photochemical production during daylight in the presence of ozone precursor gases.

The spatial distribution of the carbon dioxide flux from fossil fuel showed the cities of Nairobi and Mombasa registering high emissions. The dominant fossil fuel flux was centred at Nairobi and is up to ten times that of the rest of the country. It spreads out to the surrounding eleven counties of Kiambu, Nyandarua, Nakuru, Narok, Kajiado, Muranga, Machakos, Embu, Kirinyaga, Nyeri, Meru and parts of Makueni and Laikipia. The flux of the biosphere closely follows the march of the rainfall pattern and amounts in the country.

The Carbon dioxide column concentration has a bimodal seasonal distribution and divides the country into two. From June to November the eastern parts of the country, together with Mt Kenya GAW station register lower amounts and the western half has higher values. From December to May, the high Carbon dioxide amounts are to the north and northwest of the country; low amounts are to the southern parts, including the Mt Kenya GAW Station. The lowest amounts occur in December in the central parts of the country.

The seasonal distribution of surface Ozone shows a seasonal high in March and September. A minimum occurs in December. The Methane temporal distribution shows high values in November to February and this could be due to the higher concentrations in the northern hemisphere air. A minimum occurs in April - May and the low amounts continue into October.

These findings can be incorporated into any analysis for the greenhouse gases' emissions in environmental impact assessments reports for commercial and industrial projects. They inform the background patterns. The health authorities are encouraged to take appropriate actions and greater concern during the months of June to August incase of any rising amounts of ozone. Further, the Mt Kenya GAW Station is well placed to continue the background monitoring of greenhouse gases.

Table of Contents

List of Figures

List of Tables

ACRONYMS

ADEOS	-	Advanced Earth Observing Satellite “MIDORI”
AIRS	-	Atmospheric InfraRed Sounder
AQ	-	Air Quality
AR4	-	Fourth Assessment Report of the Intergovernmental Panel on Climate Change (IPCC)
CARIBIC	-	Civil Aircraft for the Regular Investigation of the Atmosphere based on an Instrument Container
CMDL	-	Climate Modeling and Diagnostics Laboratory
CONTRAIL	-	Comprehensive Observation Network for Trace gases by AirLiner
DU	-	Dobson Units
EALLJ	-	East African Low Level Jet
EIA	-	Environmental Impact Assessment
ENSO	-	El Nino- Southern Oscillation
ENVISAT	-	ENVIronmental SATellite
EPA	-	Environmental Protection Agency
ERS-2	-	Earth Resource Satellite- 2
ESRL	-	Earth System Research Laboratory
FAO	-	Food and Agricultural Organization
GAW	-	Global Atmosphere Watch station
GHGs	-	Greenhouse gases
GOME–2	-	Global Ozone Monitoring Experiment- 2
GOME-1	-	Global Ozone Monitoring Experiment -1
GOSAT	-	Greenhouse Observing SATellite, “IBUKI”
GRACE	-	Gravity Recovery and Experiment satellite
GrADS	-	Graphics Analysis Data Display System
GWP	-	Global Warming Potential
HDF5	-	Hierarchical Data Format version 5
HYSPLIT	-	Hybrid Single – Particle Lagrangian Integrated Trajectory
IASI	-	Infrared Atmospheric Sounding Interferometer
IMG	-	Interferometric Monitor for Greenhouse Gases
IPCC	-	Intergovernmental Panel on Climate Change
IR	-	Infrared radiation

ITCZ	-	Inter-Tropical Convergence Zone
LEO	-	Low Earth Orbit
METOP-A	-	Meteorological Operation Satellite- A
MKN GAW	-	Mount Kenya Global Atmosphere Watch station
MOPITT	-	Measurement of Pollution in the Troposphere
NCAR	-	National Center for Atmospheric Research
NCEP	-	National Center for Environmental Prediction
NetCDF	-	Net Common Data Format
NIES	-	National Institute for Environmental Studies
NIR	-	Near Infrared radiation
NMHCs	-	Non Methane Hydrocarbon compounds
NOAA	-	National Oceanic and Atmospheric Administration
OMI	-	Ozone Monitoring Instrument
READY	-	Real-time environmental applications and display system
SCIAMACHY	-	SCanning Imaging Absorption spectrometer for Atmospheric - CHartographY
SRON	-	Netherlands Institute for Space Research
SWIR	-	Short Wave Infrared Sensor
TES	-	Tropospheric Emission Spectrometer
TIR	-	Thermal Infrared Sensor
TKE	-	Turbulent Kinetic Energy
UN	-	United Nations
US	-	United States
UTC	-	Universal Time Coordinated- similar to Greenwich Mean Time (GMT)
UV	-	Ultraviolet radiation
UV-A	-	Ultraviolet- A (solar radiation in the wavelength range 320-400 nm)
UV-B	-	Ultraviolet- B (solar radiation in the wavelength range 280-320 nm)
UV-C	-	Ultraviolet- C (solar radiation in the wavelength range 200-280 nm)
WMO	-	World Meteorological Organization

SYMBOLS AND CHEMICAL FORMULAE

atm	-	atmospheres; pressure equivalent to 1013.25HPa
C	-	Carbon
CH_4	-	Methane
Cl	-	Chlorine
CO	-	Carbon Monoxide
CO_2	-	Carbon Dioxide
H	-	Hydrogen
hv	-	photon of energy
Km	-	Kilometre
ml	-	millilitres
N_2O	-	Nitrous Oxide
nm	-	nanometre
NO	-	Nitric oxide
NO_2	-	Nitrogen Dioxide
NO_x	-	Oxides of nitrogen
O	-	Atomic Oxygen
O_2	-	Oxygen
O_3	-	Ozone
OH	-	Hydroxyl radical
PM	-	Particulate Matter
ppbv	-	parts per billion by volume
ppmv	-	parts per million by volume
RH	-	Relative Humidity
Tg	-	Teragram
U	-	zonal (East- West) wind component of velocity
V	-	Meridional (North- South) wind component of velocity
W	-	vertical wind component of velocity
XCH_4	-	Column- averaged dry air mole fraction of Methane
XCO_2	-	Column- averaged dry air mole fraction of Carbon Dioxide
yr	-	Year

CHAPTER ONE

1. INTRODUCTION

A greenhouse gas (GHG) is a term used to refer to any of the atmospheric gases that may contribute to the warming of the earth's atmosphere. This occurs when the sun's radiation which passes through the atmosphere is absorbed by the planet and then reradiated as infrared radiation (IR). A GHG transmits visible light but absorbs strongly in the IR and near-infrared (NIR) spectrum. The GHGs trap the IR radiation and cause an increase in the average temperature of the earth's atmosphere; also called global warming. This is the greenhouse effect from which the gases get their name. It is commonly referred to as climate change stemming from anthropogenic release of GHGs.

The three most important GHGs are Carbon Dioxide (CO_2), Methane (CH_4) and Nitrous Oxide (N_2O) (South African National Climate Change Response Strategy, (SANCCRS), 2004). According to the Fourth Assessment Report of the Intergovernmental Panel on Climate Change (IPCC, 2007), CO_2 and CH_4 contribute about 80% of the global warming in the atmosphere. These GHGs are targeted by the Kyoto Protocol to be reduced to 5 - 8 % of the 1990 levels (United Nations, 1998).

Ozone (O_3) is one of the most important trace gases in the Earth's atmosphere. It is naturally present in our atmosphere and is a critical atmospheric trace species in the stratosphere and troposphere. Most O_3 resides in the stratosphere where it traps the Ultra Violet (UV) rays making it a GHG. The region between 20 and 40 km, where most atmospheric O_3 is located, is commonly referred to as the O_3 layer. This fractional abundance decreases again to about 1 ppmv in the mesosphere.

Ozone can have both good and bad impacts on human health and the environment. In the troposphere O_3 is a harmful pollutant that causes damage to plants and animal lung tissue. It is a major constituent of smog (Rajab *et al*., 2010). Radiation in the wavelength range 300 - 330 nm, called UV-B radiation, can penetrate through the whole atmosphere, but its intensity is significantly reduced because of O_3 absorption. In this spectral range the radiation is also biologically active and may cause skin cancer to susceptible individuals.

Ozone not only affects the Earth's radiation budget by absorption of solar UV radiation, but also because it strongly absorbs terrestrial radiation in the infrared atmospheric window near 9.6 nm, thereby acting as a GHG (Fishman *et al*., 1979).

The World Meteorological Organization (WMO) estimates that tropospheric O_3 has increased by 36% since 1750 (WMO Greenhouse Gas Bulletin, 2012). CO_2 has grown by about 40% of its pre-industrial period; when its concentration was about 280 parts per million volume (ppmv) of dry air to a concentration of 389 ppmv by 2010 (World Data Center for Greenhouse Gases (WDCGG), 2012). On the other hand, CH_4 has grown by about 150% to about 1780 parts per billion volume (ppbv) of dry air. These increases have been as a result of fossil-fuel combustion, cement manufacture and deforestation.

The rapid increase of these gases in the atmosphere has been accompanied by an increase in global surface temperature and observed decrease in snow cover and land-ice extent. Precipitation has been observed to have increased over the landmasses in the middle and high latitudes of the Northern Hemisphere. Over the sub-tropics, land-surface rainfall has decreased on average. The global mean sea level rise during the 20th century has been estimated at 1.5 mm/yr. An increase in the number of extreme weather events is being experienced in many places including eastern Africa (King'uyu, 1994; King'uyu *et al*., 2000; IPCC, 2007; SANCCRS, 2004).

Methane has a global warming potential (GWP) that is 25 times that of CO_2, using the 100 year timeframe. The total positive climate forcing attributed to CH_4 over the last 150 years is 40% that of CO_2 (Hansen *et al*., 1998). CH_4 has a short atmospheric lifetime of about 12 years. If significant reductions in individual sources are undertaken, the atmospheric concentrations can begin to reduce within a decade.

The major natural terrestrial sink for GHGs are the forests. As trees and other vegetations grow, they absorb CO_2 from the air. A forest continues absorbing CO_2 until trees reach full maturity, the trees stop growing; the forest then becomes a carbon reservoir, as long as it is not disturbed by human activities like land clearing or natural processes like forest fires, among others. These disturbances may increase or decrease carbon stocks (United States Department of Agriculture (USDA), 2004).

In addition to forestation, crops also function as carbon sinks by capturing atmospheric carbon during the process of photosynthesis. However, because of the annual nature of the crops carbon is quickly returned to the atmosphere through the decomposition of vegetation or the burning of residues. Cropping can create a more permanent sink for carbon, though the storage capacity is inherently limited. This occurs when residues are retained on the land, and carbon levels in soil organic matter are rebuilt. Once decomposition comes into balance with annual additions of carbon in vegetation, the land is fully saturated with carbon. This places some limits on the amount of carbon that can be stored in crop fields, as well as the rate of sequestration (FAO, 2003).

Kenya runs an O_3 monitoring program which was started in the mid 1980s with the use of Dobson Spectrophotometer at the Department of Meteorology, University of Nairobi. In the mid 1990s, O_3 profiles were obtained from soundings using balloons flying the ozonesondes.

In 1999 the Mount Kenya Global Atmosphere Watch (MKN GAW) station was installed on northwestern slope of Mt Kenya to automatically monitor the atmospheric concentrations of ozone and other gases. This location was chosen after a feasibility study (Schnell, 1978) in the East African region recommended the area as the most suitable for a background air pollution monitoring station. Here the measurement of other GHGs, along with the meteorological parameters, is done continuously. This automated program produces one minute averages which are archived.

The main objective of the MKN GAW station is to detect CO_2 cycles, its seasonal changes as well as the upslope – down slope winds. Since the station is located in a National Game Park, no significant changes in the land use are anticipated for the coming decades.

The Mount Kenya GAW is situated at the Equator at an altitude of 3678 metres above mean sea level. Its coordinates are 0.062ºS and 37.297ºE. It started operating when the electric power reached it in December 1999. However, a more continuous observational data is from the year 2002. The initial observational data were limited to O_3 and meteorological parameters but have been expanded recently to include aerosols, carbon monoxide and CO_2, and air flask sampling among others.

The other GAW stations, numbering only 23, are spread out across the world. They are essential in the understanding and predicting the relationship between changes in atmospheric compositions and changes in global and regional climate, the long range atmospheric transport and deposition of potentially harmful substances over different ecosystems. On the whole, there are about 280 observation points for GHGs in the world having continuous measurements.

Recently, from January 2009, a Japanese greenhouse gases observing satellite (GOSAT also called "ibuki" meaning breath) was put into orbit around the earth. It provides a massive 56,000 observation points, separated by only 160 km. It makes a sun synchronous orbit in 99 minutes at an altitude of 667 km and passes the same point every three days. The sub-point footprint is 10.5 km.

GOSAT measures the column-averaged dry air mole fractions (xCO_2 and xCH_4) of CO_2 and CH_4 (GOSAT Project, 2010). This data has a good temporal and spatial resolution. Observational data has been available from April 2009. The first public release of data on CO_2 monthly distribution was done in August 2012.

For Kenya and any country, the desirable outcome of any monitoring is to enhance the best environmental management practices which produce improved air quality and sustainable high standard of living for the citizens. This will take the centre stage with the economic and industrial developments envisaged in Kenya's Vision 2030.

1.1 PROBLEM STATEMENT

Carbon dioxide and Methane contribute up to 80% of the anthropogenic global warming. Global warming due to the increasing GHGs in the atmosphere is a major problem threatening the livelihoods of a huge section of our society. It has been associated with climate change which affects land and water resources; food and pasture availability, disappearance of plants and animal species and loss of habitat.

Tropospheric (surface) O_3 is poisonous to plants and the breathing system of humans, and cause asthma attacks, among other effects. Industrialization and associated transport activities produce the O_3 precursor gases like nitrogen dioxide (NO_2), nitric oxide (NO);

oxides of nitrogen (NO_x), Carbon monoxide among many others, that lead to the production and increase of O_3 near the ground surface. O_3 may also be transported by airflows from a source region into another area.

Methane is mainly produced in urban waste water and solid treatment works, ruminant domestic animals, coal mining and rice growing. Gas and oil pipelines leakages are other sources of CH_4. At the moment, there is a need for monitoring the temporal and spatial distribution of these GHGs in order to put in place effective control measures. These leakages cause social and environmental problems.

One of the fastest growing industrial and economic areas in the country is Central Kenya. Increased production and use of CO_2 is therefore expected even into the near future. It is an industrial gas used in the manufacture of soft drinks and other beverages, produced in cement manufacture, thermal electricity generating plants, industries and transport services. It is also produced in commercial and residential units in this region.

1.2 OBJECTIVES

The main objective of this study is to assess the concentrations of GHGs in 11 counties in Central Kenya; particularly CO_2, CH_4 and O_3 which account for more than 80% of all the GHGs.

The specific objectives of this study are to:-

(i). Investigate the temporal distribution of GHGs over Central Kenya.
(ii). Establish the spatial distribution of GHGs using the satellite data.
(iii). Identify the source regions of GHGs observed over Central Kenya and the impact of the local area, surrounding the Mount Kenya GAW Station, on its background monitoring.

1.3 JUSTIFICATION

Few studies have been made in the region regarding the levels of emissions of the GHGs. These studies have been mainly for the distribution of Ozone (Muthama, 1989; Thiongo, 1997; Bundi, 2004, Barasa, 2007). The other major GHGs have not been studied in the region. A new satellite having the capabilities to do CO_2 and CH_4 observations remotely at a good resolution has provided a unique opportunity to understand their distribution. These two gases contribute up to 80% of the anthropogenic global warming.

The 11 Counties in Central Kenya comprising of Laikipia, Meru, Tharaka, Embu, Machakos, Nairobi, Kiambu, Kirinyaga, Nyeri, Muranga and Nyandarua all combine to form a hub of industrial and economic activities of the country. In addition, parts of the counties of Nakuru, Narok, Kajiado, Makueni, Kitui, Tana River, Isiolo, Garissa and Wajir feed into this area. These counties are home to about a third of the total population of the Country (Kenya Census 2009). They are also among the fastest growing industrial and economic areas in the country.

Some of the major industrial activities in Central Kenya include processing of agricultural products like coffee, tea, milk, fruits, meat, wheat and maize among others. Vehicle assembling and the manufacturing of chemicals, textiles, shoes, ceramics, cement, steel, machinery, beer and soft drinks, soap, batteries, glass and plastics. Publishing, packaging and canning are other industrial activities carried out.

New resort towns are planned for the region (Kenya Vision 2030). Communication networks and many economic activities are expected to spring up. Oil and gas pipelines are set to traverse the area. Coal has been found in the Mui basin in Kitui County. Mining, industrial and commercial usage is set to start soon.

The levels of GHGs emissions may be expected to continue rising and this necessitates an assessment of greenhouse gas emissions in the country. Continuous monitoring is done at the ground based stations but currently remotely sensed data is also available from the orbiting satellites. The new satellite has given the impetus to establish the current GHGs concentrations and their possible sources or sinks.

The in situ observational data sets of GHGs available can also be used to validate the satellite observations. Mount Kenya GAW station has continuously observed the air from

year 2002 to date and has had regular instrument calibrations done at the station since its establishment (WMO World Calibration Centre (WCC) Reports 2010; 2008; 2005; 2002).

An assessment of the various GHGs data sets around Central Kenya will improve the understanding of the spatial and temporal distribution of these gases and establish their current distributions and trends. This could not have been done comprehensively earlier as there were only few data sets of atmospheric profiles from radiosonde observations in the region.

The characterization of these gases is needed to understand and anticipate the likely changes. A good knowledge of the background levels of GHGs is important before any additional industrial or commercial development, which may emit these gases, is considered. A clearer picture of the anticipated conditions will then be available. This knowledge will also feed the policy making processes and build effective strategies against global warming, improve air quality and build resilience against climate change. There will be opportunities for proactive measures in the region that will avert any negative consequences of the human activities.

This study will help to provide the background concentrations of GHGs upon which the anticipated additions will be built on for any impact analysis. Environmental Impact Assessment (EIA) studies for new developments need the background pollution levels in order to assess whether the anticipated additional pollution may be accommodated when the proposed project or policy is implemented. Impact assessment for any developments will consider; especially on air quality, the sources, the prevailing concentrations and the proposed routine mitigation and monitoring measures for implementation in the project.

This helps the authorities in deciding on one of the three options to take: Whether a project can be implemented as it is, or with some modifications or alternatively that project will not be implemented at all. A project is not implemented if the anticipated consequences are deemed to be of an adverse nature to the environment and/or humans. A good knowledge of the initial and the total anticipated emissions is important in the evaluation of the effectiveness of any mitigation measures considered in every case.

1.4 PHYSICAL LOCATION AND CLIMATOLOGY OF STUDY AREA

The Mount Kenya GAW station stands at 3678 metres above mean sea level at the Equator and 37ºE in the Mount Kenya National Park; well above the tree-line. The vegetation type is moorland scrubs. This Station provides unique observational opportunities; it straddles the Equator and the air masses from both hemispheres reach it. Further it is also sampling both continental and maritime air.

The map of Kenya, Figure 1, shows the physical features of the country and Central Kenya which lies between latitudes 2°N and 2°S of the Equator and Longitudes 36° and 40°E. It is a greatly diverse area in rainfall, temperature and winds due to the relief. The land rises from 500 to over 5,000 metres above mean sea level and temperatures from above 25° Celsius in the east to freezing on top of Mt. Kenya.

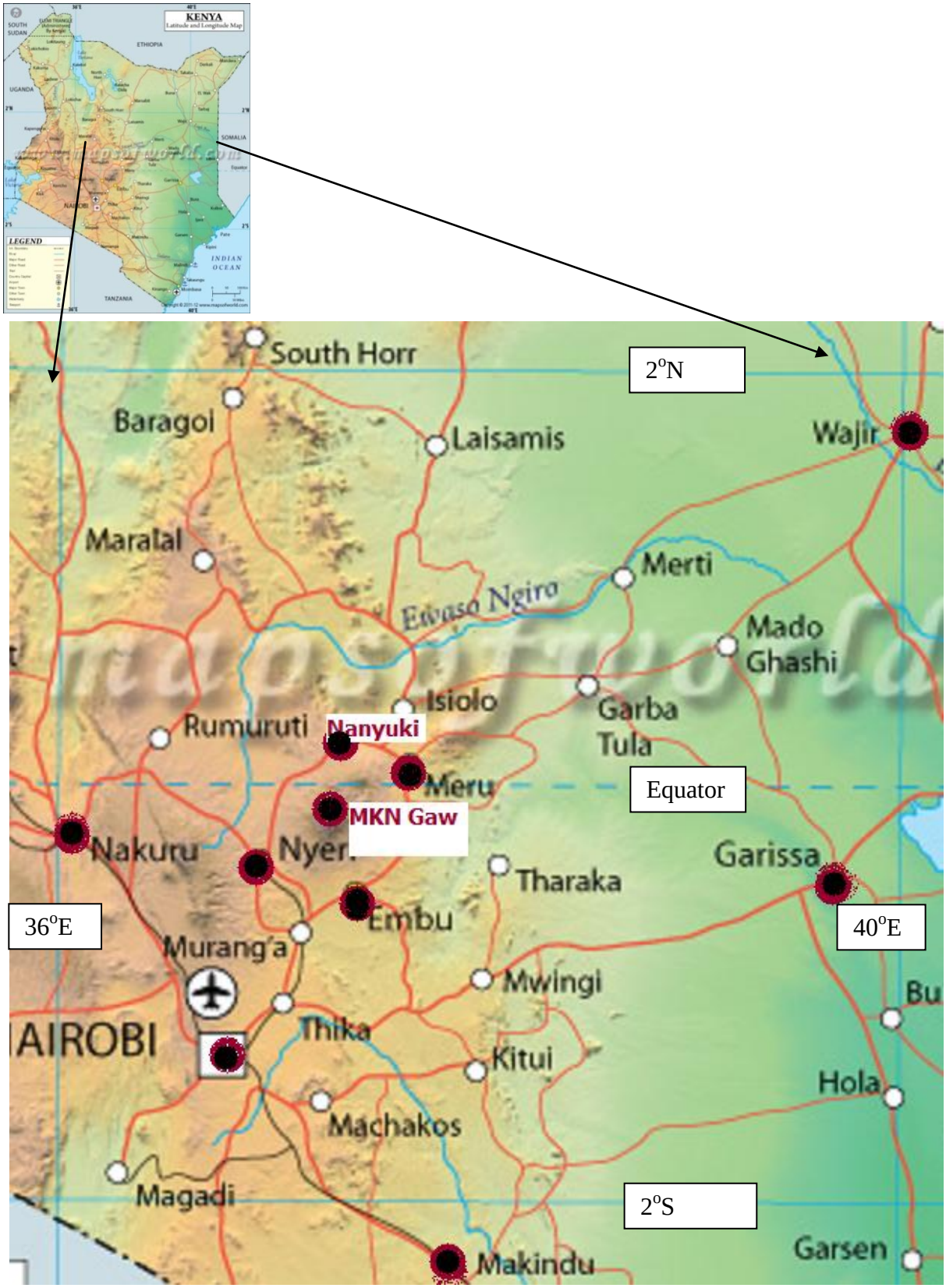

Figure 1: A Map of Kenya showing the study area and the ten stations used highlighted in black with red dots

(Source: www.mapsofworld.com)

The Mt. Kenya GAW station sits on the eastern Kenyan Highlands which experiences two rainy seasons: The long and the short rainy seasons. This climate is dominated by the seasonal displacement of the inter-tropical convergence zone (ITCZ) (Asnani 1993; Leroux 2001; Slingo *et al*. 2005). The Long rains come in March to May and the short rains in October to December. The station at this high elevation gets the rains at the beginning of March and October and in higher amounts than the lower stations in Nanyuki (Laikipia), Nyeri, Embu, or Meru.

Between May and September the East African Low Level Jet (EALLJ) is at its peak, Bunker, (1965); Findlater, (1969); Krishnamurti *et al*., (1976); Ngara, (1977), Asnani, (1993). EALLJ develops as from May in the southeast trade winds over Madagascar. As the ITCZ progresses northwards, the EALLJ strengthens and also extends further northwards. It is deflected by the East African Highlands and flows parallel to the coast before it blows eastward off the Somali coast as Somali jet. The EALLJ reaches its maximum extent in June/July when it stretches into India. The jet maximum generally occurs between 1.0 and 1.6 km above mean sea level. Wind speed maxima are usually about 20 ms^{-1}, but wind speeds may reach up to 50 ms^{-1} (Asnani 1993).

In June to August, the ITCZ is situated far to the north (10º – 20ºN), over India and along the southern coast of the Arabian Peninsula, resulting in southerly to south-easterly winds over Kenya. From September the ITCZ starts to retreat southward. This is normally followed by a rainy period, called the short rains, from mid-October to December over Kenya. In December to February, the ITCZ is situated south of the Equator (10° – 15°S), extending from the northern tip of Madagascar toward southern Tanzania and then northward toward Lake Victoria. As a consequence, East Africa is dominated by the north-easterly monsoon.

When the ITCZ starts to progress northward, it brings a second rainy period from mid-March to the beginning of June to Kenya. This is normally called the long rains season. The ITCZ moves farther north, re-establishing the southeast monsoon over East Africa, and the seasonal cycle is completed.

Studies have shown that monsoonal flows (Anyamba, 1983), subtropical anticyclones (Griffiths, 1972), easterly waves (Njau, 1982; Okoola, 1989), cyclones, tele-connections and El Nino- Southern Oscillation (ENSO) (Landsberg, 1963; Beltrando and Camberlin, 1993)

influence the rainfall and weather patterns in Kenya. Other meso scale local systems also influence the weather over the study area. These may include the presence of large water bodies, thermally induced systems and unique topography (Ogallo, 1988).

The temperatures at the Mt Kenya GAW station are 8-10ºC as maximum and 2 – 4ºC as minimum (Henne *et al*., 2008). Cloudiness during the wet seasons starts as early as mid morning and lasts till evening. The relative humidity during these months is high; 70 - 90%.

CHAPTER TWO

2. LITERATURE REVIEW

This review is subdivided into four sections: The first deals with the air flows, followed with a review on Ozone, then on Methane and finally on Carbon Dioxide.

2.1 AIR FLOWS

The categorization of the air flow over Central Kenya has always attracted interest (Gatebe *et al*., 1999; Okoola, 2000; Henne *et al*., 2007; Gicheru, 2007). Gatebe *et al*. (1999) and Henne *et al*. (2007) both showed that Central Kenya is influenced by six representative flows. These flows emanate from the following sources: eastern Africa, southern Indian Ocean, South eastern Africa, northern Indian Ocean and India, Arabian Peninsular and Pakistan and northern Africa free tropospheric air in that order. These airflows affect the region at different seasons and time spans.

Okoola (2000) showed that cold air originates from the South West Indian Ocean during cold spells especially between June and August. This was also confirmed by Gicheru (2007), that the cold air flow to Central Kenya originated from the eastern South Africa. Gicheru (2007) used the Hybrid Single – Particle Lagrangian Integrated Trajectory (HYSPLIT) in his analysis of back-trajectories. Draxler and Hess (1998) have described the HYSPLIT model. This model is sensitive to near ground-level trajectories and uses gridded meteorological data. It is also good for any spatial and temporal resolutions.

The Mt Kenya GAW station receives thermally induced wind systems that disturb the free tropospheric conditions (Henne, 2008). Henne (2008) further used the nighttime data for the analysis of long term trends of the free tropospheric air. Due to this criterion only about 14% of all the data at the station could be used in the analysis of long term trends of the free tropospheric background air. This compares to one year of the available data then.

Studies on the influence of source regions on the variation of concentrations of various gases, (Alto *et al.*, 2003 and Parish *et al*, 2010), have been done in different parts of the world. Alto *et al.*, (2003) investigated the influence of the air mass source sector on the

variations of CO_2 mixing ratios in Finland. This study used back trajectories and wind directions to identify the source regions of the air mass reaching their station. Different source sectors showed variations of up to 20 ppm. Parish *et al*. (2010) while studying the impact of transported O_3 on the air quality of California noted that the measured O_3 concentrations exhibit complex temporal behaviour on diurnal, synoptic and seasonal scales, as well as spatial variations in three dimensions. This variability results from a mix of production, loss and transport processes.

2.2 OZONE

Space-borne observations of O_3 tropospheric composition, profiles and/or columns, have been based on Low Earth Orbit (LEO) nadir viewing platforms. LEO satellites have a mean altitude of 800km above the earth and revolutions of about 90 minutes. These platforms include: Global Ozone Monitoring Experiment (ERS-2/GOME-1) (Burrows *et al*., 1999); Interferometric Monitor for Greenhouse Gases (ADEOS/IMG) (Kobayashi *et al*., 1999); Measurement of Pollution in the Troposphere (Terra/MOPITT) (Drummond and Mand, 1996b); Atmospheric InfraRed Sounder (Aqua/AIRS) (McMillan *et al*., 2005); Tropospheric Emission Spectrometer (Aura/TES) (Beer *et al*., 2001); Ozone Monitoring Instrument (Aura/OMI) (Levelt *et al*., 2006); Infrared Atmospheric Sounding Interferometer (METOP-A/IASI) (Clerbaux *et al*., 2009); METOPA/ GOME–2, (Callies *et al*. 2000); Scanning Imaging Absorption Spectrometer for Atmospheric Chartography (ENVISAT/SCIAMACHY) (Bovensmann *et al*., 1999). However, one of the setbacks of the LEO platforms is that they are not well adapted to the temporal variability and spatial gradients generally needed for Air Quality (AQ) management and forecasts.

In the upper atmosphere; stratosphere and mesosphere the production of O_3 takes place in two steps (Chapman, 1930). First, molecular oxygen (O_2) is photo-dissociated into atomic oxygen (O) by the absorption of a photon of energy *hv*, and subsequently, atomic oxygen reacts with the available molecular oxygen to form O_3. This photo-dissociation only takes place at wavelengths shorter than 242 nm.

The Ozone production is balanced by reactions in which O_3 is destroyed, as shown in the series of equations represented by equation 1 below. In the stratosphere, a catalytic O_3 destruction chain plays the most important role (Bates and Nicolet, 1950):

$$X+O_3 \longrightarrow XO+O_2$$

$$XO + O \longrightarrow X+O_2$$

$$\text{net : } O+O_3 \longrightarrow O_2 +O_2, \qquad (1)$$

where X is the catalyst species. The species X is not destroyed in this reaction, so only a small amount of X is needed to destroy a large amount of O_3. Several species have been suggested for the catalytic X in the atmosphere. The most important of these in the natural stratosphere are Hydrogen (H), Hydroxyl radical (OH), Nitric Oxide (NO), and Chlorine (Cl) (Wayne, 1985). In the troposphere O_3 is not produced by the photo-dissociation because the light at wavelengths shorter than 242nm cannot penetrate into the troposphere.

However, a catalytic reaction chain can lead to the production of tropospheric O_3. The last two steps of this reaction chain are shown in equations 2 and 3 shown below:

$$NO_2 + h\nu \longrightarrow NO + O \qquad (2)$$

$$O+O_2 \longrightarrow O_3 \qquad (3)$$

Here, the photo-dissociation of NO_2 provides an oxygen atom which in the next step reacts with molecular oxygen to produce O_3. NO and NO_2 are designated as NO_x or oxides of nitrogen. These are the precursors of surface (tropospheric) ozone. The presence of CO, CH_4 and other hydrocarbons allows the recycling of NO to NO_2.

Ozone also plays an important role in tropospheric chemistry. The photolysis of O_3 in the troposphere at wavelengths shorter than 315 nm (UV-B) leads to the production of the highly reactive OH radical. The OH radical reacts with almost all the gases in the atmosphere by natural processes and anthropogenic activities, like hydrocarbons, carbon monoxide, NO, and NO_2, and is therefore called the detergent of the atmosphere. Thus, tropospheric O_3 is of crucial importance for the removal of atmospheric pollution. The stratospheric O_3 is also important for the OH production because it affects the amount of

UV-B radiation in the troposphere, which is needed for the photolysis of tropospheric O_3 (Schlesinger, 1997).

A second source of tropospheric O_3 is transport from the stratosphere. In the lower troposphere the major source of O_3 is in situ production whereas in the upper troposphere transport of stratospheric O_3 is more important.

Ozone concentration includes that formed through photochemical reactions involving precursors from biogenic sources, wildfires and lightning, as well as O_3 transported to the station from outside the region or from the stratosphere.

2.3 METHANE

There are many sources of atmospheric CH_4 (Matthews, 2000), but the largest single source is the natural wetlands. Other sources include landfills, ruminant animals, rice cultivation, biomass burning, termites, coal mining and processing, as well as natural gas exploration, extraction, processing, transmission, distribution and usage, venting and flaring at oil and gas wells, wastewater treatment plants from domestic or urban and industrial establishments.

In general, in the sources of CH_4, there is a large proportion of anthropogenic sources composition over the natural. Among the domesticated animals are cattle, buffaloes, sheep, goats, pigs, camels, and horses. It is estimated by the United States (US) Environmental Protection Agency (EPA) that more than 50% of global CH_4 emissions are directly from human-related activities (EPA, 2011).

Other natural sources of CH_4 are natural gas hydrates; also called clathrate-hydrates, permafrost, oceans, freshwater bodies, non-wetland soils, wildfires and geologic processes. Its production is dependent on temperatures and moisture availability. Wetlands are ecosystems in which saturation with water is the dominant factor controlling soil development and the species of plants and animals that occur.

Upland soils are well-aerated, not water-saturated, and generally contain oxygen with dry soil conditions. These conditions favour microbial processes that make these soils a sink for

CH_4 and a source of N_2O. Natural sources include upland soils associated with forests and grasslands under natural vegetation, but not agricultural lands (EPA, 2011).

Methane sink strength of soils under natural vegetation (including upland and riparian soils) is estimated at 30 Tg CH_4/yr (EPA, 2011). Process-level (bottom-up) methods of estimating CH_4 budgets contain significant uncertainties due to the aggregation of local measurements, taken on short time scales and with large spatial variability. There still exists a lack of field measurements in the tropics and significant model uncertainties.

Future Methane oxidation by soils will depend on the changing human activities on these soils, as well as on climate patterns that are shifting as a result of global climate change. Clearing land for agricultural use has been shown to lead to a decreased capacity for CH_4 oxidation. Global climate models show patterns of temperature and precipitation changes worldwide. As soil moisture is a key determinant of the microbial processes that consume CH_4, the shifting climate patterns will determine the fluxes of CH_4 into the future (EPA, 2011).

Methane is chemically as well as radiatively active and its atmospheric concentrations can increase because the terrestrial sources are increasing and/or because the sinks are declining. An important atmospheric sink for CH_4 is the OH radical. The reaction of CH_4 with OH radicals is the first step in a series of reactions which eventually leads to compounds that are readily removed from the atmosphere by precipitation or uptake at the surface. OH radicals also act as a chemical sink for other trace gases.

The Environmental Protection Agency (2011) shows that since 1980, rice production has risen by over 40% through the combined effects of increased harvest areas and higher yields. CH_4 sources under anthropogenic control currently account for approximately 70% of the total annual emission. Currently, northern wetlands contribute about one-third of the world's total wetland emissions while the tropics account for most of the remainder.

Atmospheric record shows large and variable patterns in annual increases in atmospheric concentrations and uncertainties remain with respect to year-to-year variations in CH_4 emissions from various sources (EPA, 2011). Short-term variations in temperature and precipitation can affect emissions from biological sources such as rice paddies and wetlands; political and economic changes can affect levels of industrial activity and

consumption of fossil fuels; management practices can affect emissions from domestic animals and rice paddies; and development and recycling trends can affect CH_4 emissions from landfills and from wastewater. Landfill gas contains approximately 50-60% CH_4 with the remainder primarily CO_2.

Thathy *et al*. (1992), measured CH_4 fluxes by the static chamber method above three types of soils characterized by various water contents. High CH_4 emission is recorded on flooded soils while CH_4 uptake occurs in dry soil. CH_4 flux is also derived from variations of surface concentrations of CH_4 related to the variations of air stability and from vertical profiles in the lower troposphere.

Tyler *et al*. (1988) while investigating CH_4 emissions in termites, rice paddies, and wetlands in Kenya showed that the amounts compared well with those of other parts of the world. However, CH_4 in rice paddies is as high as from termites and also compares well with that from lakes and rivers in Kenya. Lal *et al*. (1993) also carried out studies of CH_4 flux values from rice paddies in southern India and showed that they were higher than estimates from some other regions in India, as well as average values for the mid-latitude region, but these values were lower than from China. The bottom- up approaches have been used to estimate the CH_4 flux but now orbiting satellites can now do the top- down measurements and fluxes done from inverse modeling.

In Kenya, a study of the GHGs by Simiyu *et al*. (2006) along the Nzoia River, in Western Kenya, revealed an increasing emission of GHGs as one moves downstream the course of the River. This study involved the sampling of emission from the river.

Schuck *et al*. (2012) studied the distribution of CH_4 in low latitudes using six years data from aircrafts CARIBIC/CONTRAIL flights and found that CH_4 had a high degree of variability, spatially and seasonally in the upper troposphere. The seasonal cycles over tropical Asia are influenced by the monsoon circulation. The study noted pronounced seasonal cycles over tropical Asia and enhanced mixing ratios over Central Africa. Further, a good correlation of CH_4, ethane, and acetylene with carbon monoxide was found and this indicated that the CH_4 high mixing ratios originated from biomass burning as well as from biogenic sources. Besides the changes in time, upper tropospheric CH_4 mixing ratios exhibit large spatial and seasonal differences. In the tropics distinct differences in the CH_4 distribution are seen for the different flight routes and longitudes bands.

These results were consistent with Meyer *et al*. (2012) who investigated biomass burning in the tropics. This study showed that CH_4 emission factors from savanna fires do not vary seasonally and that CH_4 emission factors vary across fuel types and vegetation types. The emission factor for CH_4 decreases during the dry season principally due to curing of the fuels.

A publication from the Netherlands Institute for Space Research (SRON) (2010) showed that higher temperatures can worsen climate change, and that CH_4 measurements from space reveal that fluctuations in the CH_4 emissions in the tropics are mainly determined by variations in the groundwater level but that fluctuations in the CH_4 emissions at high latitudes are mainly due to variations in the surface temperature. The data used was from the satellite which has on board SCIAMACHY and surface temperature for the period 2003-2007, and satellite measurements of variations in the gravitational field (GRACE) that were used to calculate variations in groundwater levels. An analysis of the data revealed that the total emission of the boggy areas increased by 7 % during this period.

Sinha *et al*. (2007) showed that the CH_4 average of the median mixing ratios during a typical diel (12 hour) cycle were remarkable similarity in the time series of both the boreal and tropical diel profiles. Nocturnal CH_4 emission flux of the boreal forest ecosystem, calculated from the increase of CH_4 during the night and measured nocturnal boundary layer heights yields a flux of about 45.5±11 Tg CH_4 yr^{-1} for global boreal forest area. This is a source contribution of about 8% of the global CH_4 budget. These results highlight the importance of the boreal and tropical forest ecosystems for the global budget of CH_4.

Table 1 below gives a comparison of some of the GHGs. The lifetime of the species in the atmosphere and the Global Warming Potentials (GWP) are compared. From the table, CH_4 is seen to be 25 times more potent than CO_2 in the 100 year timeframe.

Table 1: Global Warming Potential (GWP) Values for some key Greenhouse Gases

Common Name	Chemical Formula	Lifetime (years)	GWP time horizon		
			20 years	100 years	500 years
Carbon dioxide	CO_2	50 - 100	1	1	1
Methane	CH_4	12	72	25	7.6
Nitrous oxide	N_2O	114	289	298	153
Sulfur hexafluoride	SF_6	3,200	16,300	22,800	32,600

Source: 2007 IPCC AR4 (Working Group I: The Physical Science Basis)

2.4 CARBON DIOXIDE

CO_2 is a heavy colourless inert gas that is formed in animal respiration and in the combustion and decomposition of organic substances. CO_2 is a gas at standard temperature and pressure and exists in Earth's atmosphere in this state. It is a trace gas comprising 0.039% of the atmosphere; being uniformly distributed over the earth surface. In its solid state, CO_2 is commonly called dry ice.

Photosynthesis is a part of the carbon cycle whereby plants, algae, and bacteria absorb CO_2, sunlight, and water to produce carbohydrate energy for themselves and oxygen as a waste product. CO_2 is also generated as a by-product of combustion; emitted from volcanoes, hot springs, and geysers; and freed from carbonate rocks by dissolution.

Dams and water reservoirs also emit CO_2 and CH_4 (World Commission on Dams, 2000, Rosa *et al*., 2004). CO_2 is generated by the decomposition of organic materials under aerobic conditions while CH_4 is produced by decomposition processes under oxygen-deficient conditions.

One of the best ways to mitigate the greenhouse gases emissions in tropical regions is to clear the biomass from the reservoir basin before inundation. Logging a forest prior to flooding and using the timber for building can also reduce reservoir emissions.

Arau´jo *et al*. (2002) showed that in the Amazon forest, there was a lowering of the CO_2 fluxes during the dry season and that the seasonal variation was little. Other studies in Europe about reducing CO_2 in road traffic within the cities was done by Sternad *et al*., (2010) and found that high amounts were emitted even in small cities and towns and concluded that there is a need for different measures to reduce the emissions from cars.

Carbon dioxide is released into our atmosphere when carbon-containing fossil fuels such as oil, natural gas, and coal are burned in air. As a result of the tremendous world-wide consumption of such fossil fuels, the amount of CO_2 in the atmosphere has increased over the past century, now rising at a rate of about 1ppm per year (Earth System Research Laboratory, 2013). Major changes in global climate could result from a continued increase in CO_2 concentration.

In addition to having an influence on climate, CO_2 has a direct, measurable effect on plant growth. Plants tend to grow better under conditions of higher CO_2 levels (Mooney and Luo, 1999) when other factors are not limiting. This effect has been given the name "CO_2 fertilization." This effect implies increased: Photosynthetic production rate, biomass (plant dry weight), water use efficiency, tolerance for low light levels and optimum temperature for photosynthesis,

Carbon dioxide at low concentrations is odourless. At higher concentrations it has a sharp, acidic odour. It can cause asphyxiation and irritation. When inhaled at concentrations much higher than usual atmospheric levels, it can produce a sour taste in the mouth and a stinging sensation in the nose and throat. Carbon dioxide is toxic in higher concentrations: 1% (10,000 ppm) will make some people feel drowsy. Concentrations of 7% to 10% cause dizziness, headache, visual and hearing dysfunction, and unconsciousness within a few minutes to an hour. Amounts above 5,000 ppm are considered very unhealthy, and those above about 50,000 ppm (equal to 5% by volume) are considered dangerous to animal life.

Some of the uses of CO_2 include the following: food, oil, and chemical industries, in many consumer products that require pressurized gas because it is inexpensive and non-flammable, and because it undergoes a phase transition from gas to liquid at room temperature at an attainable pressure of approximately 60bar, allowing far more CO_2 to fit in a given container than otherwise would. Life jackets often contain canisters of pressured CO_2 for quick inflation.

Aluminium capsules of CO_2 are also sold as supplies of compressed gas for airguns, paintball markers, inflating bicycle tires, and for making carbonated water. Rapid vaporization of liquid CO_2 is used for blasting in coal mines. High concentrations of CO_2 can also be used to kill pests.

The combustion of all carbon containing fuels, such as CH_4 (natural gas), petroleum distillates (gasoline, diesel, kerosene, propane), but also of coal and wood, will yield CO_2 and, in most cases, water. Iron smelting in blast furnace produces pig iron and CO_2.

Yeast metabolizes sugar to produce CO_2 and ethanol in the production of wines, beers and other spirits. Commercially, CO_2 finds uses as a refrigerant (dry ice is solid CO_2), in beverage carbonation, and in fire extinguishers. Since the concentration of CO_2 in the atmosphere is low, it is not economical to obtain the gas by extracting it from air. Most commercial CO_2 is recovered as a by-product of other processes, such as the production of ethanol by fermentation and the manufacture of ammonia. Some CO_2 is obtained from the combustion of coke or other carbon-containing fuels.

The six main industrial processes for CO_2 production is listed briefly below:

a) Directly from natural CO_2 springs, where it is produced by the action of acidified water on limestone or dolomite.
b) As a by-product of hydrogen production plants, where CH_4 is converted to CO_2;
c) As a by-product of the industrial production of ammonia. The process also begins with the reaction of water and CH_4;
d) From combustion of fossil fuels and wood;
e) As a by-product of fermentation of sugar in the brewing of beer, whisky and other alcoholic beverages;
f) From thermal decomposition of limestone, $CaCO_3$, in the manufacture of lime, CaO.

According to the Earth System Research Laboratory (2013), the global CO_2 in the Earth's atmosphere was at a concentration of 395.09 ppm by volume as of January 2013. Atmospheric concentrations of CO_2 fluctuate slightly with the change of the seasons, driven primarily by seasonal plant growth in the Northern Hemisphere. Concentrations of CO_2 fall during the northern spring and summer as plants consume the gas, and rise during the northern autumn and winter as plants go dormant, die and decay. There is a seasonal cycle

in CO_2 concentration associated primarily with the Northern Hemisphere growing season. Taking all this into account, the concentration of CO_2 grew by about 2 ppm in 2009.

Recent studies (Cogan *et al*., 2012) comparing the satellite observed column- averaged CO_2 and the in situ measurements have showed good correlation of about 0.75 and mean differences of 0.1 ppm. Other studies (Ohyama *et al*., 2012) comparing the total and tropospheric columns of O_3 retrieved from GOSAT found them to have a good agreement with the ground-based data from the Dobson spectrophotometers with a correlation coefficient of about 0.98 over Japan.

The seasonal trends and patterns were also consistent with those of Dobson measurements. However, there was a positive bias of 8.8 DU (3.0%) with a root-mean-square difference of 10.9 DU (4.1%) compared to the Dobson measurements.

CHAPTER THREE

3. DATA AND METHODOLOGY

The data and methods applied to this study are discussed below:

3.1 DATA USED IN THE STUDY

Five different data sets were used in this study and are discussed below. They are:

a) Meteorological data from the synoptic stations in the study area,

b) Background greenhouse air pollution data from the Mt. Kenya GAW station

c) The Nairobi Ozone data comprising the total column, surface and profiles of ozone.

d) The satellite observational data.

e) Reanalysis meteorological fields from National Center for Environmental Prediction – National Center for Atmospheric Research (NCEP- NCAR)

3.1.1 Meteorological data

The meteorological data was obtained from the Kenya Meteorological Department for the stations in Central Kenya. This data is from the synoptic meteorological stations surrounding the Mount Kenya GAW Station. These Stations are as shown in Figure 1. The synoptic stations near the Mt Kenya GAW station include Wajir, Garissa, Meru, Nanyuki (Laikipia), Embu, Nyeri, Nakuru, Dagoretti Corner, Narok and Makindu. The meteorological element of interest at these surrounding stations was the monthly rainfall total.

3.1.2 The Background greenhouse air pollution data from Mt Kenya GAW station

The greenhouse gases data was obtained from the Kenya Meteorological Department for the Mt Kenya GAW Station. This data comprises of one minute averages of surface O_3 data from the year 1999 to 2010. The other data for the station include the weekly CO_2 and CH_4 amounts for the period December 2003 to November 2011.

This weekly data is obtained from the Earth System Research Laboratory (ESRL); formerly Climate Modeling and Diagnostics Laboratory (CMDL of NOAA) where air-filled flasks from the Mt Kenya GAW Station were sent for analysis by Gas Chromatographs. The website is www.esrl.noaa.gov/gmd. or via ftp://ftp.cmdl.noaa.gov/

3.1.3 The Nairobi Ozone data

The total column ozone measurements with the Dobson spectrophotometer from September 1984 to December 2012 will be used. The monthly values were considered along with the weekly ozonesonde profiles data that are also available from May 1996 to December 2012. These data sets were obtained from the Kenya Meteorological Department headquarters.

In addition a one year data for surface ozone measured in Nairobi from July 2012 to May was also compared with the surface ozone data from Mt Kenya GAW station for their diurnal characteristics. The surface ozone measuring equipment was installed in 2012 in Nairobi at KMD headquarters.

3.1.4 The Satellite observations data

The satellite data from the GOSAT (Greenhouse Observing SATellite), "ibuki" will be obtained from the National Institute for Environmental Studies (NIES) of Japan. The data can be accessed on the web, by registration and can be obtained by en email request. The registration web page is: https://data.gosat.nies.go.jp/gateway/gateway/MenuPage/open.do and different categories of users are allowed. GOSAT uses Thermal and Short Wave Infrared Sensors (TIR and SWIR) to measure the CO_2 and CH_4 column amounts and profiles from clear skies during the day. Other data sets that can be obtained are the monthly distributions and flux of GHGs, especially CO_2 at a 1° x 1° (latitude- longitude) grid for flux and 2.5° X 2.5° for spatial distribution.

The flux and distribution data sets are the level four data type and are in text format for flux but the column abundances are in Net Common Data Format (NetCDF). The Grid Analysis Display System (GrADS) software can read and display NetCDF data. ArcView GIS can be used for the spatial display of the CO_2 flux data.

The other levels (1 to 3) of the satellite data are in the fifth version of the Hierarchical Data Format (HDF5). The Level 1 data are radiance data, level 2 are column amounts and vertical profiles of CO_2 and CH_4 while Level 3 are monthly averaged global distributions. The level

3 data_are generated by interpolating, extrapolating, and smoothing the Level 2 column-averaged mixing ratios of CO_2 and CH_4 on a monthly basis. Kriging method, which is a geostatistical calculation technique, is applied. The values are gridded to 2.5-degree cells. The Level 3 data products are global maps of CO_2 and CH_4 at several pressure levels that are processed in the same manner as above. These data products can be utilized for visualizing local highs and lows of the greenhouse gases on a global scale.

The Level 4A data product shows monthly CO_2 source/sink strengths (fluxes) in 64 global regions that are inversely estimated from the Level 2 column-averaged mixing ratios and ground-based observational data using a global atmospheric transport model. The other Level_4B data product presents global CO_2 concentrations in three dimensions calculated from the Level 4A data product by using the atmospheric transport model. The data product has a horizontal resolution of 2.5^o x 2.5^o and a time step of six hours.

GOSAT makes a sun synchronous orbit in 99 minutes at an altitude of 667 km. It has a spatial resolution of 160 km and passes the same point every three days; after making about 56,000 observations. The sub-point footprint is 10.5km. This data has been used in other areas apart from Eastern Africa.

GOSAT has been progressively making public the different levels of their data and products. The most recent public release of CO_2 data on flux and distribution (satellite level 4 data) was in August 2012 for. The initial level 2 data release, to the general users, was in August 2010.

3.1.5 Gridded meteorological data

These data sets are obtained through the web from the National Centre for Environmental Prediction- National Centre for Atmospheric Research (NCEP- NCAR) global re-analyses. These monthly global reanalysis data sets at a resolution of 2.5^o X 2.5^o grid, given six hourly are for use with the HYSPLIT model. The data spans from 1948 to present for every month. The monthly data from the period 2005 to 2008 were used in this study and can be accessed through: http://www.ready.noaa.gov/archives.php or ftp://arlftp.arlhq.noaa.gov.

These data sets have been used successfully in different studies in East Africa (Bundi, 2004; Sakwa, 2006; Omeny 2006; Gicheru, 2007; Mungai, 2008; Mbithi, 2010) among others.

3.1.6 Data Quality Control

Involves filling in of missing data and doing data homogeneity tests. Data in-homogeneity can arise as a result of changes in exposure site, change of instrument, or change of personnel.

3.1.6.1 Missing Data

Missing data is filled in, using the mean ratio formula given in equation 4 below, so long as the missing data is less than 10% of the data set. To meet this objective, the ratio of the long term means of two stations, X and Y, which have a strong positive correlation is used. To get the missing value, x, in Station X, a corresponding value, y, in Station Y is used with the mean ratio.

$$\frac{\bar{X}}{\bar{Y}} = \frac{x}{y} \qquad (4)$$

In equation 4, x is the missing value in Station X, y is the corresponding value for Station Y and $\bar{X}$ and $\bar{Y}$ are the respective long term means of the stations X and Y.

3.1.7 Homogeneity

In this study inconsistency was tested using the mass curves method. A graphical plot was done of time versus accumulated values of each meteorological element of interest, GHGs at Mt Kenya GAW station and Ozone in Nairobi. When the time series of cumulative values form a straight line, then record is homogeneous. On the other hand, strictly heterogeneous record is shown by significant deviations of some of the plots from the straight line.

3.2 METHODS

The methods applied to the data to meet the stated objectives include data quality control, time series analysis, temporal and spatial distribution, trajectories and correlation analyses. Some descriptions of each method are given below.

3.2.1 Time series analysis

The time series analysis involves a graphical plot of the element of interest against time. The graphical representation shows the spread of the data over time. Any gaps of missing

data become apparent; unless a smoothing function is applied. Seasonal cycles may also be deduced in the plotted data.

The seasonal, monthly and diurnal graphs are made for each of the element of interest. The range of spread of the data is also seen.

Trend is the long- term behavior of the time series. Both graphical and statistical methods may be used for trend analysis. In the graphical method, the rate of change of slope is used to describe the trend of the time series. A positive slope shows an increasing trend, whereas a negative slope shows a decrease. The statistical significance of the slope is tested. Since the data available is for durations of about 10 years or less, the Student‘s t-test is used in testing the significance. The confidence level for the testing of the hypothesis will be set to 95%. No trend; stationary trends do not have a slope.

It is against the hypothesis that the slope is significantly different from zero at 95% confidence level that the testing is done. The Student’s t- test for the means takes the form given in equation 5 shown next:

$$t = \frac{\bar{x} - \mu_0}{s/\sqrt{n}} \qquad (5)$$

In equation 5, t is the statistic to be used in the student’s t- test computed tables. The degrees of freedom used in this test is $n - 1$, $\bar{x}$ is the sample mean, μ_0 is the population mean, the desired mean, s the standard deviation of the sample, and n is the sample size; usually less than 30 for the Student’s t- test.

Surface ozone data at Mt Kenya GAW station was subjected to trend analysis. There are some disadvantages of using the graphical method for trend analysis as it is highly subjective to individual visual interpretation.

3.2.2 Spatial Distribution

The mean monthly GHGs concentrations and fluxes are displayed on spatial maps to show their distributions in the study area. ArcView GIS software is used to facilitate this exercise. Other packages like Surfer can also be used. They have the same principle that data has to be interpolated between the grid points so as to show areal spread over the region.

3.2.3 Comparison of GOSAT data with in situ Observations

The satellite GHGs abundances are compared with the in situ observations in Mt Kenya. Monthly mean values will be used for this comparison as some of the GHGs data sets for Mt Kenya GAW station are done weekly. Comparisons will be by correlation as was done in studies by Cogan *et al*., (2012) and Ohyama *et al*., (2012).

The testing of results for significance is also carried out. The data set is small and the Student's t- test is most appropriate in handling these samples. The correlation analysis equation is given by, r, for the correlation coefficient between x and y is given by equation 6 below:

$$r_{xy} = \frac{\sum(x-\bar{x})(y-\bar{y})}{\sqrt{\sum(x-\bar{x})^2\ (y-\bar{y})^2}} \qquad (6)$$

where $\bar{x}$ and $\bar{y}$ are the sample means.

The test of significance of the computed correlations is by the student's t-test, where the test statistic, t, is given by equation 7 stated below:

$$t = \frac{\sigma\sqrt{(n-2)}}{\sqrt{(1-r^2)}} \qquad (7)$$

with n-2 degrees of freedom, r^2 is the coefficient of determination, found by getting the square of the coefficient of correlation and σ is the pooled standard deviation of the two samples.

3.2.4 Determination of Air Trajectories

Air trajectories can either be forward, moving away, from the station or backwards; where the air flow is into the station. Different models for air trajectories can be used depending on the availability of input data. Each model requires gridded fields of meteorological variables at regular temporal intervals. The time interval between fields should be constant for each defined grid; the fine grid regional data may be available at three hour intervals while the coarser grid global model fields may be available only every six hours.

The Hybrid Single - Particle Lagrangian Integrated Trajectory (HYSPLIT) is used for two primary applications of trajectories or concentrations. The model structure consists of a modular library with main programs for each application. It has two independent operational

options; it can be installed in a personal computer and run or done on the over the web-based http://ready.arl.noaa.gov/.

The data sets are the monthly reanalysis fields available from the National Centre for Environmental Prediction- National Centre for Atmospheric Research (NCEP- NCAR) global re-analyses. The start or end of the trajectories was determined from the time series plots of the surface ozone concentrations at the Mt Kenya GAW Station. A sudden sustained rise or fall in the ozone concentration could be indicative of changed air source characteristics or path. For a rise or fall in the ozone concentration, the timing is supposed to coincide with the start (of a backwards trajectory to indicate the path and source region of airflow. Forward air trajectories merely indicate the outflow from the Mt Kenya GAW Station.

The back and forward-trajectories for air mass source region is done using the HYSPLIT model. The HYSPLIT model, version 4.9, of National Oceanic and Atmospheric Administration (NOAA), is described by Draxler and Hess (1998). HYSPLIT runs by making the initial time ($t+\Delta t$) step; normally of 6 hours for low resolution but the time period can be as low as 10 minutes and domain of about 300m. The computational errors increase with the distance travelled.

HYSPLIT integrates the horizontal and vertical fields as provided by the reanalysis data. The first guess for the vertical motion is given by equation 8 shown below (Draxler, 1998):

$$P(t+\Delta t) = P(t) + V(P,t)\Delta t \qquad (8)$$

Where $P(t+\Delta t)$ is the three- dimensional parcel motion and $V(P, t)$ is the parcel velocity and Δt is the time step.

The outputs, showing the paths and time of the air parcels took, are shown on aerial maps. The map projection can be in any of the three map projections; Lambert, Polar, or Mercator. The time intervals are defined by the user. A vertical view is also appended to show the air parcel through different altitudes.

The model takes care of the diabatic and adiabatic processes in the vertical dimension. The boundary condition at the surface, where we assume no vertical motion, together with the

consideration of atmospheric stability, permits trajectories to follow the terrain or go around obstacles when the trajectories approach the surface.

The choice of start or end times at the station is determined from the time series plots of surface ozone detected at the Mt Kenya GAW station. A sudden fall or rise in surface Ozone amount, which is sustained for long period at the station is a good indicator of a changed source region or source characteristics. Clusters are also calculated to indicate the most common directions and their proportions during the month.

The air reaching or leaving the station at different periods is traced backwards for five days to show the source region. The forward trajectories are done for only 72 hours to indicate the general flow patterns out of Mount Kenya GAW Station. These results are available on six hourly basis, at 0000, 06000, 1200 and 1800, as determined by the HSPLIT model.

Backward trajectories are useful in tracing aerosols and trace gases back in time and space to their source regions. Forward trajectories of air parcels provide a guide on the locations where pollutants are likely to be advected to.

(Gicheru, 2007; Bundi, 2004) used these methods in their studies on trajectories. Gicheru (2007) investigated the circulation patterns and trajectories associated with cold air outbreaks over Central Kenya and Bundi (2004) studied the distribution of tropospheric ozone and synoptic circulations over southern Africa.

The NCEP / NCAR reanalysis data has been used successfully to characterize the wind fields, (Mungai, 2008; Mafimbo, 2008) over the Kenyan coastal region. Mbithi (2010) used these data sets to investigate the transport patterns of aerosols over East Africa.

The HYSPLIT model can run interactively on the Web through the READY system on NOAA's site. The PC based version of HYSPLIT has also been used. Similar results are obtainable from both versions. Except that the Web based version does not do the clustering.

The model is based on the principle of Lagrangian advection with the zonal (u), meridional (v) and the vertical (w) wind components at a time, atmospheric layer and grid used to compute a new upstream (or downstream) location of an air parcel at chosen time steps. This location is then iteratively re-determined using the components at the new position to

calculate the next location. The procedure is then repeated for a specified starting time on a desired date for six days to produce a backward trajectory over five days.

The following are some of the assumptions that are necessary to have the HYSPLIT model run according to Draxler and Hess (1998):

(a) When the input data are given on pressure-sigma surfaces it is assumed that these surfaces are the native grid of the meteorological model, hence moisture is expected as specific humidity and temperature is assumed to be a dry temperature.
(b) In a puff model, the source is assumed to be releasing pollutant puffs at regular intervals over the duration of the release. That each puff contains the appropriate fraction of the pollutant mass and the puff is advected according to the trajectory of its centre position while the size of the puff (both horizontally and vertically) expands in time to account for the dispersive nature of a turbulent atmosphere.
(c) In a particle model, the source is assumed to be releasing many particles over the duration of the release. In addition to the advective motion of each particle, a random component to the motion is added at each step according to the atmospheric turbulence at that time.
(d) Pollutant vertical mixing is assumed to follow the coefficients for heat. If the Turbulent Kinetic Energy (TKE) field is available, the mixed layer depth can also be computed from the TKE profile instead of the temperature profile.
(e) For puff dispersion, when the puff is larger than the meteorological model grid size it is assumed that the meteorological model is capable of resolving turbulent motions on that scale. In the vertical direction, a puff distribution is always assumed to be a constant value inside the puff and zero outside.
(f) For wet deposition one of the two assumptions taken is that the polluted air is continuously ingested into a cloud from a polluted boundary layer and those in which rain falls through a polluted layer.
(g) At the grid points where it is raining, the cloud bottom is defined at the level when the RH first reaches 80% and the cloud top is reached when the RH drops below 60%. All removal amounts are adjusted by the fraction of the pollutant mass that is within the cloud layer by defining the fraction of the pollutant layer that is below the cloud top and the fraction of the pollutant layer that is above the cloud bottom.

CHAPTER FOUR

4. RESULTS AND DISCUSSIONS

The results obtained using the methods described in Chapter Three are presented in the following sections. The initial discussion is from the data quality control.

4.1 RESULTS FROM DATA QUALITY CONTROL

The data quality control methods outlined in Sections 3.2.1 and 3.2.2 were employed. These included estimation of missing data and homogeneity tests. The results are as given below:

4.1.1 Estimation of Missing Data Using the Mean Ratio Method

Missing data were estimated using the arithmetic mean ratio method as was described in section 3.1. This was for the data that had less than ten percent. The Nairobi Dobson spectrophotometer monthly data had more than ten percent missing and this data was not used in the analysis.

All the data used was subjected to quality control before they were used in the analysis. The results of data quality control are presented in the next section.

4.1.2 Results of Data Quality Control

The homogeneity test used on the data was the single mass curve homogeneity test. Good results were obtained, showing that the records were homogeneous. The mass curves were almost linear. Some of the results from this test are displayed in Figures 2 to 5. The different data sets were therefore declared to be of high quality and useful for further analysis.

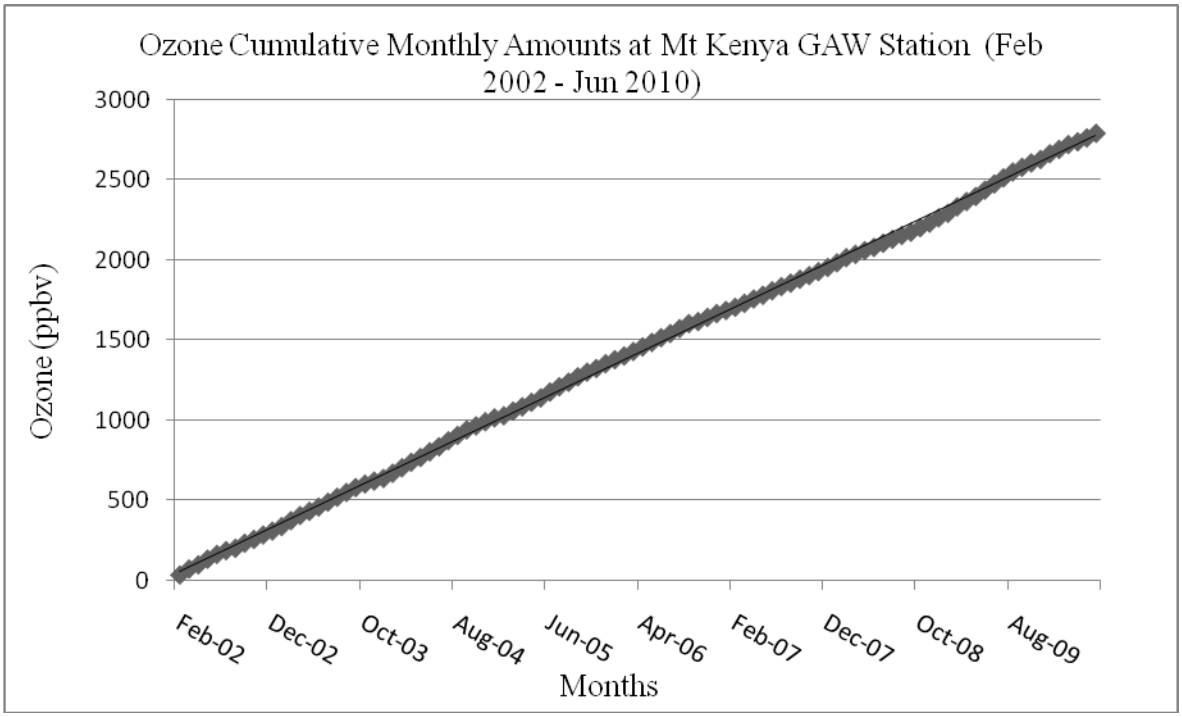

Figure 2: Time series of cumulative surface ozone amounts for Mt Kenya GAW Station.

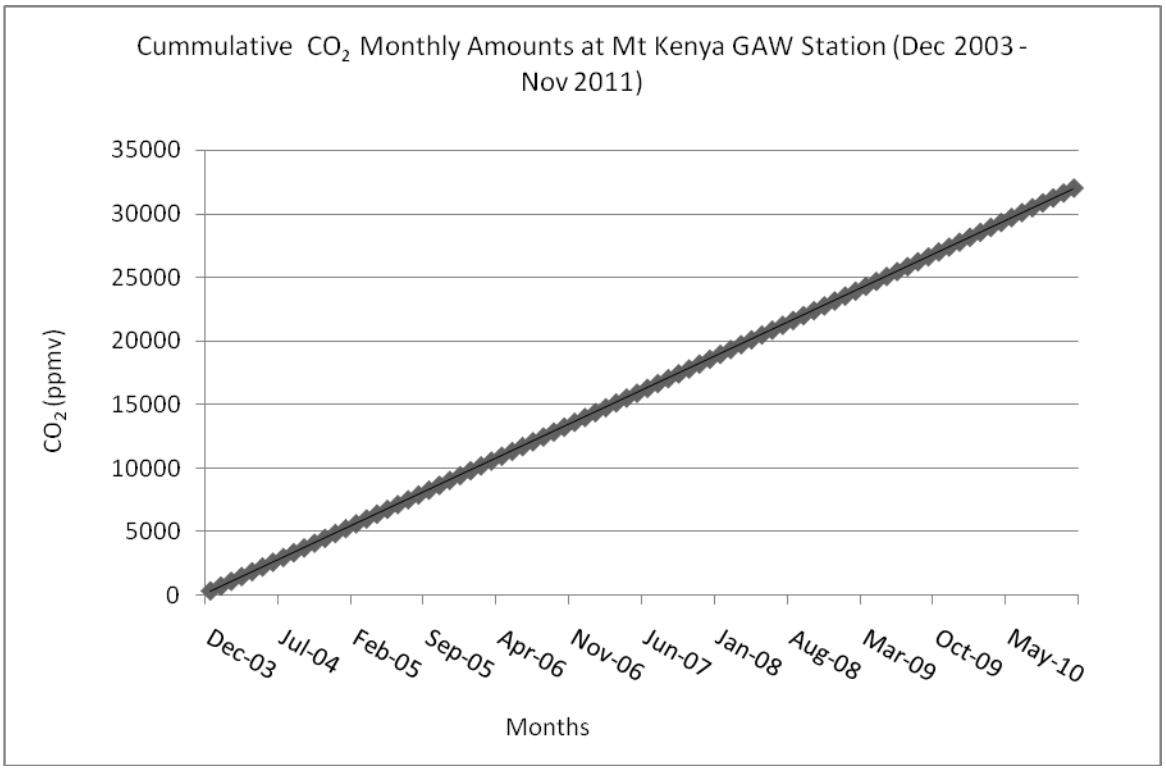

Figure 3: Time series of cumulative CO_2 amounts for the Mt Kenya GAW station.

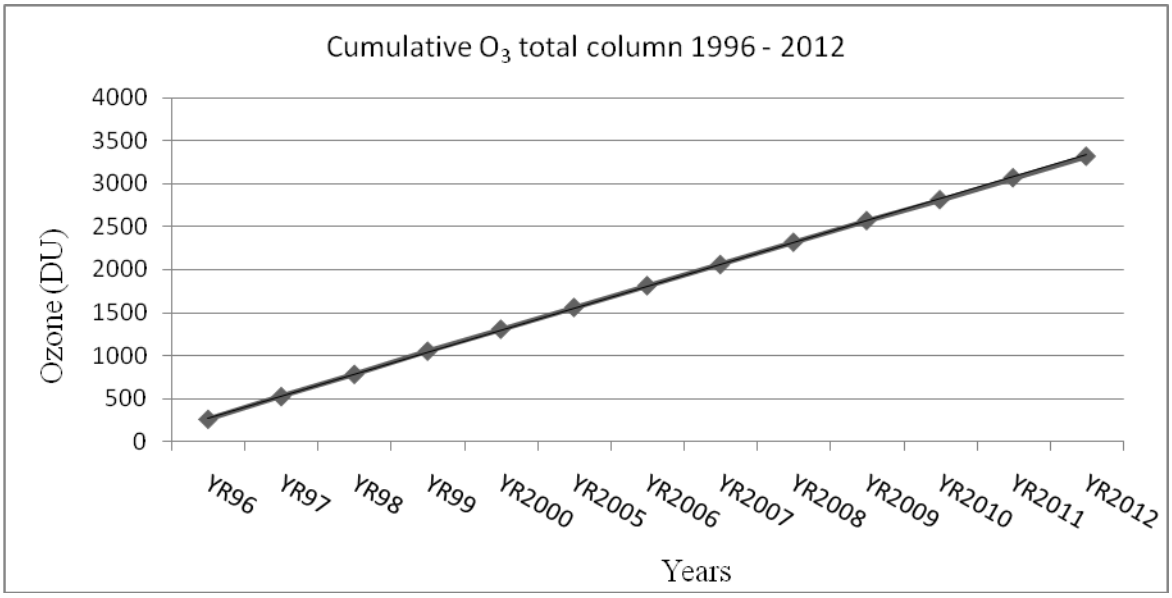

Figure 4: Time series of cumulative Total Ozone Column amounts for Nairobi.

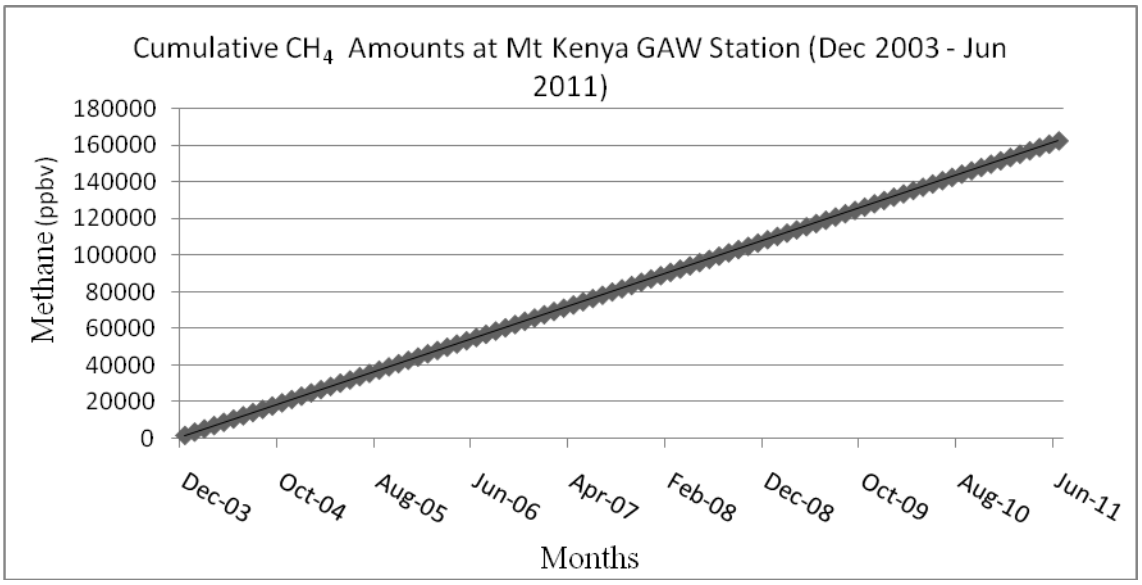

Figure 5: Time series of cumulative Methane amounts for Mt Kenya GAW Station.

4.2 RESULTS FROM TIME SERIES ANALYSIS

All the data sets used were subjected to time series analysis and displays, as shown in Figures 6 to 9. The key result in these plots is to detect whether there are any trends.

Some gaps were noted for methane, ozone and carbon dioxide. However, they were each less than ten percent of the data set. Some data sets had outliers as shown in Figure 6 where some two values were far too low values for December and August in the monthly means.

Throughout the period (December 1999 to June 2010), surface ozone has been ranging between 20 and 40 ppbv.

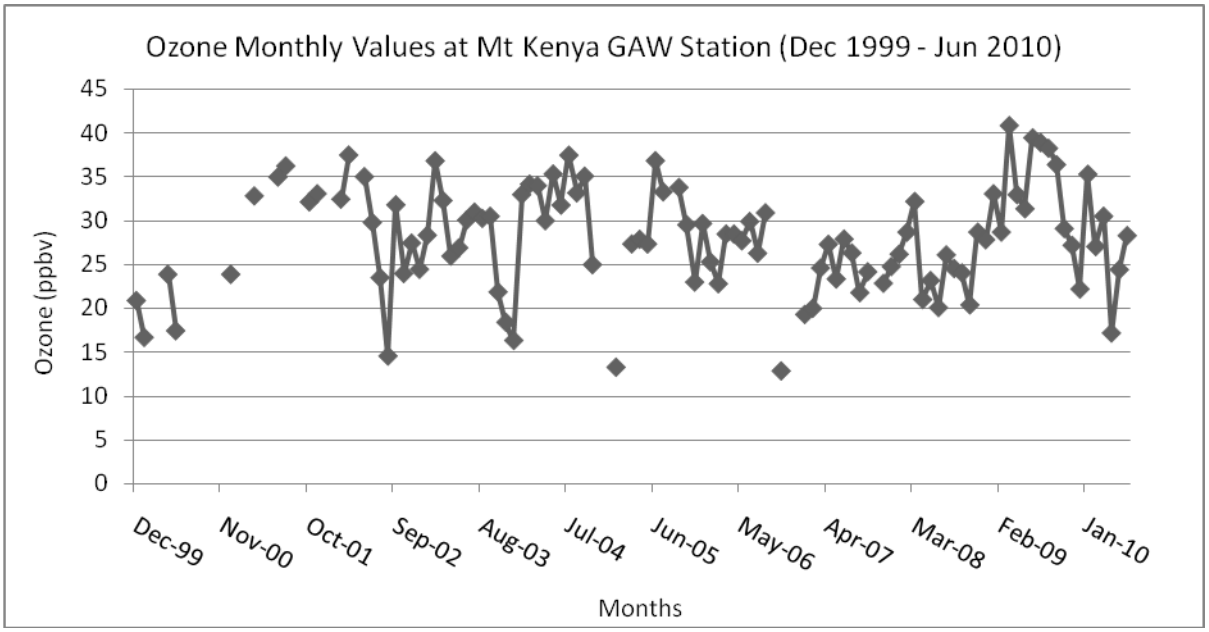

Figure 6: Time series for monthly ozone means at the Mt Kenya GAW Station.

Figure 7 shows the time series for Carbon dioxide. The continuing rise in CO_2 concentrations is discernable at the Mt Kenya GAW station and the Keeling curves in each season. Figure 8 shows the time series of Methane and rise is discernable. The seasonal cycles for Carbon dioxide and Methane show some periodicity due to the strong influence of air from the two hemispheres at different times. A discernable rising trend can also be deduced from Figures 7 and 8.

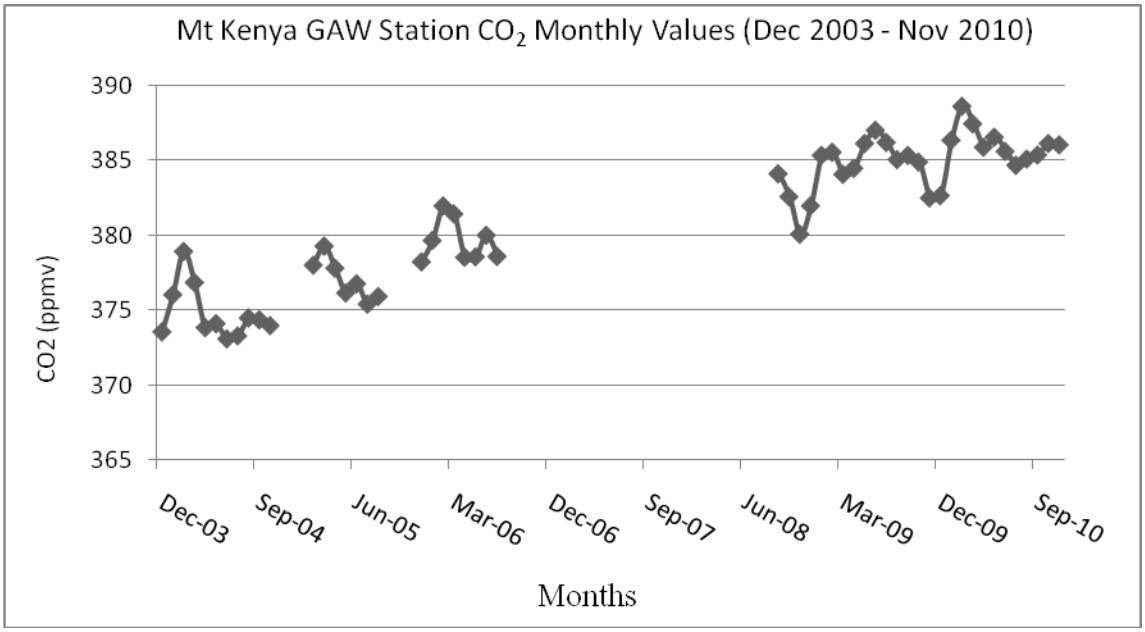

Figure 7: Time series for Carbon Dioxide at the Mt Kenya GAW Station.

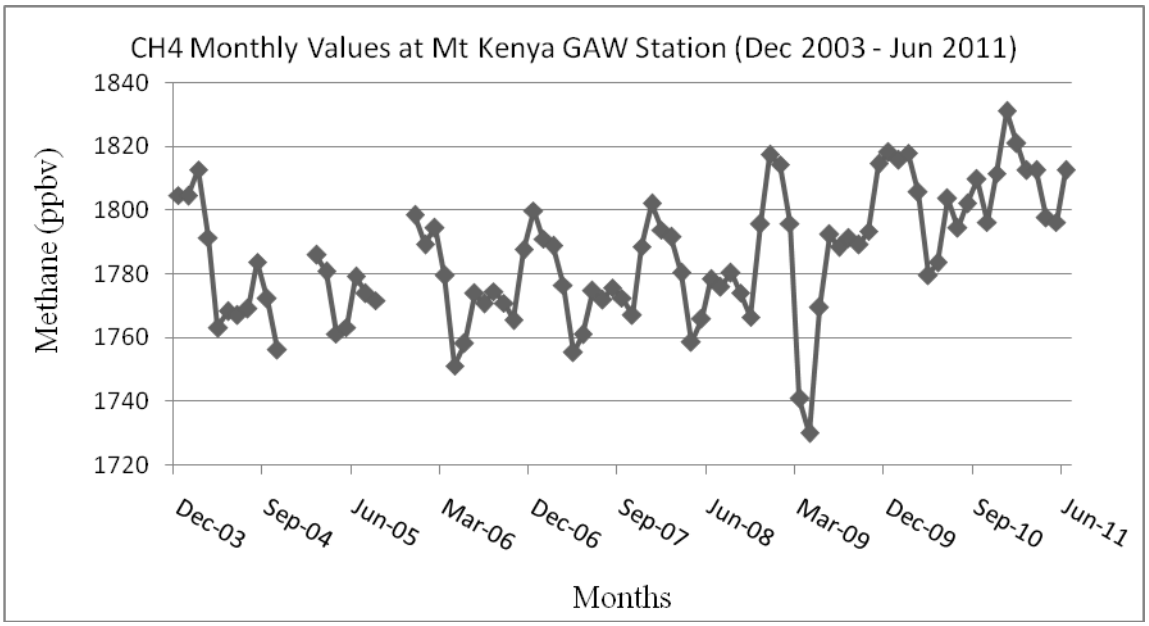

Figure 8: Time series for Methane at the Mt Kenya GAW Station

The Mt Kenya GAW station surface (tropospheric) ozone data is on one minute averages. The One month data for December 2007 is displayed as Figure 9. Sometimes the Ozone amounts are steady with the discernable diurnal cycles. At times the gentle but steady rise or fall is detected. The continuous rise or fall of ozone values are later subjected to trajectory analysis for the source region of the air the caused the change.

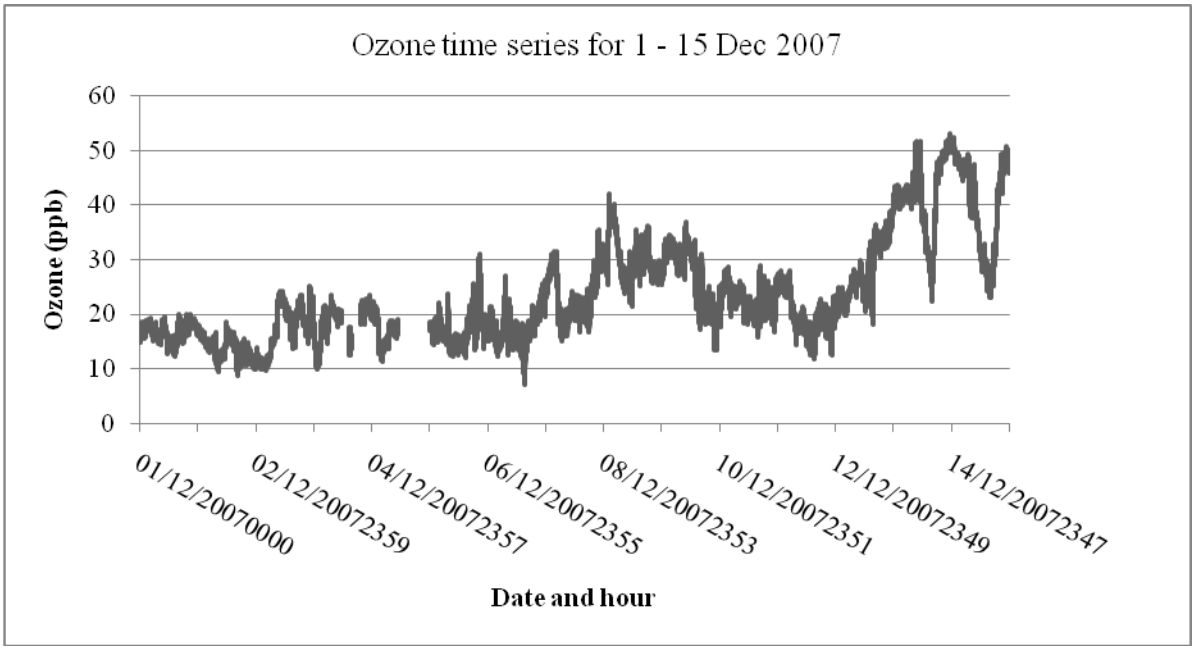

Figure 9: Time series for Surface Ozone at the Mt Kenya GAW Station for December 2007

Further two other analyses were done on the time series data to get the seasonal and the diurnal cycles. The seasonal cycles of Methane, Carbon Dioxide and Ozone are shown in Figures 10 - 13. Peak Methane amounts, Figure 10, are from November to February around Mt Kenya GAW station. Low methane amounts are witnessed from March to October. It dips steeply in March reaching a minimum in April; a second minimum is in October.

The low amounts are consistent to the exposure of the station to the southern hemisphere air and the high amounts to the northern hemisphere air.

Though the length of the data set is short, the GAW station is exposed to the air from the southern hemisphere where the CH_4 amounts are low. From October, the northern hemisphere air which is rich in CH_4 reaches the station. The amplitude of the seasonal cycle is about 50 ppbv.

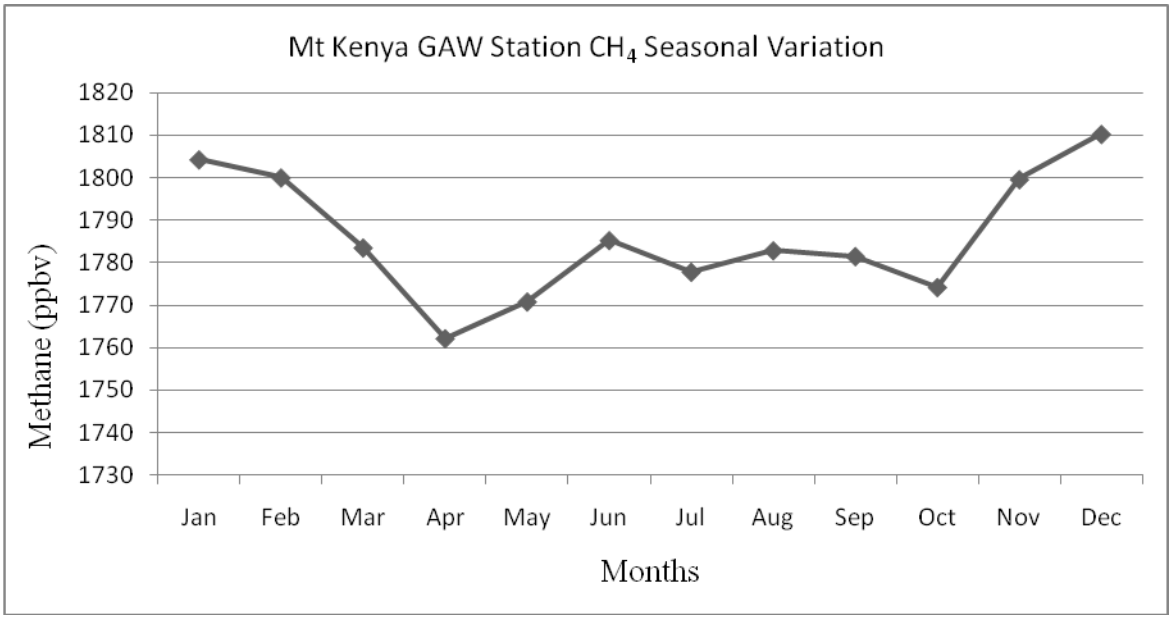

Figure 10: Seasonal cycle of Methane at the Mt Kenya GAW Station.
(Data from gas filled flasks sent to ESRL for analysis).

The Mt Kenya GAW station CO_2 amounts shown in Figure 11, has low amounts in April to August with a minimum in December. A second minimum is in July. High amounts are in January to March. This could be due to exposure to the air from the northern hemisphere. A second peak is in September to November. The amplitude of the seasonal cycle is about 4ppmv.

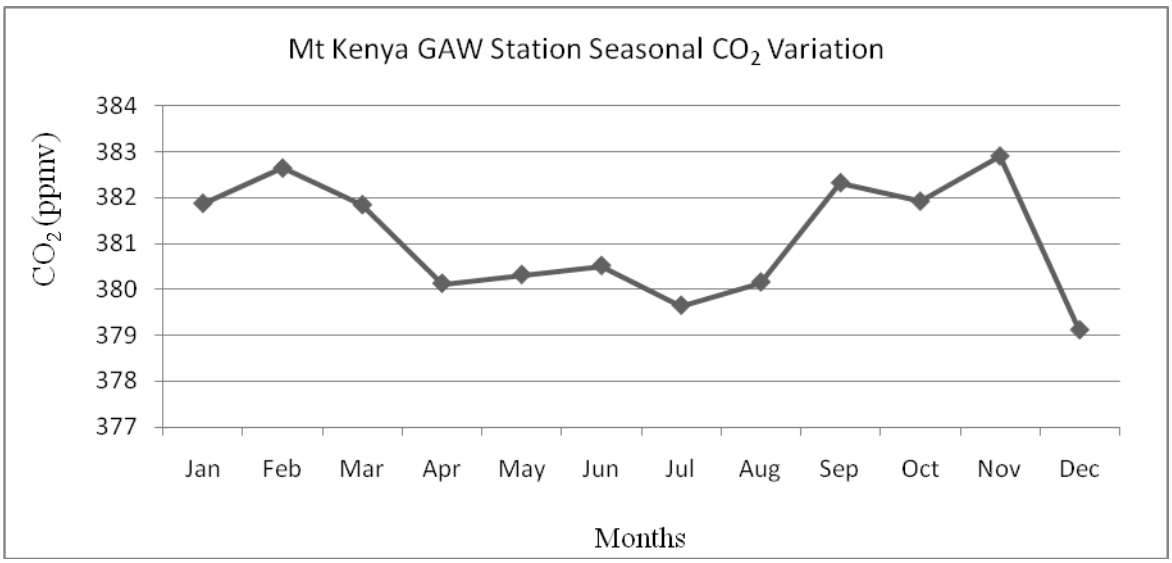

Figure 11: Seasonal Cycle of Carbon Dioxide at the Mt Kenya GAW Station

Figures 12 and 13 show the surface ozone amounts of two stations of Mt Kenya GAW and Nairobi station. The peaks are in March and September, being the time of passing of the

ITCZ, area of convergence of air before it rises. This represents a convergence of the precursor gases along with ozone to raise the concentration at these stations. One urban, Nairobi, and the other remote from human habitation. The lowest amounts are from November to December in the two stations. These two patterns are also reflected in the total column ozone in Figure16. The peaks also occur in March and September but the lowest amounts occur in January, a lag of one month. The amplitude of the seasonal cycle is about 8ppbv.

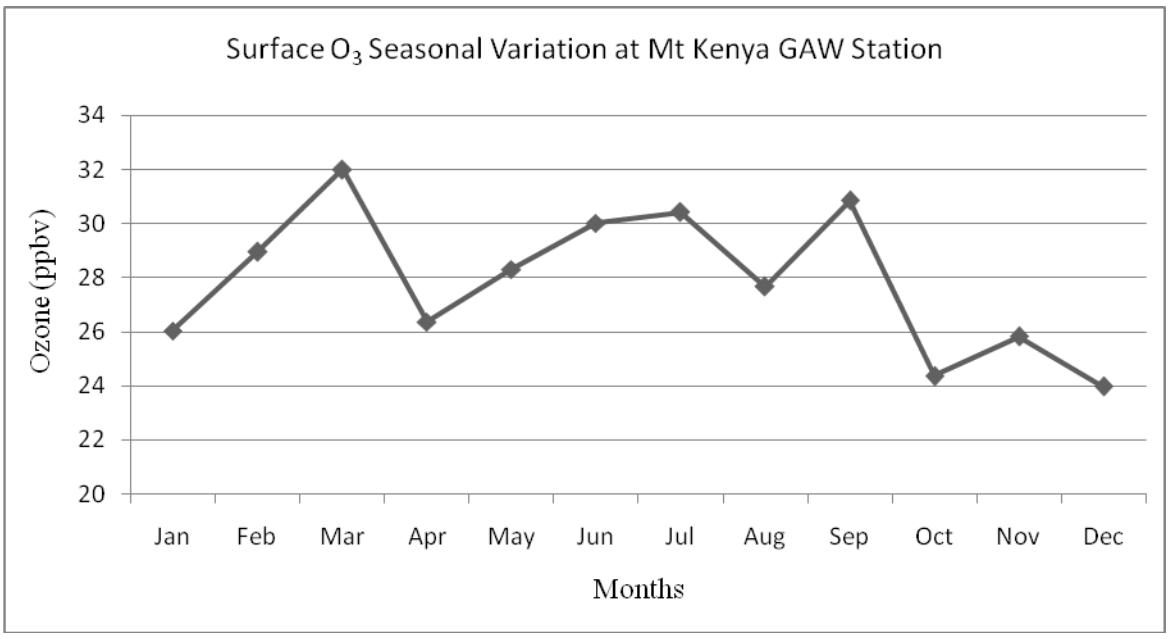

Figure 12: The seasonal Ozone amount at the Mt Kenya GAW Station

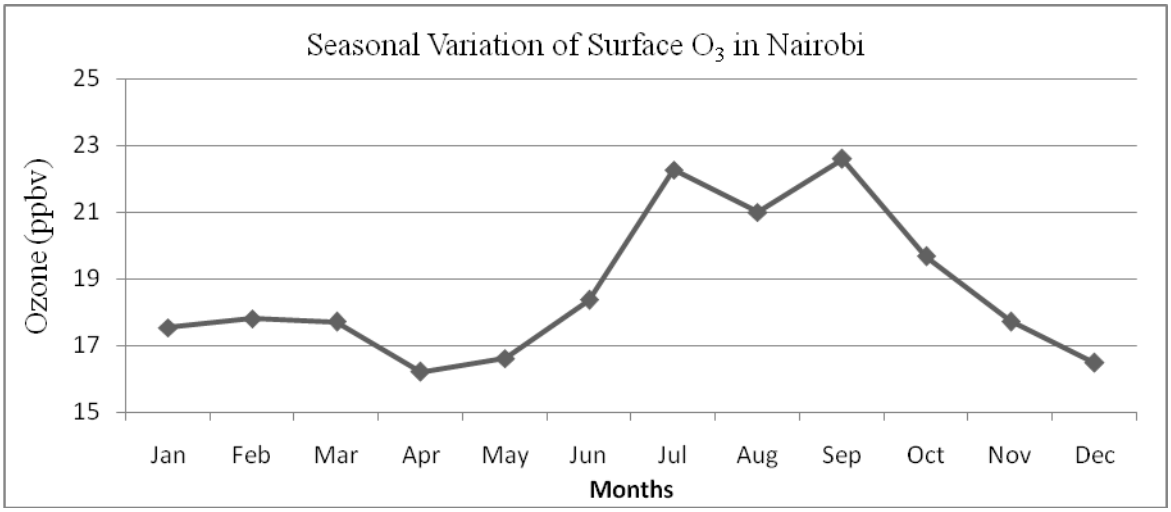

Figure 13: Seasonal Cycle of Surface Ozone in Nairobi

Though the Nairobi station has been operating for barely a year, the two stations have similar patterns and comparable concentrations. The seasonal ranges are about 8 ppbv. This

might be due to the greater influence of the large scale synoptic systems than the local systems. However Nairobi shows large diurnal range of 24 ppbv, as compared with the Mt Kenya GAW Station having a small range of about 4 ppbv as shown in Figures 15 (a) and (b).

The start of the two rainy seasons are in April and October. Sharp dip are noticable in the two months for mt Kenya GAW Station. A slight rise, peaking in July may be due to the capping of the surface air due to inversions as the air is stable during the June – July period.

The seasonal total column ozone variation is shown in Figure 14. The peaks fall on the months of the March and September coinciding with the passage of the overhead sun over station. The surface convergence brought about by the ITCZ accounts for this. However the September peak is higher than in March. The sun is marching south and more continental air convergences at the station. A minimum occurs in January and a second minimum is in June. The amplitude of the seasonal cycle is about 8 DU.

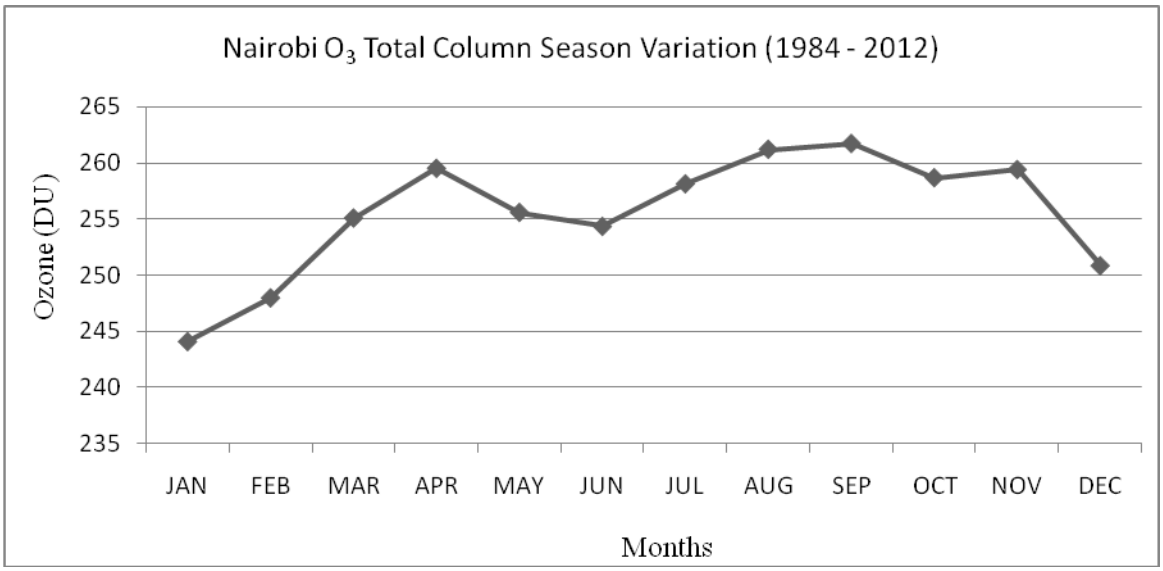

Figure 14: The Seasonal Cycle of Total Column Ozone in Nairobi

Surface ozone diurnal cycles shown in Figures 15(a) and 15(b). These cycles are different form each other. Figure 15(a) for Mt Kenya GAW station has peaks at night and dip during the day, reaching a minimum at 15UTC; 6pm local time. This is consistent with the findings of Henne *et al*. (2007) and (2008). This dip could be due to the behavior of the thermally influenced air increasing the mixing and dilution of ozone. At night fall the amount of ozone rises, largely due to lack of strong mixing and also due to the subsiding cold air bringing in the ozone rich air aloft.

On the other hand, the Nairobi station is in a large metropolis and ozone peaks during the day but dips as the sun sets at 16 UTC. It remains low throughout the night. Sunlight must be playing a big role in the process of accumulation of ozone during the day; with a peak at 1pm local time. The presence of precursor gases that are emitted by the industries and motor vehicle are converted to ozone in the presence of sunlight. The reactions take the form given by the equations 2 and 3 given in Section 2.2.

Nairobi has a large diurnal range of about 24 ppbv whereas at the Mt Kenya GAW the range is about a third that of Nairobi; 8 ppb. The amplitude of the seasonal cycle is about 4ppmv

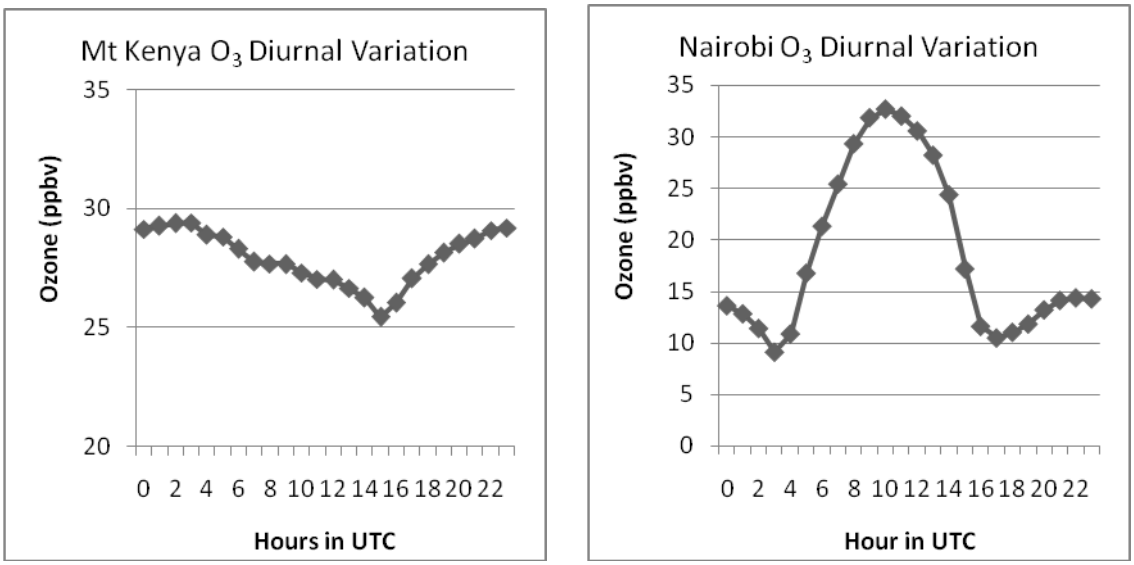

(a) (b)

Figure 15: Surface ozone diurnal cycles for (a) Mt Kenya GAW station and (b) Nairobi

The trend analysis for the Mt Kenya GAW station ozone data was undertaken for each month. The resultant slopes as shown in Figures 16 to 17 were tested for significance at 95% confidence level but were found not to be significant.

Table 2: Student t-test on the trends of surface Ozone at Mt Kenya GAW Station

	JAN	FEB	MAR	APR	MAY	JUN	JUL	AUG	SEP	OCT	NOV	DEC
standard error of slope	0.13	0.17	0.20	0.18	0.18	0.19	0.17	0.13	0.23	0.18	0.29	0.20
degrees of freedom	7	6	7	6	7	7	6	5	5	6	5	7
t value testing slope =0	1.55	-1.7	-0.2	-1.1	-1.8	-0.1	0.52	1.05	-0.5	-0.6	-0.3	-0.2
Highest significance level (%)	16.6	13.7	84.2	33.1	11.5	93.5	62.0	34.2	62.4	55.3	79.4	84.1
R squared	0.25	0.33	0.01	0.16	0.32	0	0.04	0.18	0.05	0.06	0.02	0.01

The slopes are rising for January, July, August, and December. It is note worthy here that the air circulation over Kenya in the July- August period is mainly a recirculation within the county and that less air is injected in from the sources outside the country as is seen in the trajectory analyses. This is also consistent with the findings of Gatebe *et al*. (1999).

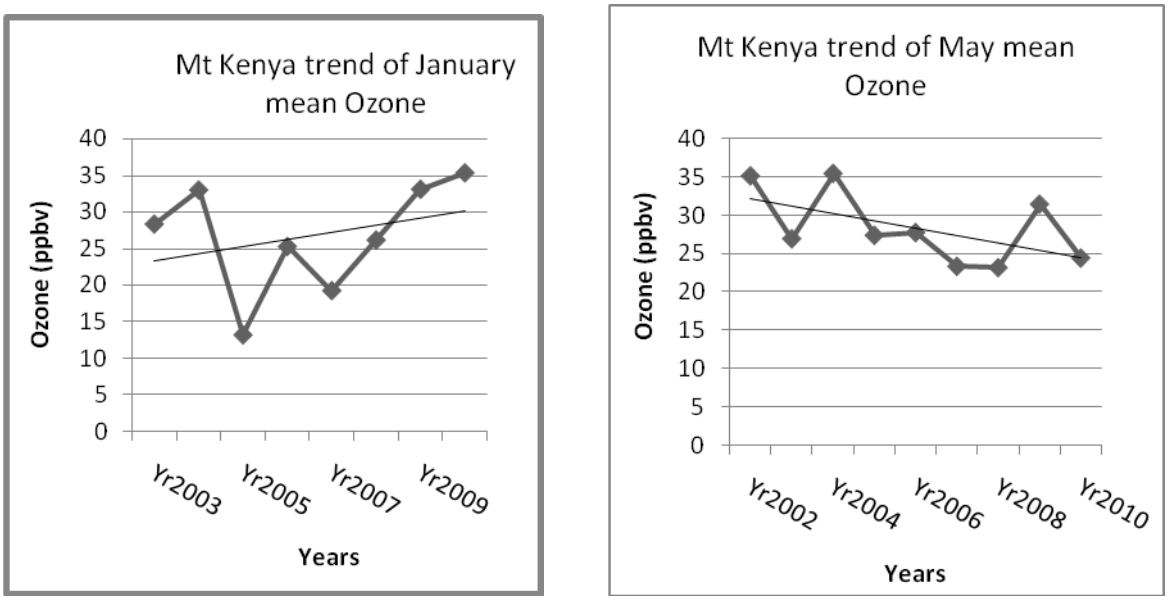

(a) (b)

Figure 16: The trend for the Mt Kenya surface ozone for (a) January and (b) May

From February to May, September to November there is a decreasing trend of ozone, while that for June is stationary. Combining all these scenarios, there is no significant change on the ozone trend in Mt Kenya. One can also deduce this in the time series shown in Figure 6.

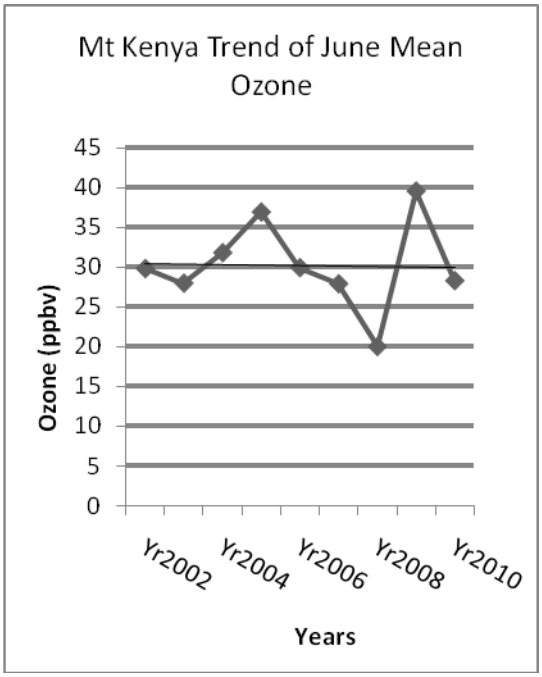

(a)

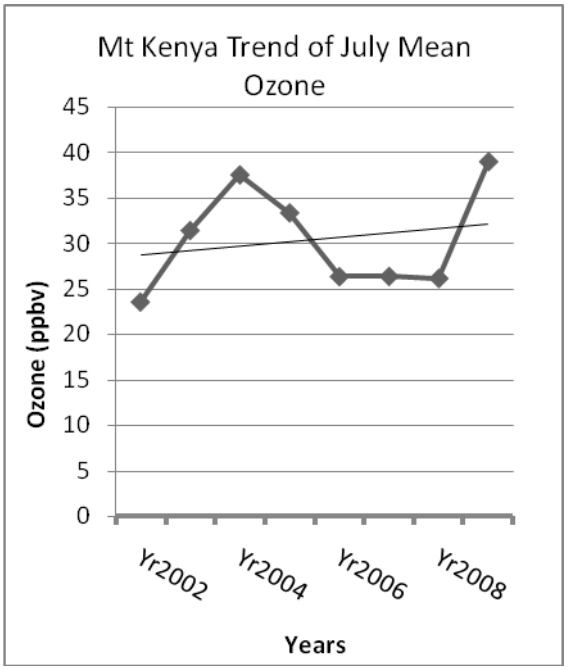

(b)

Figure 17: The trend for the Mt Kenya surface ozone for (a) June and (c) July

4.2.1 Results from Correlations and Significance Tests

The mean monthly CO_2 concentrations; column averaged dry air mole fraction and surface were compared. Figure 18 below shows the curves for the amounts from the flask sampling and the satellite observations. They are close but the correlation coefficient is 0.413 and was not found to be statistically significant at 95% confidence level, using the Student's T - test. The data used here were for only one year, as was released by GOSAT.

However other studies in Japan by Cogan *et al*. (2012) who compared the satellite observed column- averaged CO_2 and the in situ measurements found a high correlation of about 0.75 and mean differences of 0.1 ppm.

Data sets for a longer period may present an improved correlation coefficient. The data points presented here were only twelve. Further analysis need to done with more data in the near future.

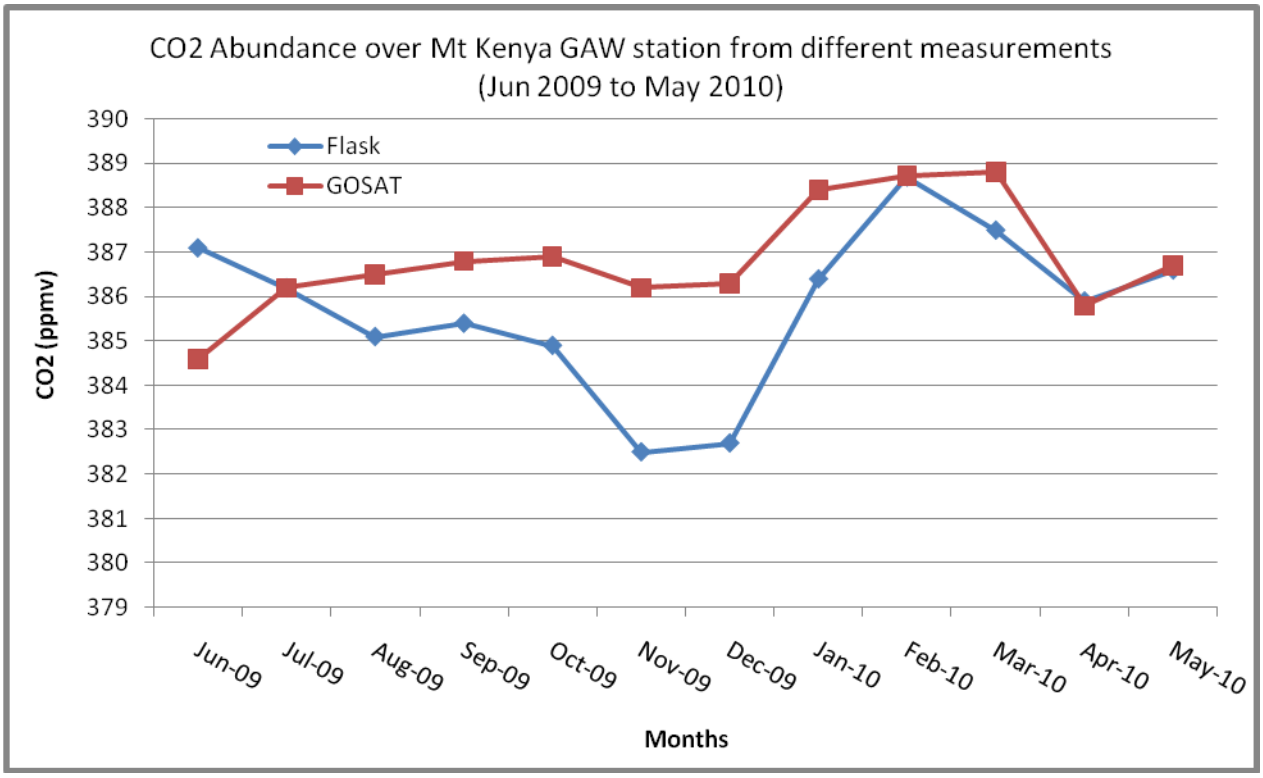

Figure 18: Comparison of CO_2 concentrations from the GOSAT satellite and that from the air flask samples at the Mt Kenya GAW station.

4.3 SPATIAL AND TEMPORAL DISTRIBUTIONS

The spatial distributions of CO_2 over the country are discussed under the column abundance, as a flux derived from fossil fuel, from the biosphere flux and when optimization has been done.

4.3.1 CO_2 Spatial Distributions

The general pattern of the spatial distribution of CO_2 over the country is consistent with the movement of the ITCZ, the overhead sun and the plants activity or emergence. Figures 19 to 22 show the CO_2 abundance over the country averaged over the month.

The higher concentrations are to the west especially between June and October as shown in Figures 19 to 20. The eastern parts of the country have lower concentrations than the west and south west. This could be due to the proximity of the Indian Ocean to the east. Oceans are natural sinks of CO_2. Air blowing over the Ocean into the Country brings in less CO_2

across the eastern parts. A good convergence occurs in September and October, during the passage of the overhead sun, raising the levels of CO_2 in the Country.

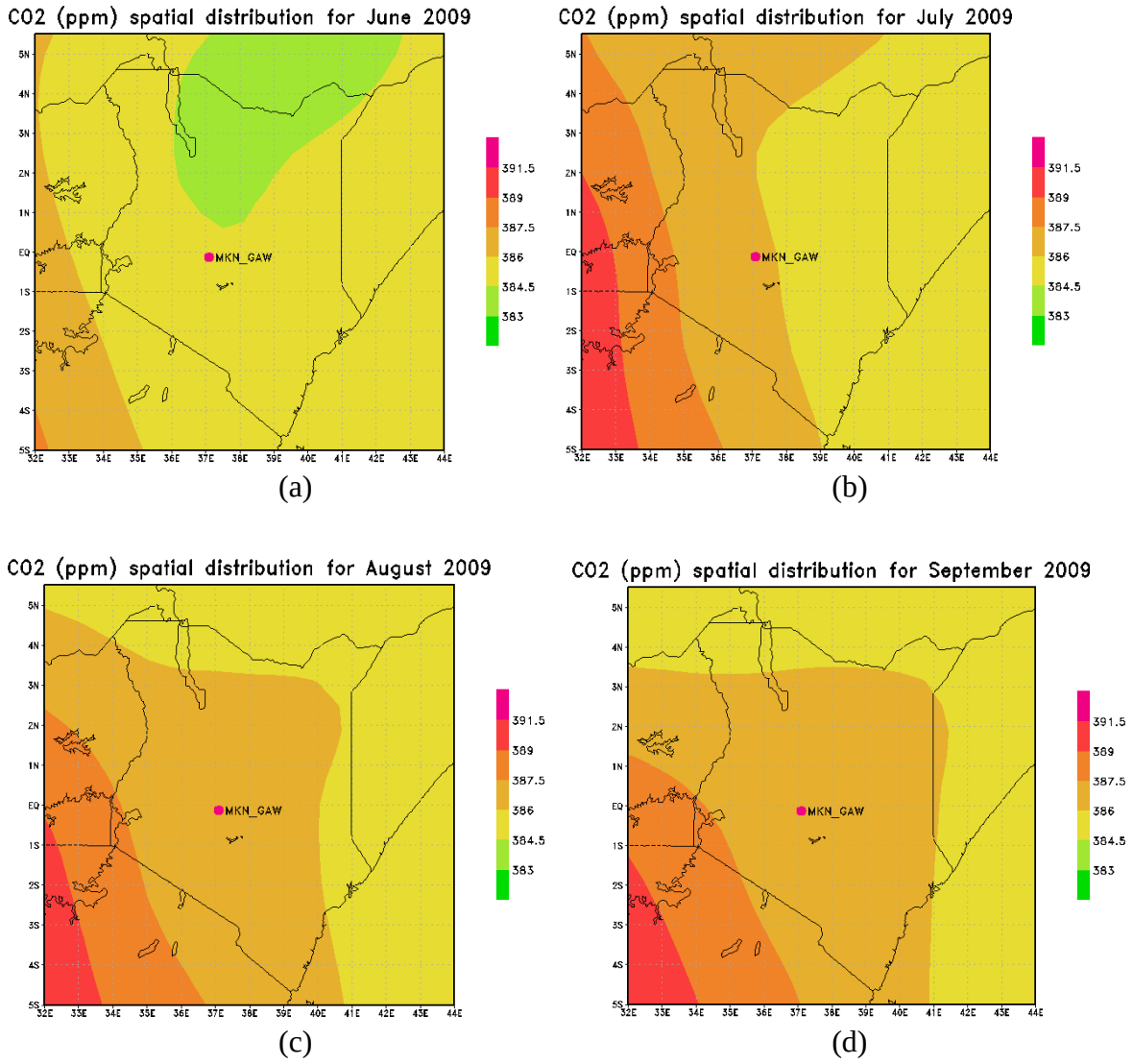

Figure 19: The Spatial distributions of CO_2 over Kenya in year 2009: (a) June, (b) July, (c) August and (d) September. (Data from GOSAT)

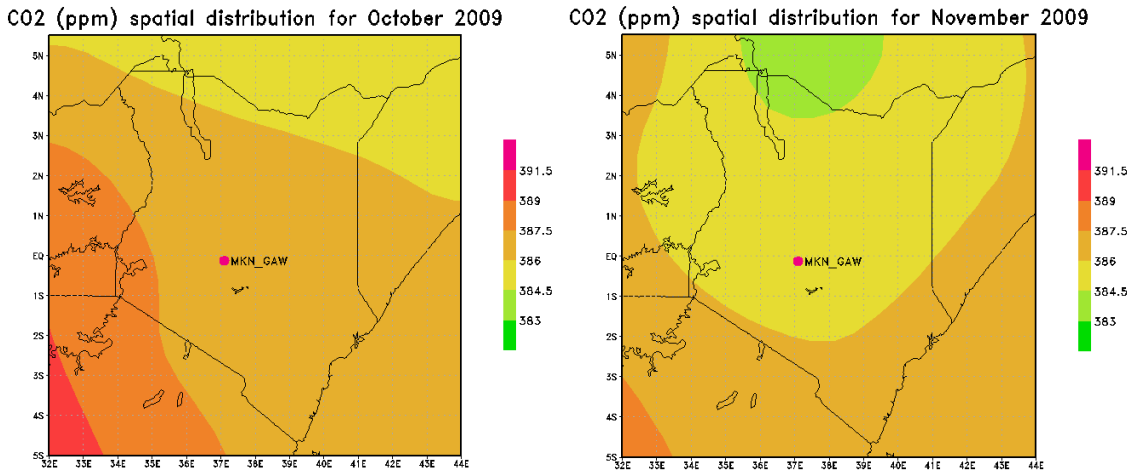

(a) (b)

Figure 20: The spatial distribution of CO_2 over Kenya in year 2009 (a) October and (b) November.

In November and December, as shown in Figures 20 (b) and 21 (a), the concentrations are especially low in the country, particularly in the central parts. Higher concentrations set in from January and persist to March, as is shown in Figures 21(b) to 21(d), but the lower concentrations shift south gradually.

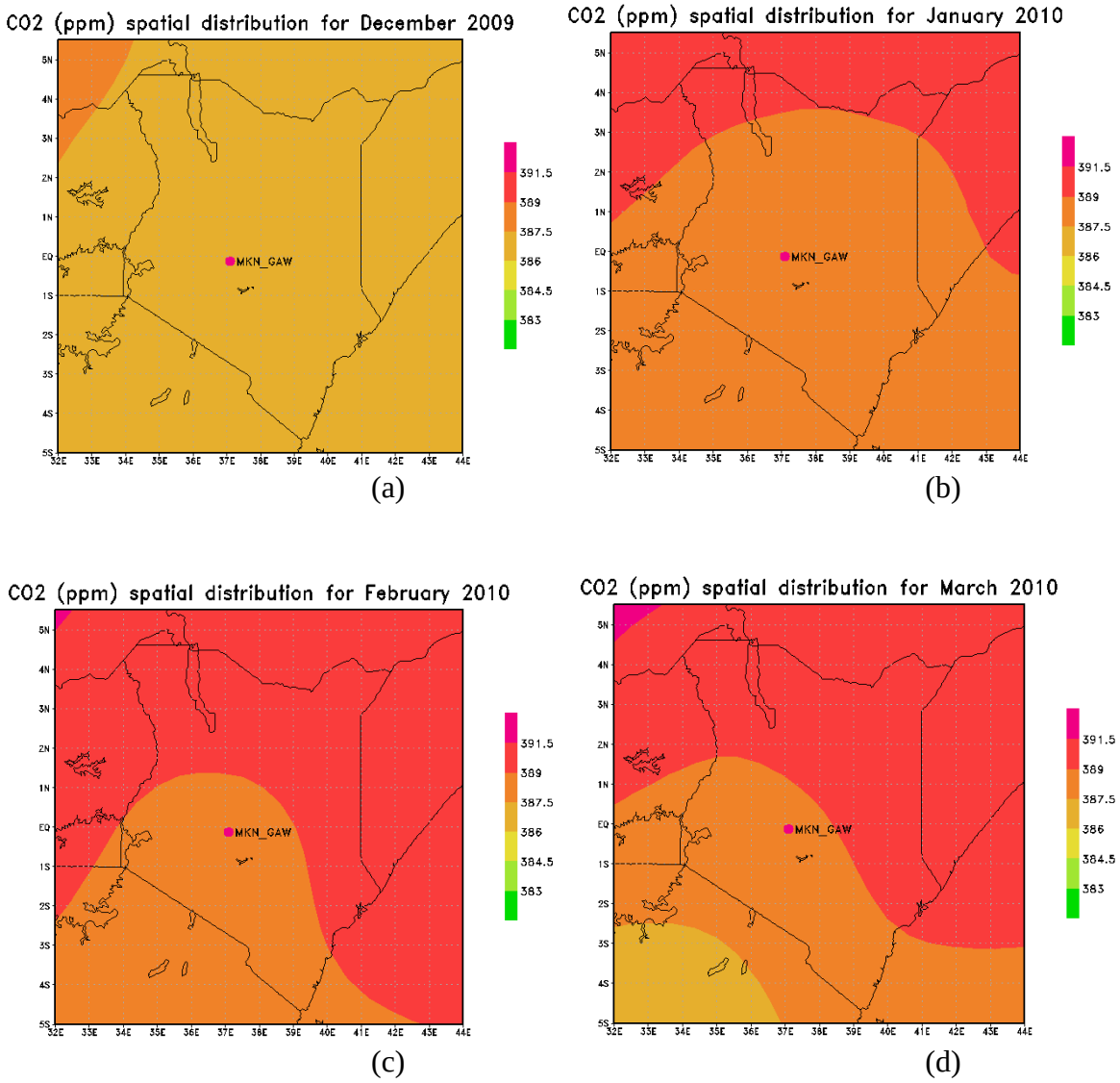

Figure 21: The spatial distribution of CO_2 over Kenya in (a) December 2009, (b) January 2010 (c) February 2010 and (d) March 2010.

In April and May the low concentrations are on the southern half of the country while the north western has higher concentrations. See Figure 22(b). This marks the transition to the June- October scenario described above.

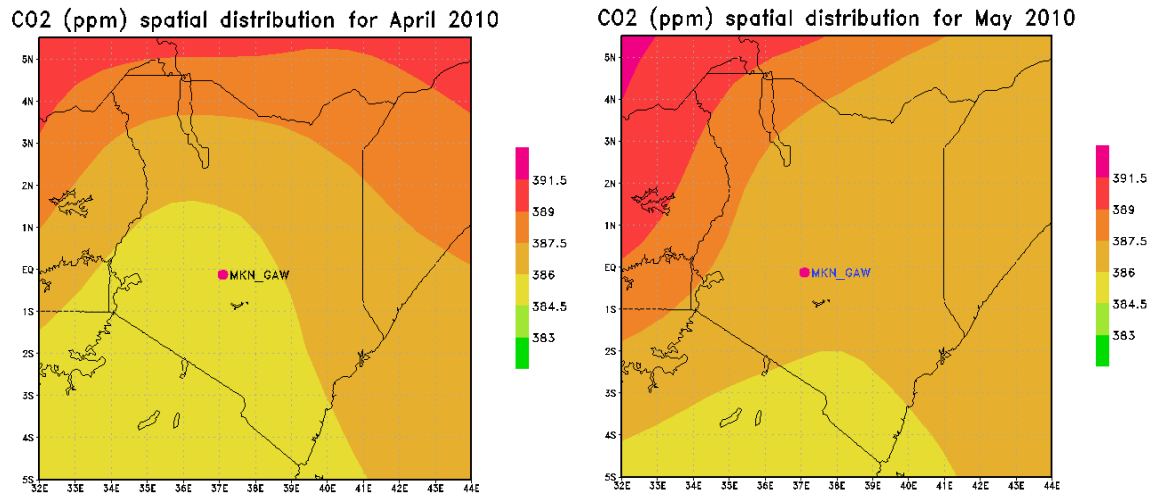

Figure 22: The spatial distribution of CO_2 over Kenya in year 2010: (a) April and (b) May

4.3.2 CO_2 Flux from Fossil Fuel

The Carbon dioxide flux from the fossil fuels and the biosphere were also shown over the Country with the spatial maps showing the counties by use of ArcView GIS software. A brief discussion is given here for the CO_2 flux from fossil fuel as all the maps, represented by Figure 23 which shows the same features. There was little change in the amounts shown over the one year period of observation.

Nairobi County in Central Kenya stands out as the major source of CO_2 flux from fossil fuels. This may be due to the proportion of vehicular traffic in Nairobi and the number of industries. Another part of the country where some amounts were also discernable was in Mombasa at the coast. This area is known for the cement manufacture and oil refining with some vehicular traffic. These results are consistent with the investigations done in Europe (Sternad *et al*. 2010) which also showed that high CO_2 amounts were emitted even in small cities and towns from cars.

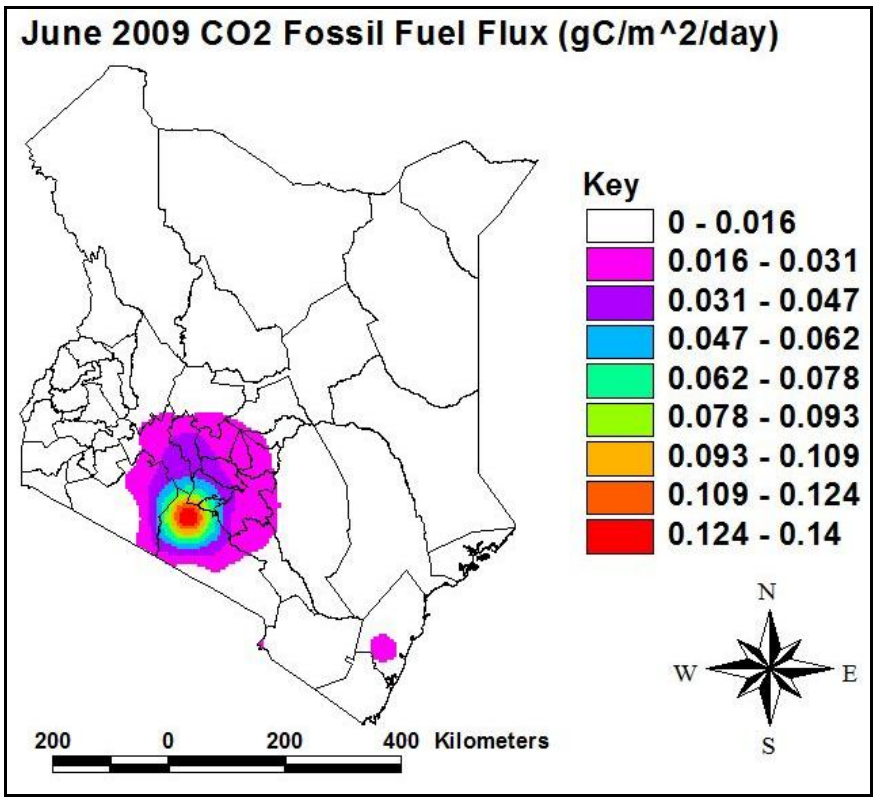

(a)

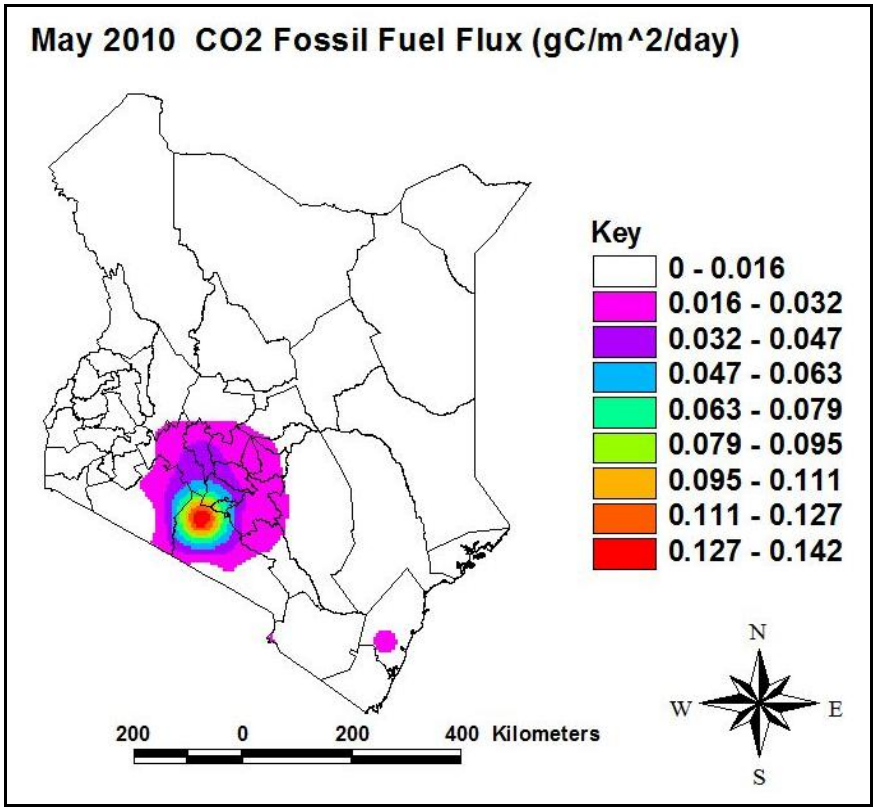

(b)

Figure 23: The CO_2 Fossil fuel flux for Kenya in (a) June 2009 and (b) May 2010. (Data from GOSAT)

4.3.3 CO_2 Flux from the Biosphere

The biosphere responds to the performance of the seasons (Earth System Research Laboratory, 2013) and according to the studies done in the Amazon forest (Arau´jo *et al*., 2002), in particular rainfall in the tropics. There is a lowering of the CO_2 fluxes during the dry season and that the seasonal variation is little.

During the year 2009, a relatively dry period occurred between June and September which was more severe over eastern Kenya than at the areas west of Mt Kenya GAW station, as shown in Figures 24 and 25. The Figures show the accumulated rainfall in five stations. The stations to the east of the Mt Kenya GAW Station are shown in Figure 24 and those to the west are in Figure 25. When these two figures are compared, the eastern stations were particularly dry from June to September 2009 and only two stations, Embu and Meru had some rain in January 2010. Some rain was experienced in the stations west of the Mt Kenya GAW Station, Figure 25, in June to September 2009. This was not much when compared with the other months.

These rainfall deficits are reflected in the CO_2 biosphere flux for the corresponding months. In Figure 24, three dry spells were experienced in Garissa and Wajir in the periods of November 2009, January and February 2010 and May 2010.

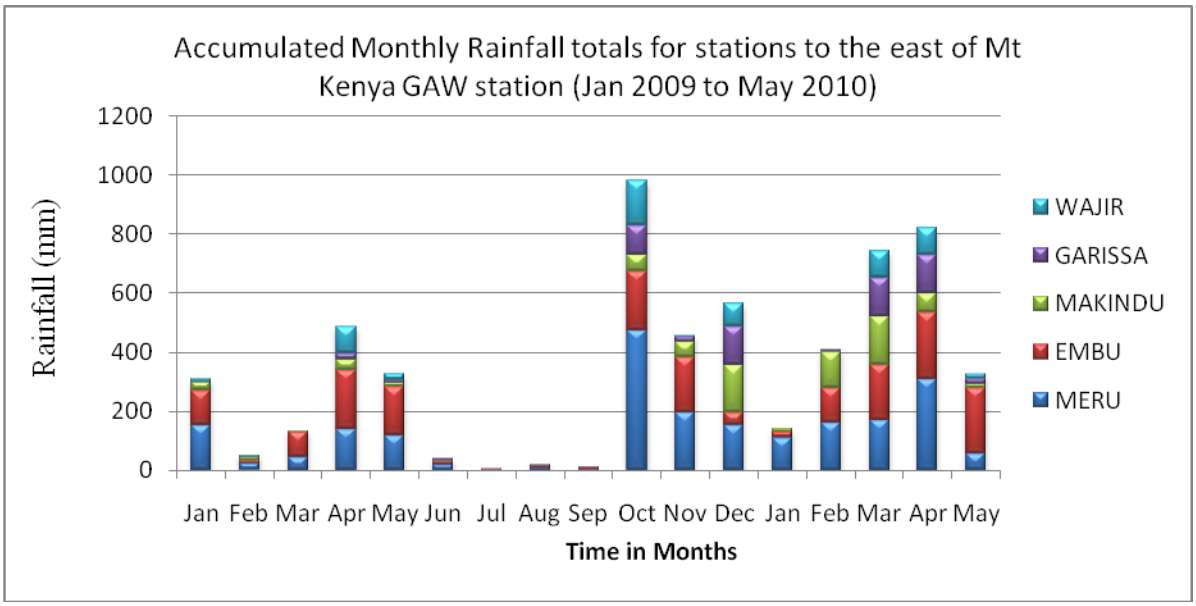

Figure 24: Accumulated monthly rainfall for some meteorological stations to the east of the Mt Kenya GAW station between January 2009 and May 2010

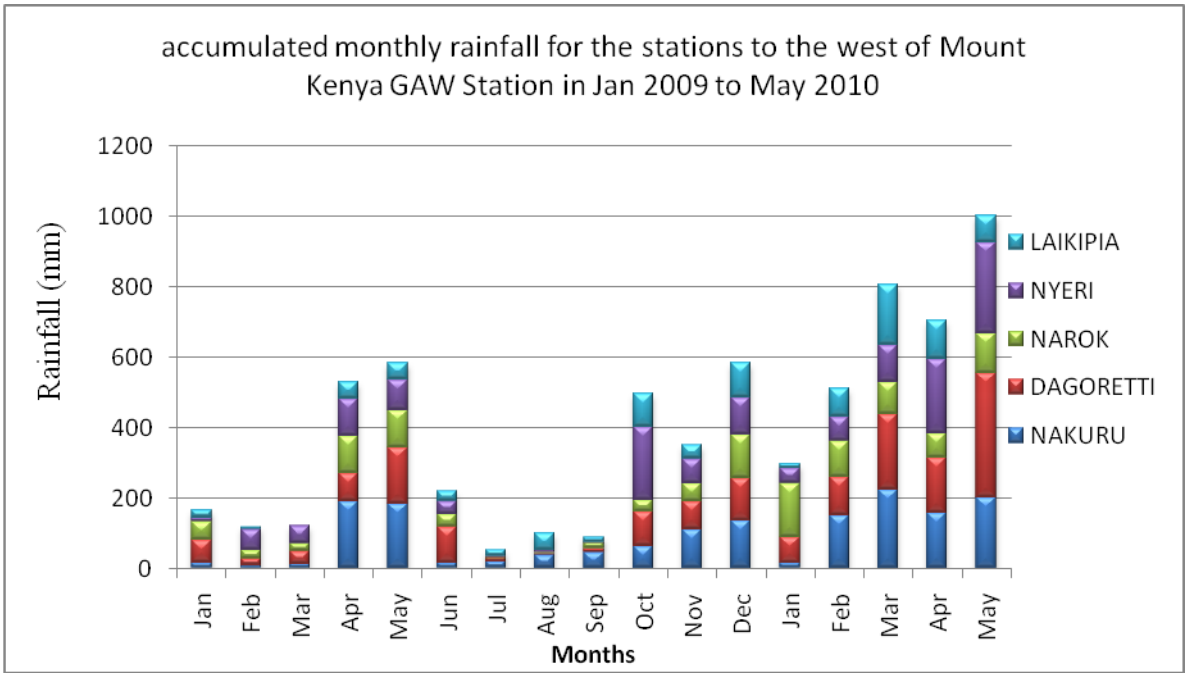

Figure 25: Accumulated monthly rainfall for some meteorological stations to the west of Mt Kenya GAW station between January 2009 and May 2010.

The biosphere fluxes from CO_2 are shown in Figures 26 to 30. The dry period corresponds to Figures 28 (a) and 28 (b). The fluxes were remarkably reduced and even reversed during this period. Other Figures are in the appendices (Figures 42 and 43).

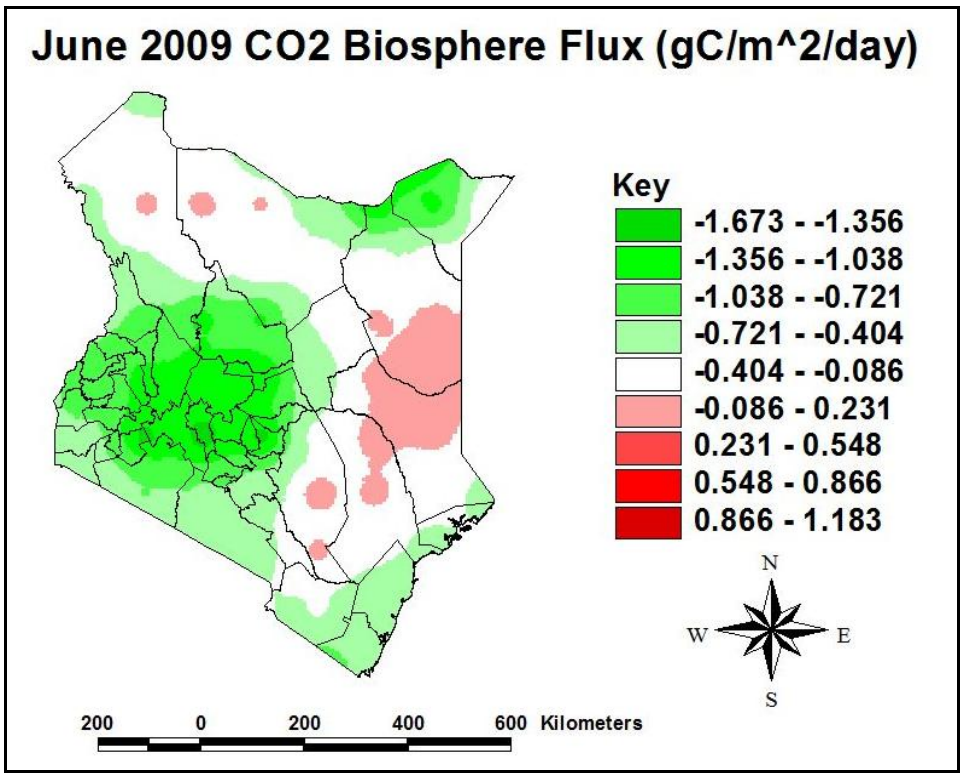

(a)

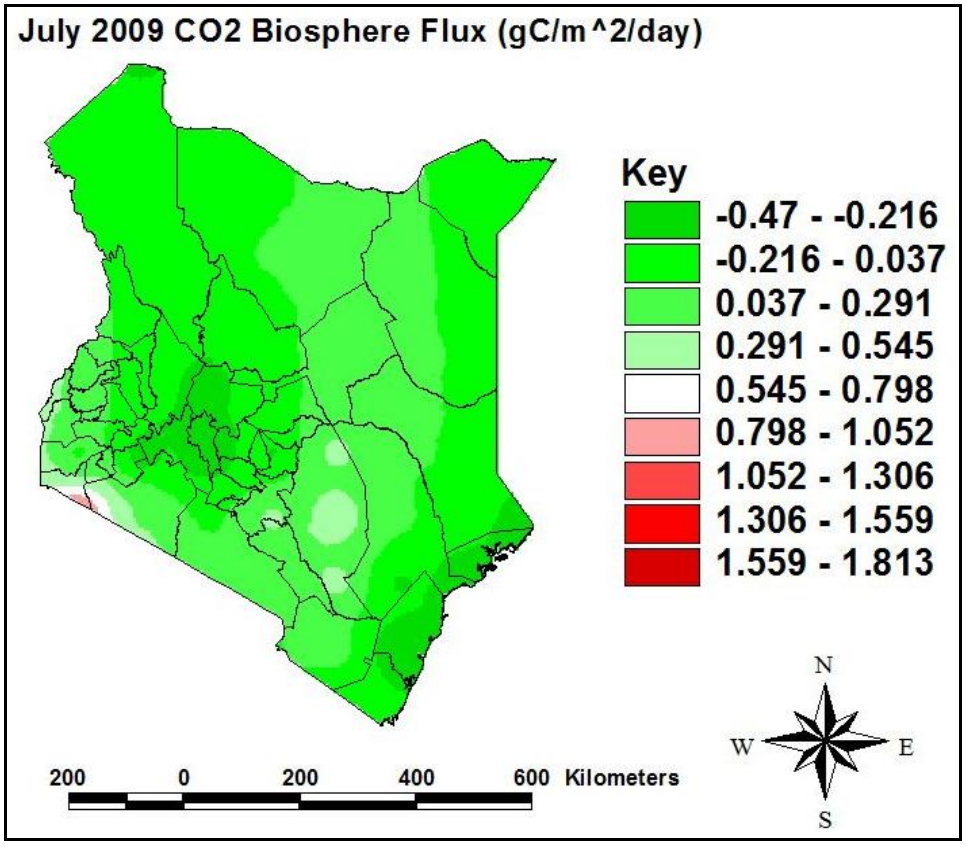

(b)

Figure 26: CO_2 Biosphere flux in Kenya for year 2009 (a) June and (b) July. (Data from GOSAT)

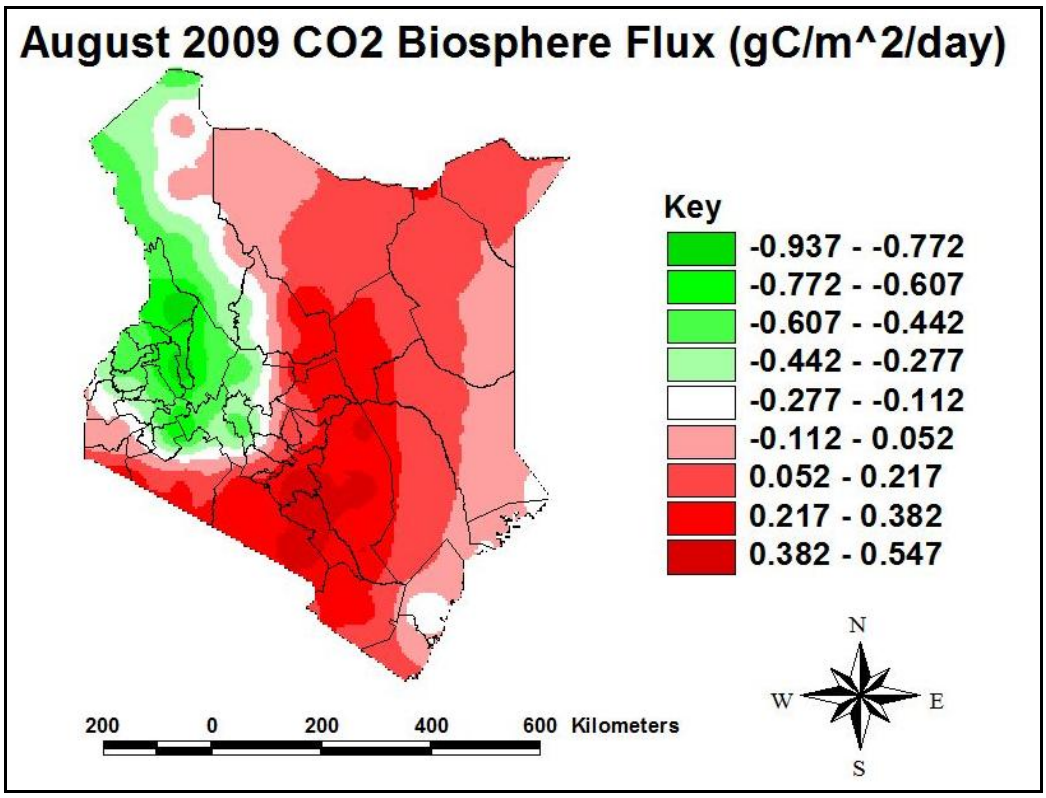

(a)

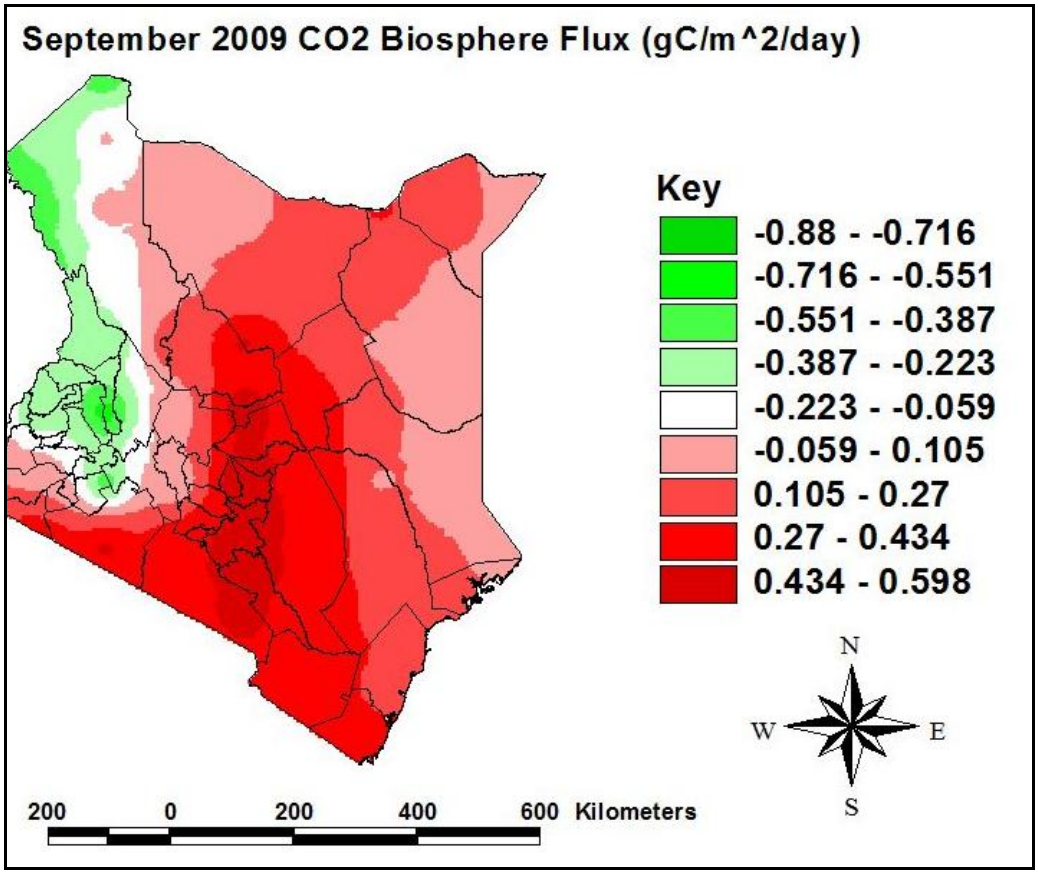

(b)

Figure 27: CO_2 Biosphere flux in Kenya for year 2009 (a) August and (b) September.

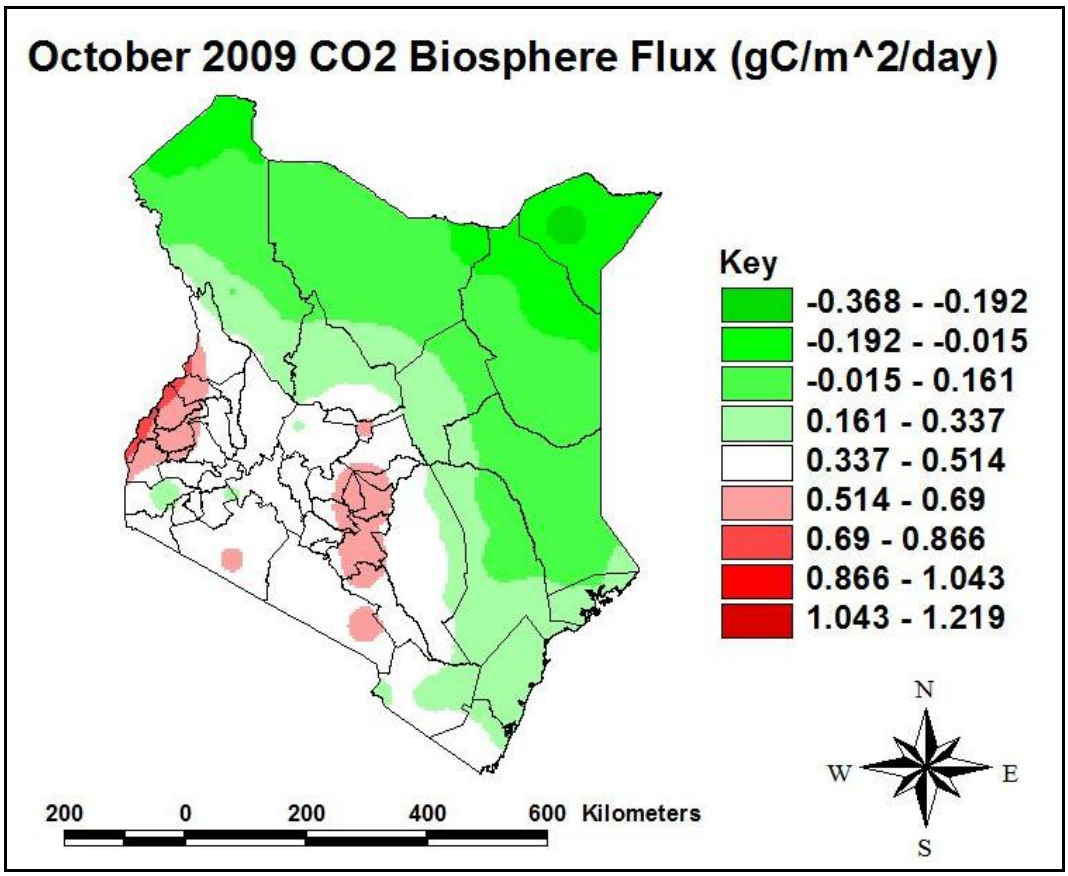

Figure 28: CO_2 Biosphere flux in Kenya for October 2009

Further, three dry spells were recorded over the two stations of Wajir and Garissa in November 2009, between January and February 2010 and also in May. The biosphere flux also responded accordingly near these stations. These are shown in Figures 29 and 30. The flux was higher at these stations periods than before for the area. These results are consistent with the findings of Arau'jo *et al*. (2002).

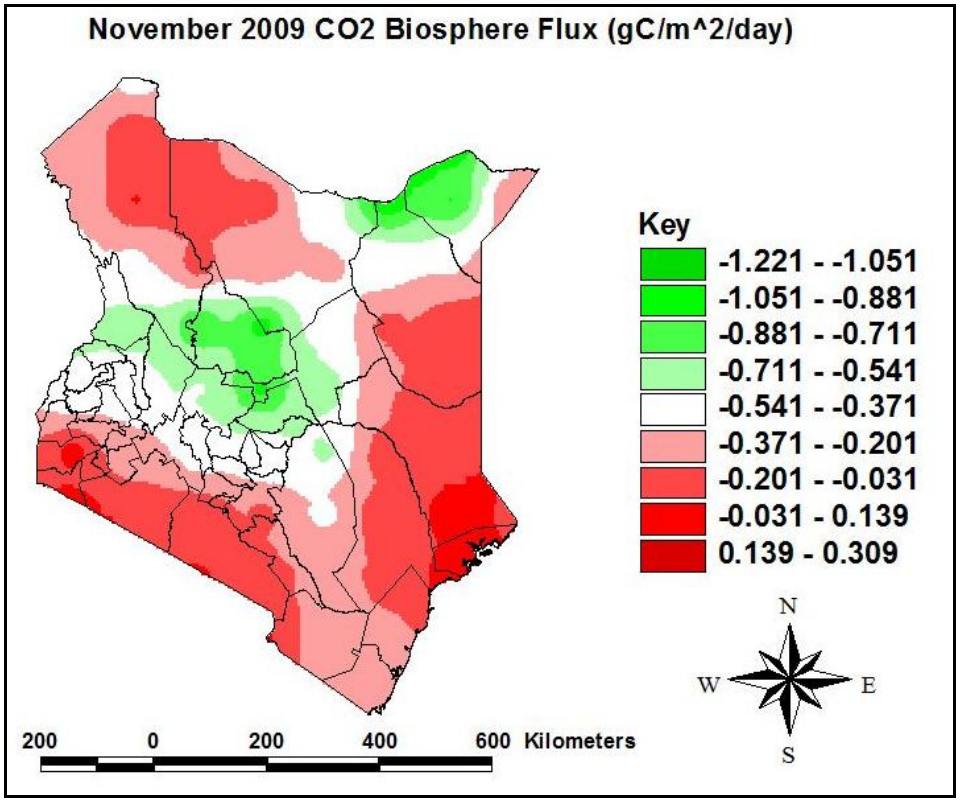

(a)

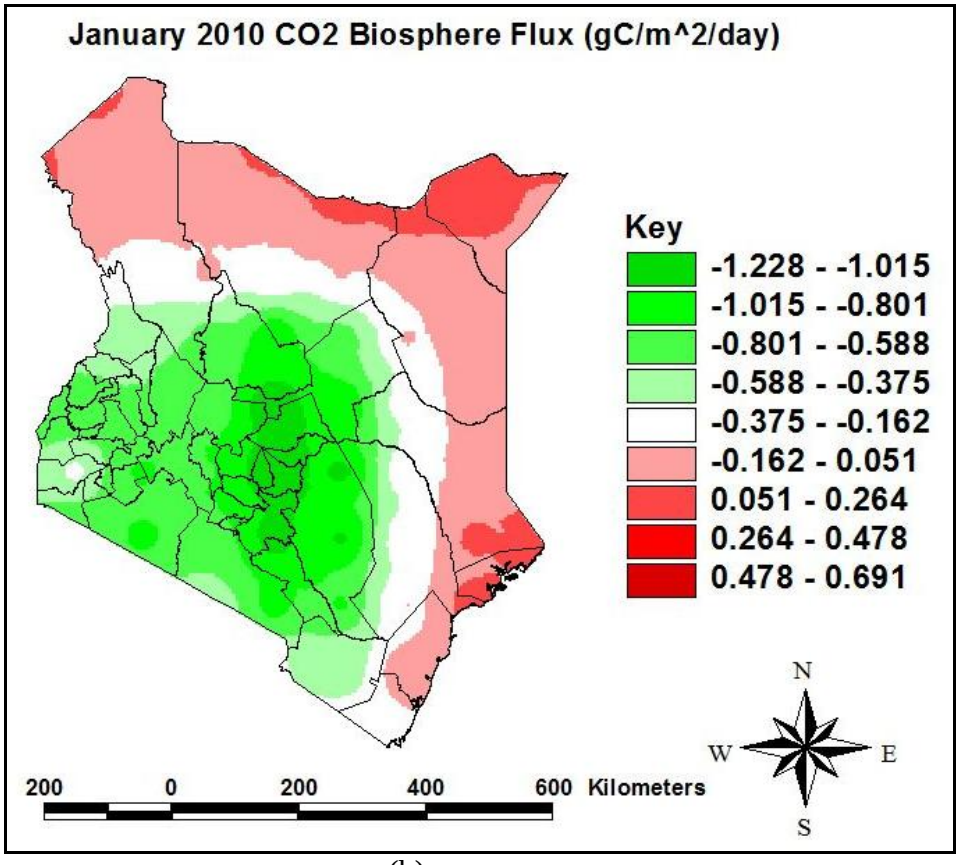

(b)

Figure 29: CO_2 Biosphere flux in Kenya for (a) November 2009 and (b) January 2010.

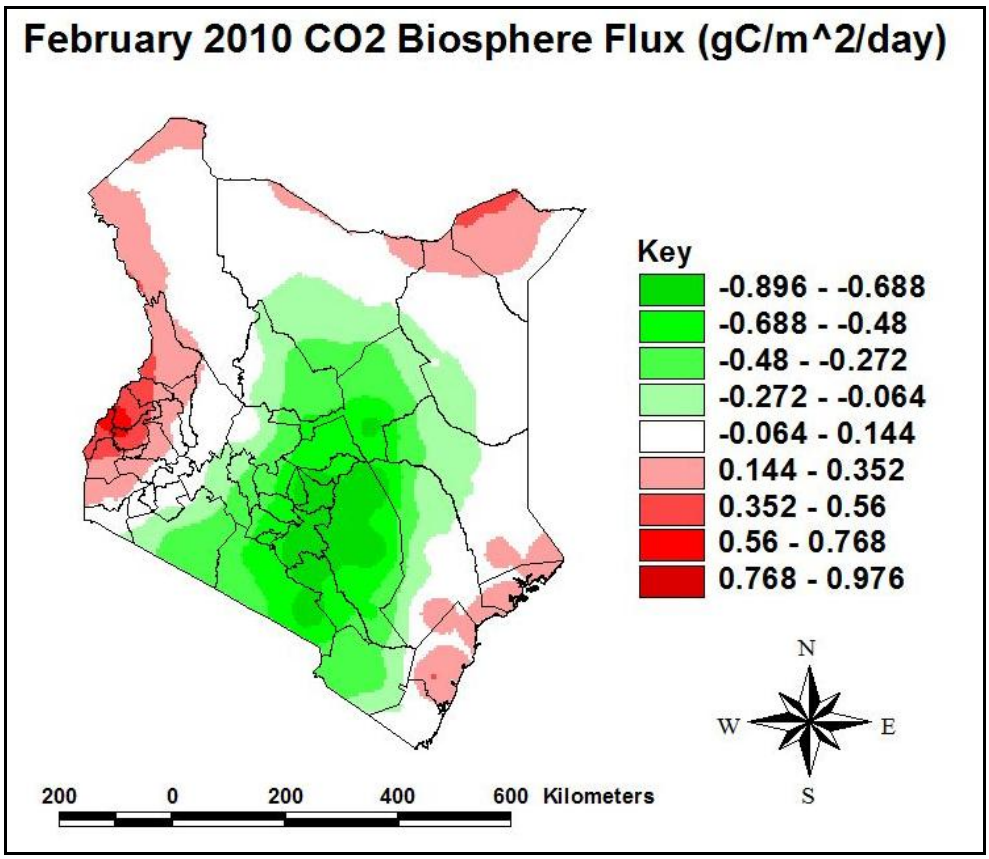

(a)

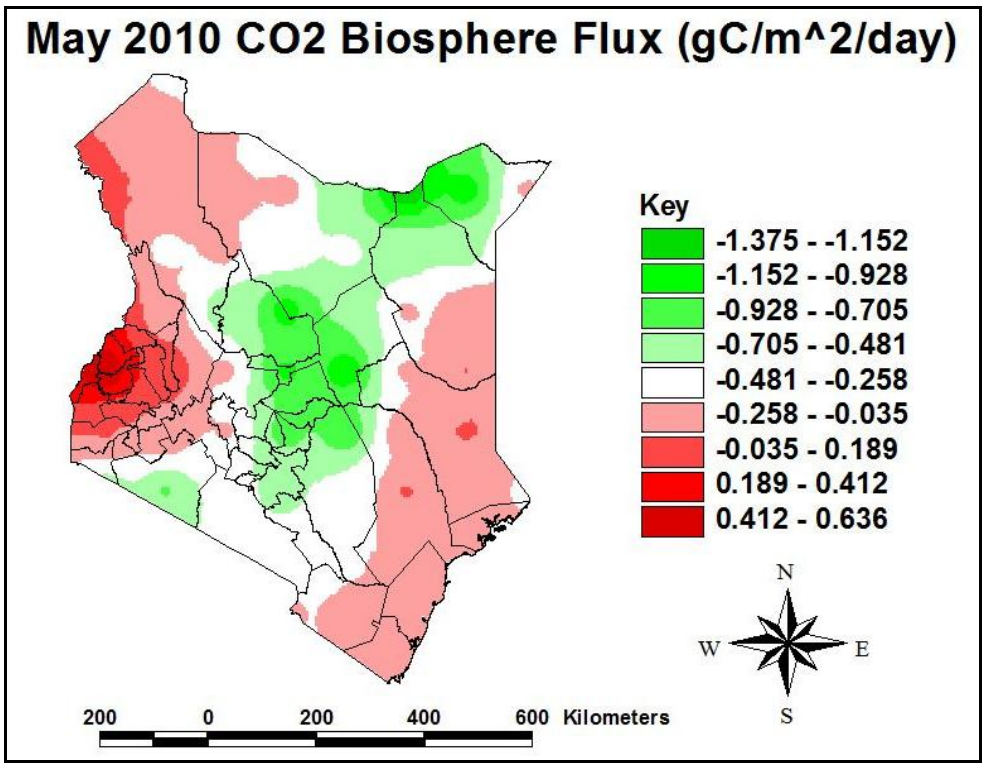

(b)

Figure 30: CO_2 Biosphere flux in Kenya for year 2010 (a) January and (b) February.

4.3.4 CO_2 Optimized Flux

The results from the optimized CO_2 flux are presented in the diagrams shown in Figures 31 and 32. Optimization results from minimizing the model outputs with the in situ observations. In general the results show that the fluxes follow the rainfall patterns with July, mostly being a cool month.

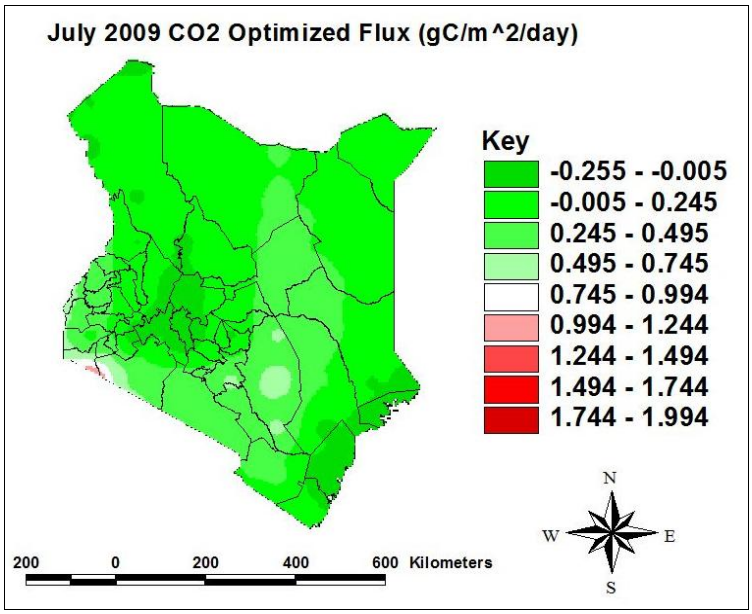

(a)

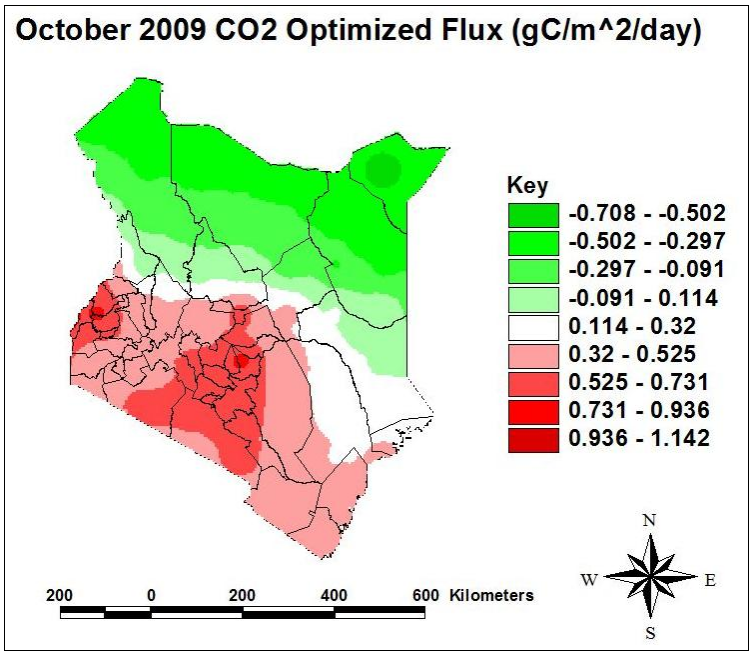

(b)

Figure 31: CO_2 Optimized flux in Kenya in 2009 (a) June and (b) October.

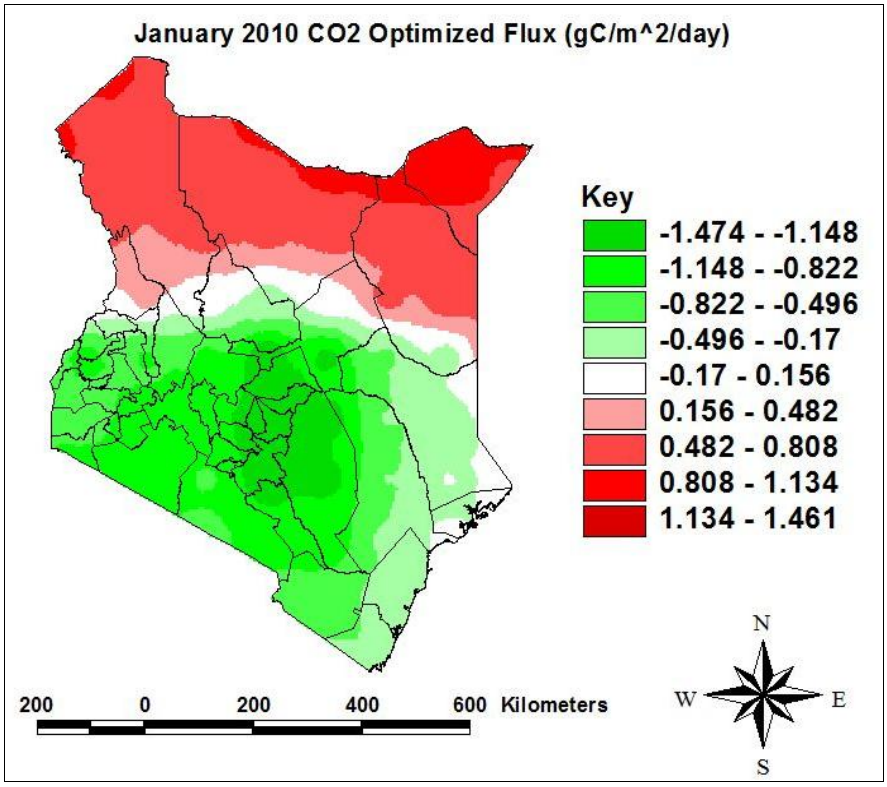

(a)

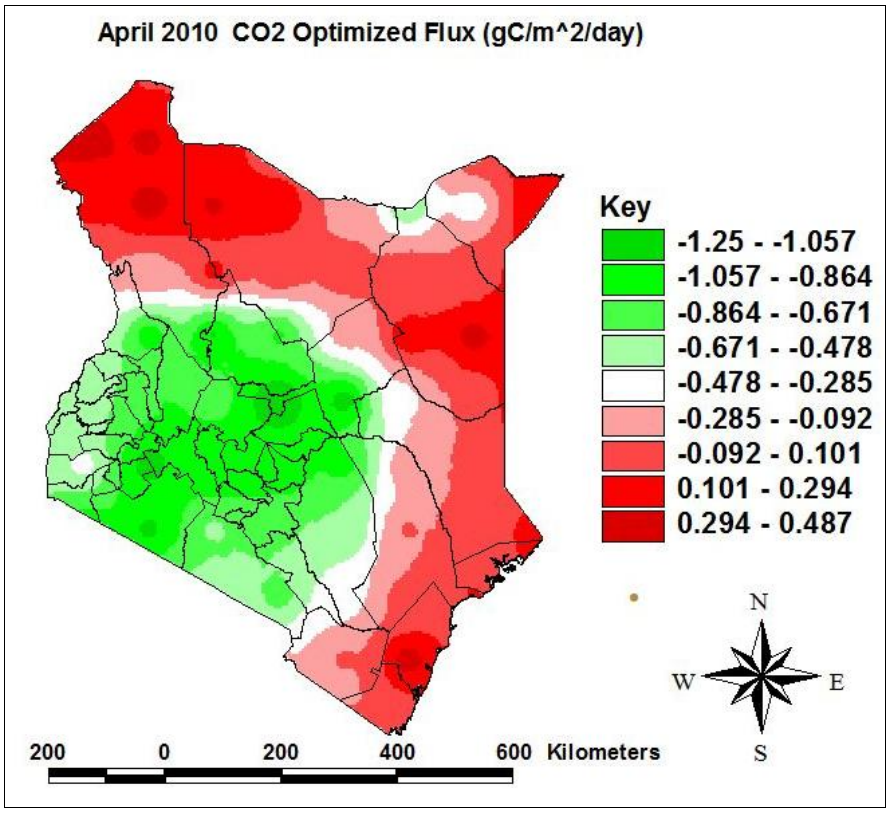

(b)

Figure 32: CO_2 Optimized flux in Kenya for 2010 (a) January and (b) April.

4.4 RESULTS FROM TRAJECTORY ANALYSIS

Trajectory analysis is discussed in the four sub-sections below under back-trajectories, forward- trajectories and trajectory clusters. These trajectories are for some 15 diverse months spanning the years 2005 to 2008. All the months of the year were considered.

There are six characteristic flows to the country as shown from Figures 37 to 38. These flows occur during different seasons of the year. The discussions are presented below.

4.4.1 Selection of start/ end time of trajectories

As discussed in section 3.2.5 the choice is determined from the time series plots of surface ozone at Mt Kenya GAW station. A sudden sustained fall or rise of ozone amounts is taken as an indicator of a changed source region characteristics. Such times where identified as shown in Figure 33 below. The time series plots were done monthly with one minute averaged data. One day has 1440 minutes.

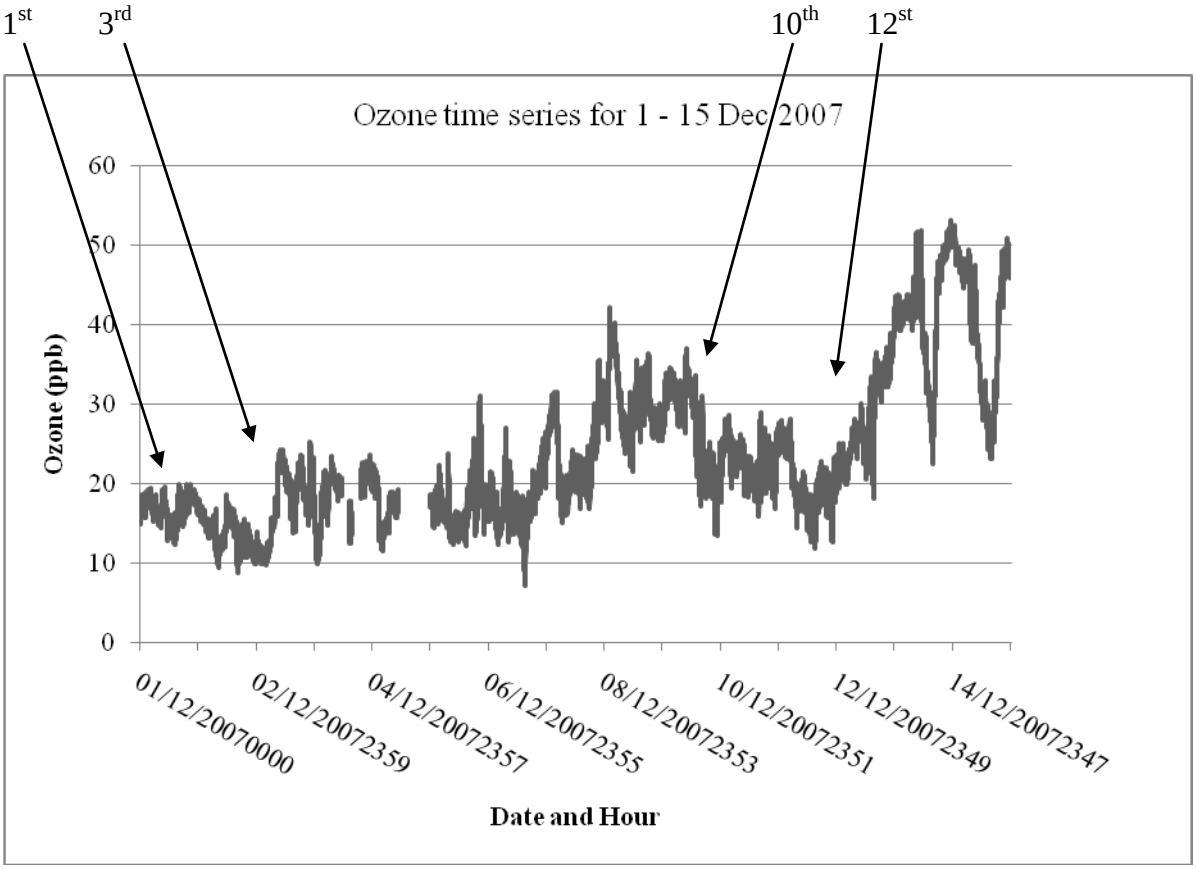

Figure 33: Time series plot for Surface Ozone for Mt Kenya GAW Station for December 2007 showing the various dates when back trajectories were terminating at the station

The resultant back trajectories over five days, using the HYSPLIT model to locate, the possible source regions for the surface ozone for the corresponding dates and hours are as shown in Figures 34 (a) to 34(d).

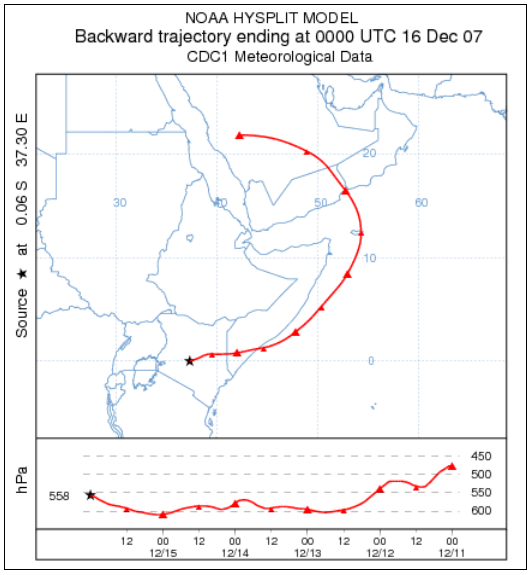

(a)

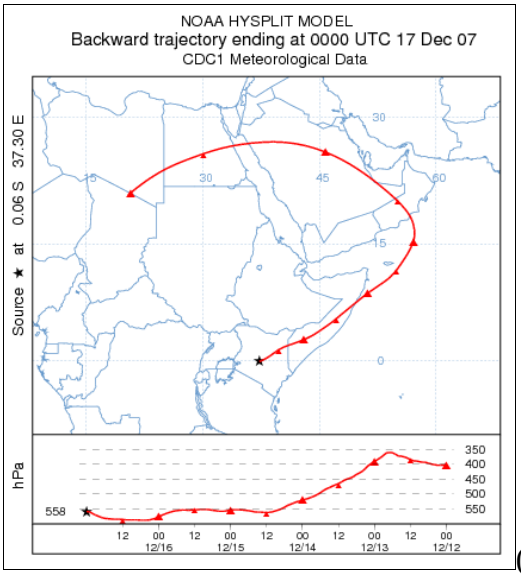

(b)

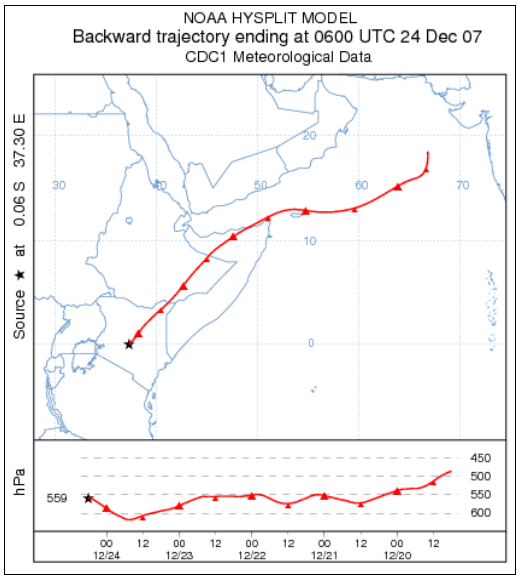

(c)

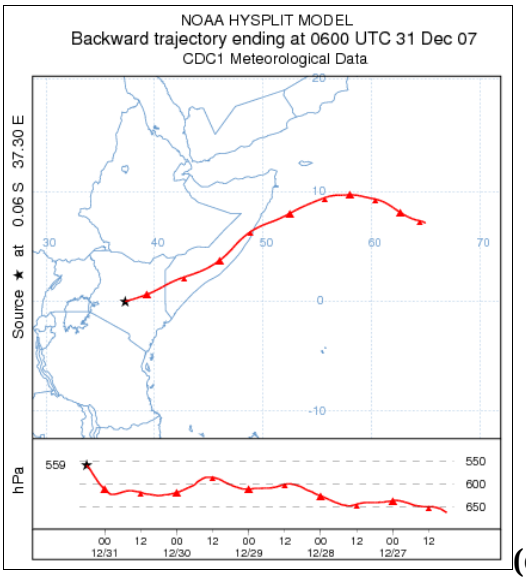

(d)

Figure 34: Back trajectories from Mt Kenya GAW Station for December 2007 (a) 16th, (b) 17th, (c) 24th and (d) 25th.

4.4.2 Back Trajectories

Source regions were of three types: Continental, Marime or internal. The first major difference is whether it is continental or maritime then either a second difference is whether it is a recirculation or from outside the country. Figures 35 and 36 show these representative flows. The circulations can be described as northerly, northeasterly, easterly,

southeasterly, westerly and recirculation flows in the country. These circulations are of different proportions but the major flows are easterly. The recirculations occur in July and August. Westerly flows are fewest.

These results showing the paths/ source regions are consistent with those of Gatebe *et al*. (1999), Okoola (2000), Henne *et al*. (2007) and Gicheru (2007).

The sudden sustained changes were targetted as these could have some indication of air of different characteristics entering the measuring system. The possible source regions of the air was sought using back trajectories over five days. Some months like March, July and August were each considered taken for two years. Some of the monthly surface ozone time series plots used are presented in Figures 43 to 46 in the appendix.

The flows bring in different air charcteristics. Easterly and southerly air flows generally lowers the ozone amounts, while the northerly or northesaterly flow increases the ozone concentrations. The recirculations have low amounts of ozone at about 20 – 25 ppb. The recirculations occur in July and August. The westerly flows also have low amounts than those of July- August.

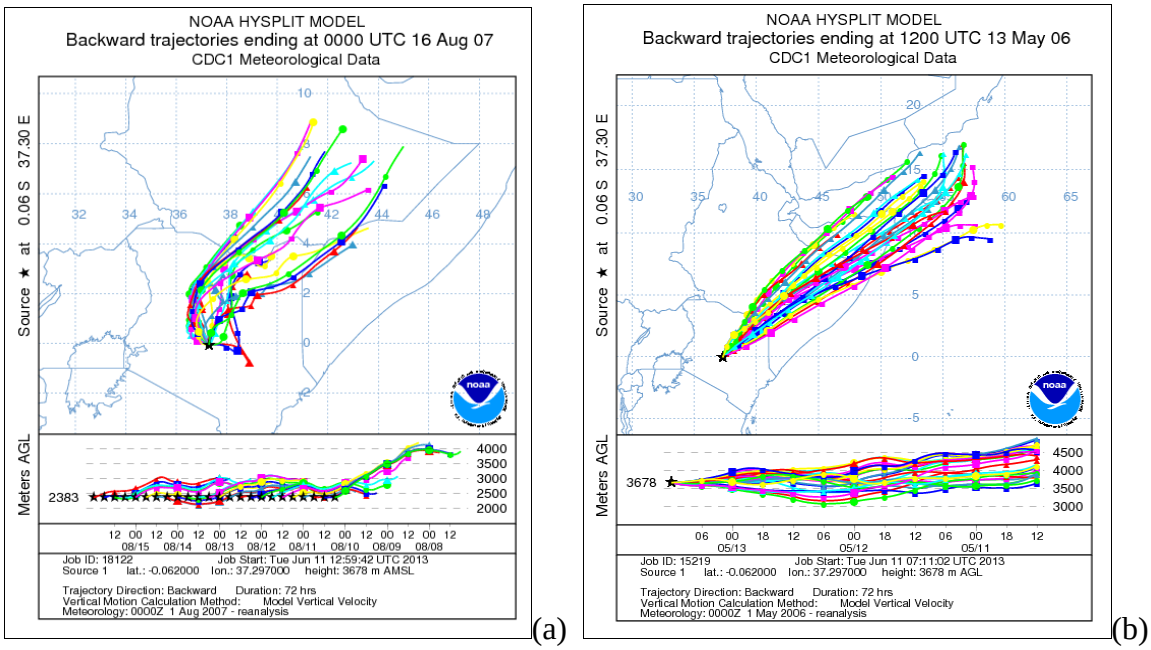

(a) (b)

Figure 35: Some of the six representative flows to Mt Kenya GAW Station from the five days back trajectories (a) northerly, (b) northeasterly

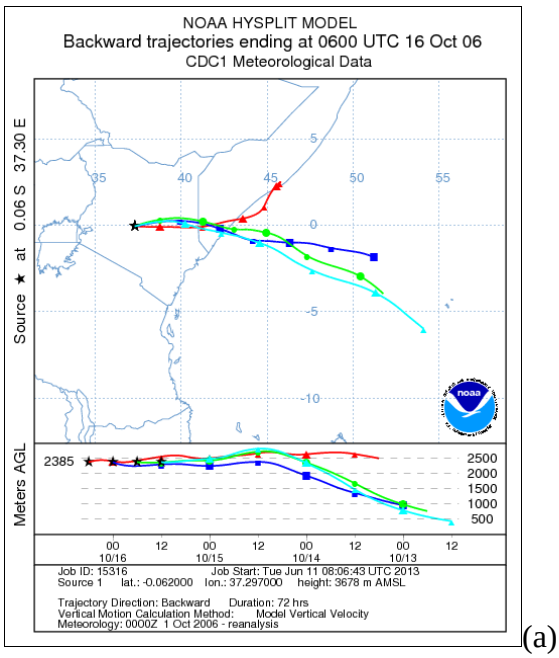

(a)

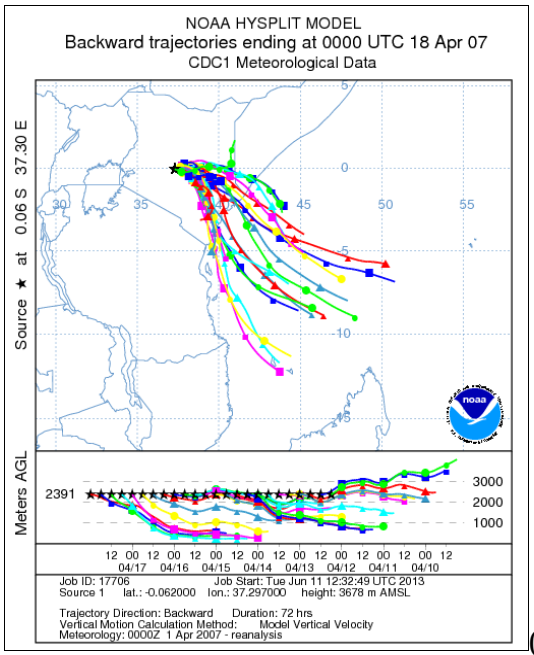

(b)

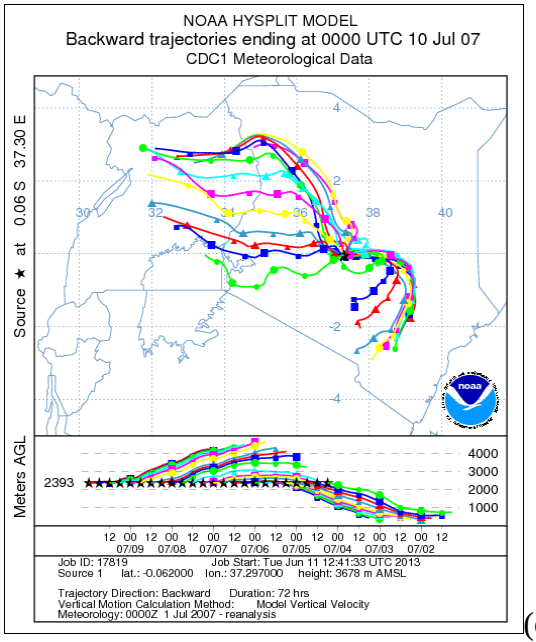

(c)

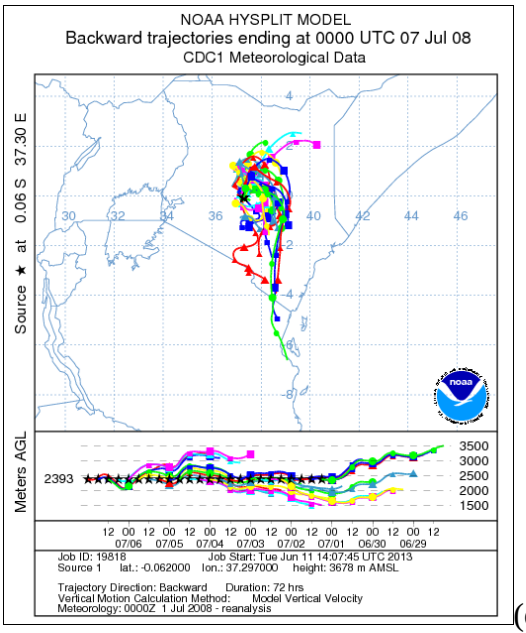

(d)

Figure 36: Some of the six representative flows to Mt Kenya GAW Station from the five days back trajectories (a) easterly, (b) southeasterly, (c) westerly and (d) recirculation.

4.4.3 Forward Trajectories

The airflow out of Mt Kenya is mostly to the west, followed by the southwest. See Figures 37 and 38). There are also outflows in other directions. Another flow is a recirculation especially in the months of June to September when it is the predominant flow. The flow is outwards from Mt Kenya GAW station and the arrows on the track are time stamps and should not be construed to be showing the direction of the trajectory.

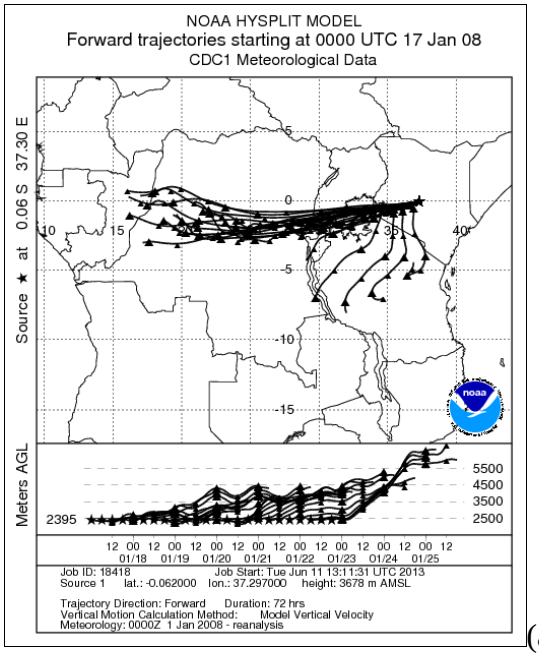

(a)

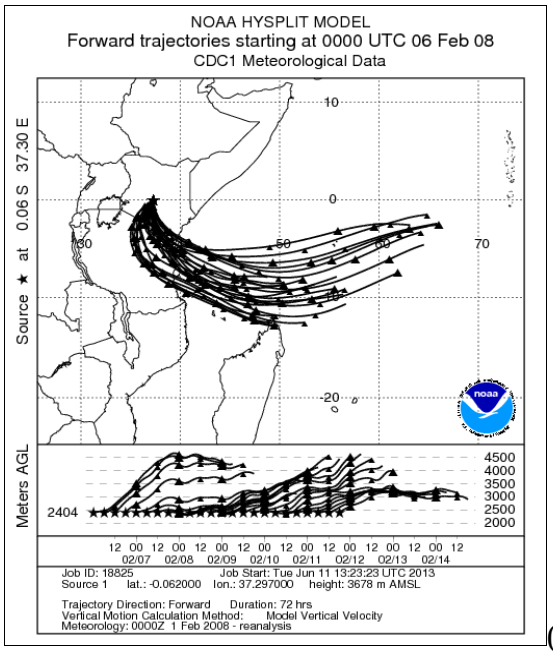

(b)

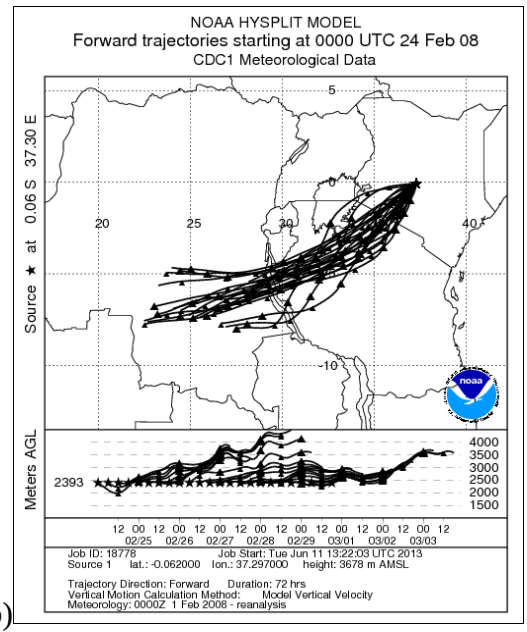

(c)

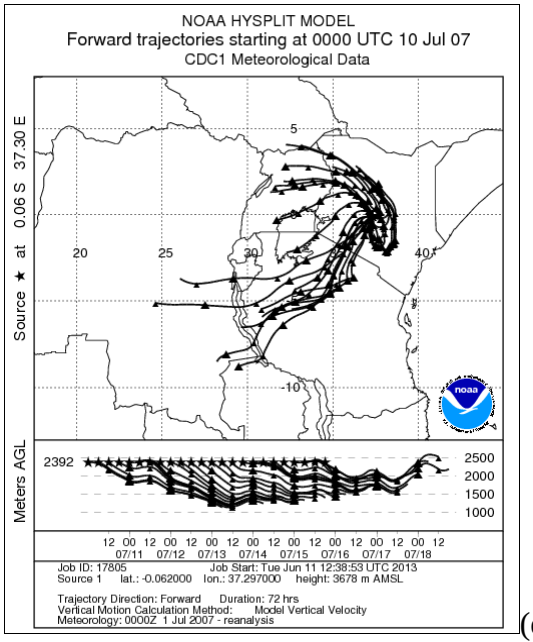

(d)

Figure 37: Directions of the Air out flows from Mt Kenya GAW station to (a) west, (b) east, (c) southwest and (d) north west

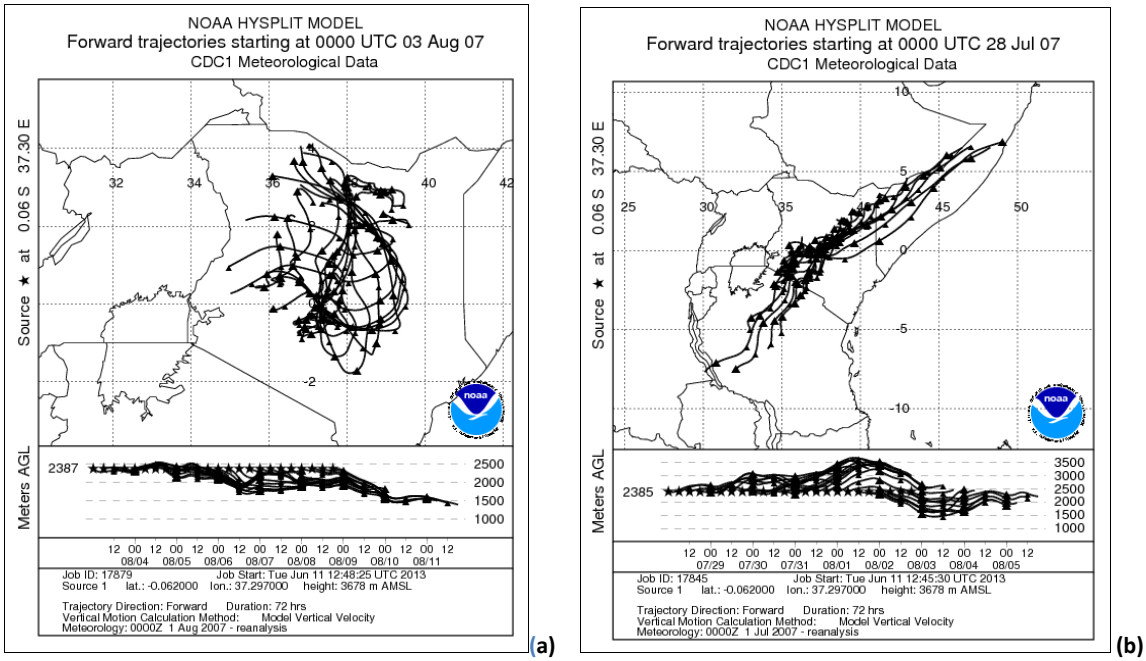

Figure 38: Directions of the Air out flows from Mt Kenya GAW station (a) recirculation and (b) north east and south west

4.4.4 Trajectories clusters

The mean tracks in July 2007 for the five days back trajectories are presented in Figure 39(a) while those of the three days forward trajectories are presented in Figure 39(b). The cluster number is given and the relative proportions of the individual trajectories in the cluster are also given in the parenthesis, as a percentage of the total trajectories. For July the recirculation flow is predominant and the tracks are in all directions.

The three days forward trajectories are presented, also for July but year 2008. Much of the flow is southwards; about 67%. Other flows are to the west, as represented by cluster number 3 with 4%, and south turning east at a proportion of 39%.

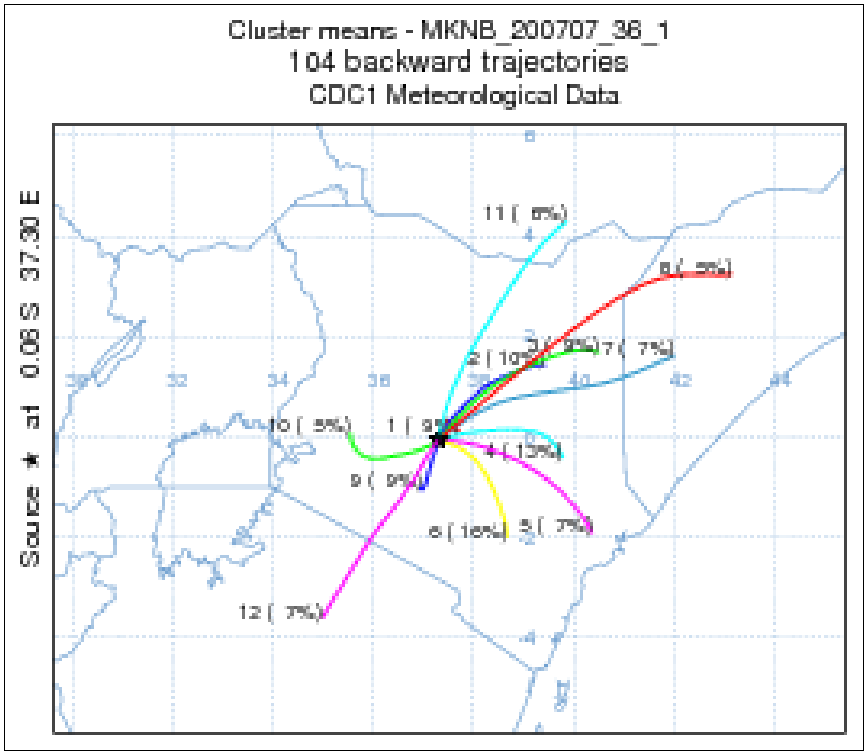

(a)

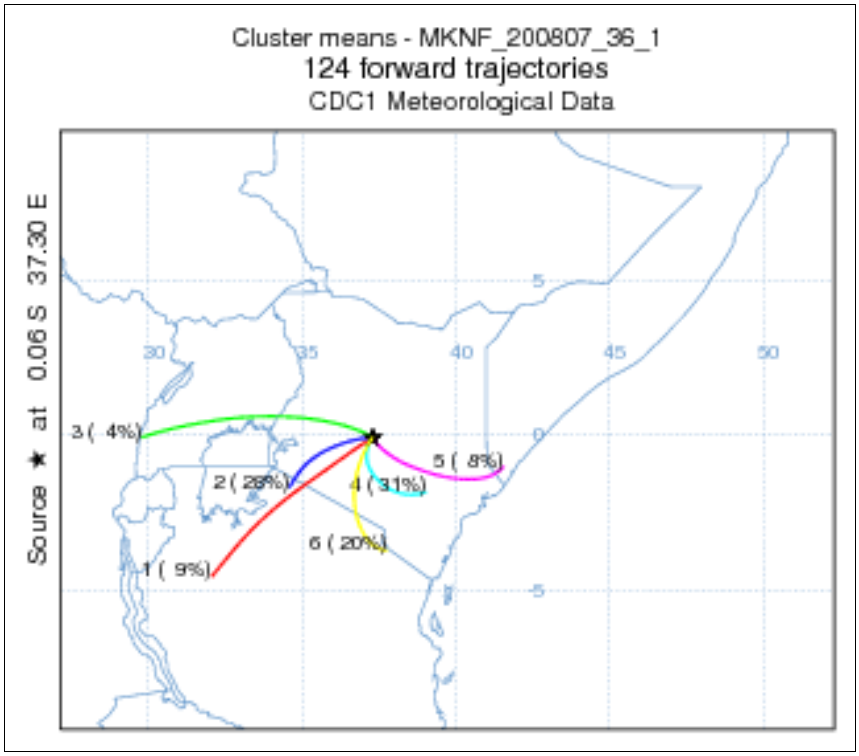

(b)

Figure 39: The HYSPLIT generated trajectories for Mt Kenya GAW Station (a) backward trajectories for July 2007 and (b) forward trajectories for July 2008.

The forward trajectories are mostly westwards for most of the year. A representative flow is shown in Figure 41. It is only when there is a recirculation in the months of July and August that this flow is not characteristic. The flow out of Mt Kenya GAW station is generally westwards since the station is in the tropics where the easterlies predominate.
These results are consistent with the findings of Gatebe *et al*. (1999).

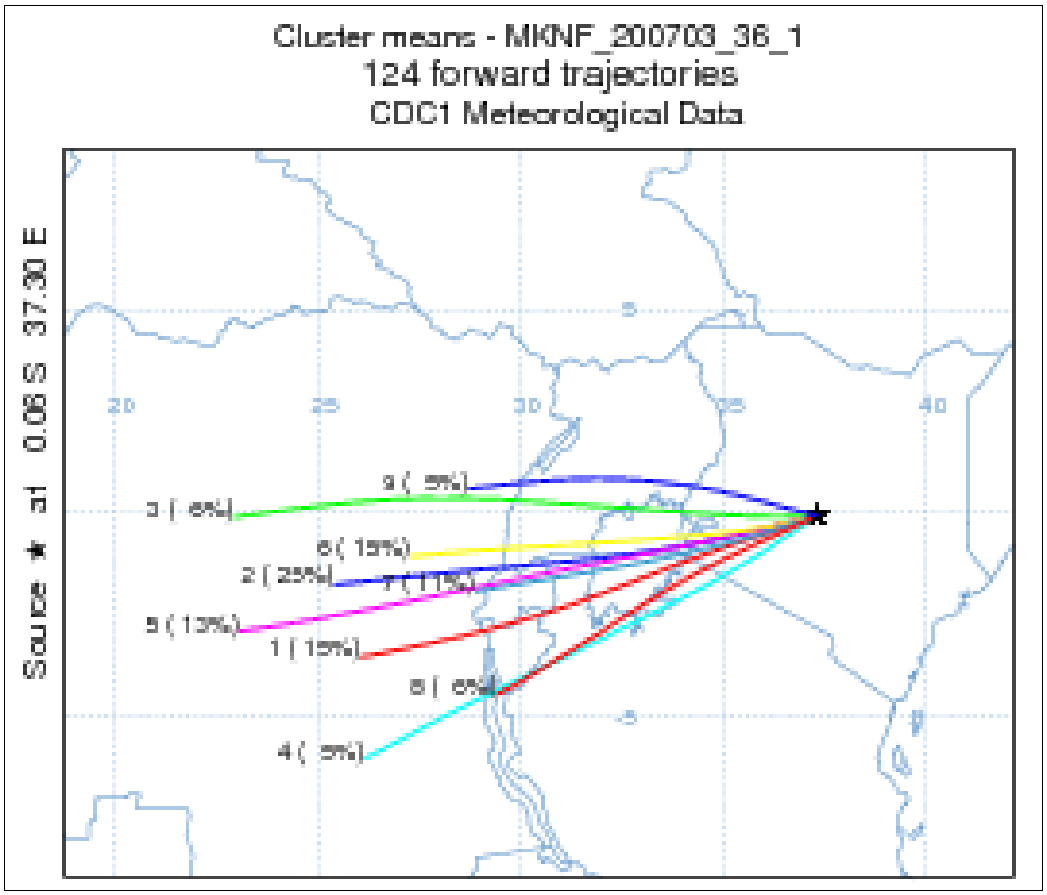

(c)

Figure 40: The HYSPLIT generated forward trajectories clusters from Mt Kenya GAW Station for March 2007. The numbers ahead represent the cluster number and the numbers in parenthesis show the proportion of the trajectories.

CHAPTER FIVE

5. SUMMARY, CONCLUSIONS AND RECOMMENDATIONS

Below is a summary of the study and the main conclusions are presented. In addition, recommendations for further studies are suggested.

5.1 SUMMARY

The main objective of this study was to assess the spatial and temporal distribution of greenhouse gases in Central Kenya. The specific objectives were to investigate the temporal distribution and establish the current spatial distribution. Further, the source regions of GHGs observed were identified and the impact of the surrounding area on background monitoring station on Mount Kenya was to be evaluated. The period of study was mainly from the year 2002 to 2010. The study dwelt on CO_2, CH_4 and O_3 which account for more than 80% all the GHGs. The relevant literature on the various aspects of the GHGs were reviewed in chapter two.

The details of the data used in this study are presented in Chapter three. There were five sets of data from various sources. The major data source was the Kenya Meteorological Department which provided all the ozone data and the associated meteorological fields. The reanalysis daily/monthly meteorological fields were provided by the NCEP – NCAR. Data from air filled flasks from Mt Kenya were retrieved from the Air Resources Laboratory (ARL); formerly the Earth Systems Resources Laboratory (ESRL) of the National Oceanic and Atmospheric Administration (NOAA). The satellite observations were from GOSAT satellite, a Japanese satellite.

The methods adopted in this study are described in Chapter two. Statistical and graphical methods were used to investigate the trends and their significance, temporal and spatial characteristics of the GHGs. The identification of the source regions and transport paths into central Kenya was done using the HYSPLIT model for trajectories.

The results from the various methods are discussed in Chapter Four. The main highlights are given below.

The data was of high quality and it confirmed that the air transport paths into the country are about six. These results agree with the observations by Gatebe (1999), Okoola (2000), Gicheru (2007) and Henne (2008). Continental sources have higher concentrations of Ozone than maritime ones. The highest concentrations emanated from the Arabian Peninsular. Air recirculation takes place in Kenya during July – August period and the concentration of Ozone also rises with it. The diurnal variation of Ozone at Mt Kenya has a nighttime maximum and a minimum in the afternoon. The converse is true for Nairobi; Ozone concentrations start rising at sunrise reaching a maximum in the afternoon.

Much of the country experiences lower concentrations of CO_2 as compared to the western and northern neighbours bordering the country. The lowest amounts of CO_2 in Central Kenya are in December to June. Much higher amounts occur the rest of the months. CO2 displays a bimodal pattern.

The Carbon dioxide fluxes from fossil fuels are highest in Central Kenya, up to ten times in Nairobi and extends to cover the 11 neighbouring counties. The fossil fuels emissions at the port city of Mombasa are also higher than the surrounding regions but do not have a large spatial spread. The flux from the biosphere follows the rainfall pattern and amounts.

The temporal distribution of surface Ozone shows a seasonal high in March and September. A minimum occurs in December. The concentrations are affected by the source regions.

The temporal distribution of Methane shows high values in November to February and a minimum in April- May. Low amounts continue into October. The northern hemisphere air is richer in Methane concentration.

5.2 CONCLUSIONS

From this study, the sources of highest concentrations of ozone are from continental sources outside the country. Saudi Arabian Peninsular consistently registered the highest amounts of ozone. This could be due to the lack of wash out of the precursor gases or that of the ozone in the desert region. The second highest concentrations were from the air recirculation in the country in July – August. This recirculating air maintains a higher concentration than the

maritime air. The implications to the human health of the concentrations higher than 50ppb for more than an hour are adverse.

The Mt Kenya GAW Station is well placed to continue monitoring the GHGs. The surrounding area has little or no significant impact on its background monitoring.

The Carbon dioxide flux from fossil fuels in Nairobi City is far much higher than at the countryside farther away from. The Counties bordering the City also feel this. This could be due to the high vehicular traffic, its industries and the high population density.

The fluxes from the biosphere follow the rainfall pattern and amounts as was. During the drought of the year 2009 in Eastern Kenya, the fluxes were reversed. The biosphere in these areas was severely affected by the drought and could no longer be a net takes of CO_2 out of the atmosphere.

Tropospheric ozone has a minimum concentration in December and two maxima in March and September. Converging airflows bring about the higher concentrations during the passage of the ITCZ. Extra precautions should be taken during the months of June through August as there is bound to be air recirculation within the country. Reinforced monitoring is vital during this period as it is a health need.

5.3 RECOMMENDATIONS

This study has identified the following areas for further investigations.

1). The relationship between the column averaged CO_2 (xCO_2) as measured by GOSAT and the in situ CO_2 was found to be very low for the Mt Kenya GAW station. Other studies have found a high correlation of about 0.75. Further work need to be done when more data is available to accent this assertion over Central Kenya.

2). The effect of temperature or radiation on the CO_2 biosphere flux should be investigated. In addition the cropping pattern in the country can also be taken into consideration. In this study only rainfall amount and distribution in some parts of the country was investigated in the conjunction with the spatial distribution of the CO_2 flux.

3). As GOSAT makes more data available to the public, the spatial distribution of methane and its temporal characteristics should be compared with that of Mt Kenya GAW station. This, however, was not possible in this study as the data was not yet available.

4). The distributions of the other GHGs over Kenya should be investigated. Gases like nitrous oxide and sulfur hexafluoride whose data is available from flask samples should also be investigated over Kenya and can be extended to cover the entire continent.

5). An investigation is necessary to determine the relationship of rain days and the concentrations of the GHGs. The distribution of GHGs seems to suggest lower concentrations during the rainy seasons.

6). The potential impacts on health of possible high concentrations of surface ozone in urban areas should be investigated. There is air recirculation in the country in the Months of July and August.

7). The Mt Kenya GAW Station is well placed to continue monitoring the GHGs since the surrounding area does not have any or has little significant impact on its background monitoring.

ACKNOWLEDGMENTS

I am indebted to my supervisors, Prof. N.J. Muthama and Dr. R.E. Okoola for the invaluable guidance and encouragement through this study. Their constant counsel and correction have made this dissertation to take this shape.

Further, I acknowledge and am grateful for the part played by the Chairman of the Department of Meteorology, University of Nairobi, Dr. A.O. Opere, and all the members of the Department for their valuable criticism and good guidance. This has helped me in the course of this study.

I give my appreciation to the Director of the Kenya Meteorological Department, Dr. J.R. Mukabana, who helped me to secure this scholarship. Other members of his staff have also facilitated in one way or another.

Members of my family have given me much encouragement and understanding during the course. I enjoyed the support of my wife, Mary, and our children; Dora, Faith, Felix, Aaron and Prince.

Many friends and colleagues have availed valuable help and prayers at one time or another. I am unable to give all their individual names or specific incidences when they were most helpful. My gratitude is to all of them.

REFERENCES

Anyamba, E. K. 1983: On the Monthly Mean lower Tropospheric Circulation and the Abberrant Circulation during 1961/62 floods over East Africa. *Msc Thesis*, University of Nairobi.

Alto, T., J. Hutakka and Y. Viisanen 2003: Influence on air mass source sector on variations in CO_2 mixing ratios at a boreal site in northern Finland. *Boreal. Env. Res.* **8**, 385 – 393.

Arau´jo, A. C., A. D. Nobre, B. Kruijt, J. A. Elbers, R. Dallarosa, P. Stefani, C. von Randow, A. O. Manzi, A. D. Culf, J. H. C. Gash, R. Valentini, and P. Kabat 2002: Comparative measurements of carbon dioxide fluxes from two nearby towers in a central Amazonian rainforest: The Manaus LBA site. *J. Geophys Res*. **107**, NO. D20, 8090, doi:10.1029/2001JD000676, 2002.

Asnani, G. C., 1993: *Tropical Meteorology*. **1**. Noble, 603 pp.

Bates, D. R. and M. Nicolet 1950: The photochemistry of atmospheric water vapour. *J. Geophys. Res*, **55**, 301.

Barasa, T.M.S., 2007: An Investigation on the effects of column ozone on the variability of UV Radiation in a Tropical African Region. M *MSc Dissertation*, Dept. of Met., UoN.

Beer, R., T. A. Glavich, and D.M. Rider 2001:Tropospheric emission spectrometer for the Earth Observing System's Aura satellite. *Appl Opt.* **40,** nos. 15, 20.

Beltrando, G. and P. Camberlin 1993: Interannual variability of rainfall in the eastern horn of Africa and indicators of atmospheric circulation. *Int. J. Climatol*., **13,** 533–546. doi: 10.1002/joc.3370130505

Bovensmann, H., J. P. Burrows, M. Buchwitz, J. Frerick, S. No¨el, V.V. Rozanov, K. V. Chance, and A. H. P. Goede 1999: SCIAMACHY - Mission objectives and measurement modes, *J. Atmos. Sci*., **56(2),** 127–150.

Bundi, P.M. 2004: Spatial and Temporal Distribution of Tropospheric Ozone over Southern Africa. *MSc Thesis*, Faculty of Science, Univ. of the Witwatersrand, Johannesburg

Bunker, A.F. 1965: *Interactions of the Summer Monsoon air with the Arabian Sea. Symp. on Met. Results of the Indian Ocean Expt*. Bombay 7-9. Indian Met. Dept. New Delhi.

Burrows, J.P., M. Weber, M. Buchwitz, V. Rozanov, A. Ladstatter-Weißenmayer, A. Richter, R. Debeek, R. Hoogen, K. Bramstedt, K.U. Eichmann, and M. Eisinger 1999: The Global Ozone Monitoring Experiment (GOME): Mission Concept and First Scientific Results. J. Atmos. Sci. **56**, 151-175.

Callies, J., E. Corpaccioli, M. Eisinger, A. Hahne, and A. Lefebvre 2000: GOME-2 – Metop's Second Generation sensor for Operational Ozone Monitoring, *ESA Bulletin*, **102**.

Chapman, S., 1930: A theory of upper atmospheric ozone. *Quar. J. Royal Met. Soc.*, **3**, pp. 103.

Clerbaux, C., A. Boynard, L. Clarisse, M. George, J. Hadji-Lazaro, H. Herbin, D. Hurtmans, M. Pommier, A. Razavi, S. Turquety, C. Wespes, and P. –F. Coheur 2009: Monitoring of atmospheric composition using the thermal infrared IASI/MetOp sounder, *Atmos. Chem. Phys*., **9,** 6041–6054, doi:10.5194/acp-9-6041-2009.

Cogan, A.J., H. Boesch, R. J. Parker, L. Feng, P. I. Palmer, J.-F. L. Blavier, N. M. Deutscher, R. Macatangay, J. Notholt, C. Roehl, T. Warneke, D. Wunch 2012: Atmospheric carbon dioxide retrieved from the Greenhouse gases Observing SATellite (GOSAT): Comparison with ground-based TCCON observations and GEOS-Chem model calculations. *J. Geophys. Res: Atmospheres* (1984–2012) **117**, Issue D21. DOI: 10.1029/2012JD018087.

Draxler, R.R., and G.D. Hess 1998: An Overview of the HYSPLIT_4 Modelling System for Trajectories, Dispersion and Deposition. *Aust. Met. Mag*. **47,** 295-308.

Drummond, J. R., and G. S. Mand 1996: The Measurements of Pollution in the Troposphere (MOPITT) instrument: Overall performance and calibration requirements, *J. Atmos. Oceanic Technol*., **13,** 314– 320.

Earth System Research Laboratory (ESRL) 2013: www.esrl.noaa.gov/gmd. last accessed 27th June 2013.

EPA (Environmental Protection Agency), 2011: *U.S. Emissions Inventory 2011; Inventory of U.S. Greenhouse Gas Emissions and Sinks: 1990-2009*. Available on: http://www.epa.gov/climatechange/Downloads/ghgemissions/US-GHG-Inventory-2011-Executive-Summary.pdf. Last accessed 27th June 2013.

FAO (Food and Agriculture Organization) 2003: *World Agriculture: Towards 2015/2030 An FAO Perspective*, Earthscan Publishing Ltd, London: 3.

Findlater, J. 1969a: A Major Low Level Air Current near the Indian Ocean during the Northern Summer. *Quarterly J. Roy Met Soc*. **95,** 362-390.

Findlater, J. 1969b: Inter-hemispheric Transport of Air in lower Troposphere over the Western Indian Ocean. Quarterly *J. Roy Met Soc*. **95,** 400-403.

Fishman, J. and V. G. Brackett 1997: The climatological distribution of tropospheric ozone derived from satellite measurements using version 7 Total Ozone Mapping Spectrometer and Stratospheric Aerosol and Gas Experiment data sets. *J. Geophys. Res.*, **102,** 19 275–19 278.

Gatebe, C., P.D. Tyson, H. Annegarn, S. Piketh, and G. Helas 1999: A Seasonal Air Transport Climatology for Kenya. *J. Geophys. Res*. **104**, 14,239 – 14,244.

Gicheru, W.N. 2007: Cold Air Outbreaks over Kenya and the Associated Atmospheric Circulations. *MSc Dissertation*, Dept of Meteorology, University of Nairobi.

GOSAT Project, 2010: Published by the Center for Global Environmental Research, National Institute for Environmental Studies URL: http://www.gosat.nies.go.jp/index_e.html . Last accessed 27th June 2013.

Griffiths, J. F. 1972: *Climates of Africa. World Survey of Climatology*. **10** . Edited by Landsberg, H. E. Elsievier Publishing Co. Amsterdam- London- New York.

Hansen, J., M. Sato, A. Lacis, R. Ruedy, I. Tegen and E. Mathews 1998: Climate Forcings in the Industrial Era, *Proceedings National Academy of Sciences [USA]*, **95**, 12753-12758.

Henne, S., J. Klausen, W. Junkermann, J.M. Kariuki, J.O. Aseyo, and B. Buchmann 2007: Representativeness and climatology of carbon monoxide and ozone at the global GAW Station Mt. Kenya in Equatorial Africa. *Atmos. Chem. Phys.* **8,** 3119 – 3139.

Henne, S., W. Junkermann, J.M. Kariuki, J.O. Aseyo, and J. Klausen 2008: Mount Kenya Global Atmosphere Watch Station (MKN): Installation and Meteorological Characterization, *J. Appl. Clim.* **47,** 2946 – 2962.

Intergovernmental Panel on Climate Change (IPCC) 2007: *The Physical Sciences Basis, Contribution of Working Group I to the Fourth Assessment*, Cambridge University Press.

Kenya Census 2009: *Kenya 2009 Population and Housing Census Highlights.* Kenya Nat Bureau of Statistics.

Kenya Vision 2030: *A Globally Competitive and Prosperous Kenya*. The Government of the Republic of Kenya 2006. http:// www.vision2030.go.ke. Last accessed 23rd July 2013.

King'uyu, S. M. 1994: The space-time characteristics of minimum and maximum temperature values over the tropical Eastern African Region. *MSc Thesis*, Dept of Meteorology, UoN.

King'uyu, S. M., L. A. Ogallo, E. K. Anyamba 2000: Recent Trends of Minimum and Maximum Surface Temperatures over Eastern Africa. *J. Climate* **13**, 2876–2886.

Kobayashi, H., A. Shomota, K. Kondo, E. Okumura, Y. Kameda, H. Shimoda, T. Ogawa 1999: Development and Evaluation of the interferometeric monitor for

greenhouse gases: A high - throughput fourier- transform infrared radiometer for nadir earth observations. Appl. Opt. **38**, 6801-6807.

Krishnamurthi, T.N., J. Molinari, and H.L. Pan 1976: Numerical Simulation of the Somali Jet. *J. Atm. Sci*. **33,** 2350-2360.

Lal,S., S. Venkataramani, B.H. Subbaraya 1993: Methane flux measurements from paddy fields in the tropical Indian region. *Atmos Environ.* **27,** 1691–1694.

Landsberg, H. E. 1963: Surface Signs of the Biennial Atmospheric Pulse. *Mon. Wea. Rev.* **99**, 549- 556.

Leroux, M., 2001: *The Meteorology and Climate of Tropical Africa*. Springer, 548 pp.

Levelt, P.F., E. Hilsenrath, G.W. Leppelmeier, G.H.J. van den Oord, P.K. Bhartia, J. Tamminen, J.F. de Haan and J.P. Veefkind 2006: Science Objectives of the Ozone Monitoring Instrument. *IEEE Trans. Geo. Rem. Sens.*, **44**, 1199-1208. (http://ieeexplore.ieee.org/search/wrapper.jsp?arnumber=1624600).

Mafimbo, A. J. 2008: Characteristics of wind fields and air-sea interactions over the upwelling region of the Somali Coast. *MSc Dissertation*, Dept of Oceanography, Univ. of Cape Town.

Matthews, E. 2000: Wetlands, pp 202-233 in *Atmospheric Methane: Its Role in the Global Environment*, edited by M A K Khalil, Springer-Verlag, New York.

Mbithi, D.M. 2010: Transport and Dispersion Patterns of Aerosols over the East African Region. *MSc Dissertation*, Dept. of Met., UoN.

Meyer, C. P. G.D. Cook, F. Reisen, T.E.L. Smith, M. Tattaris, J. Russell-Smith, S. Maier, C. Yates and M.J. Wooster 2012: Direct measurements of the seasonality of emission factors from savanna fires in northern Australia. *J Geophys Res.*, **117** doi:10.1029/2012JD017671.

McMillan, W. W., C. Barnet, L. Strow, M. T. Chahine, M. L. McCourt, J. X. Warner, P. C. Novelli, S. Korontzi, E. S. Maddy, and S. Datta 2005: Daily global maps of

carbon monoxide from NASA's Atmospheric Infrared Sounder. *Geophys. Res. Lett.*, **32**, L11801, doi:10.1029/2004GL021821.

Mooney, H.A. and Y. Luo (Editors) 1999: *Carbon dioxide and Environmental Stress.* Academic Press, San Diego

Mungai, J.G. 2008: A Numerical Investigation of the Influence of Monsoonal Wind Reversals over the East African Coastal Ocean. *MSc Dissertation*, Dept of Oceanography, Univ. of Cape Town.

Muthama, N.J. 1989: Total Atmospheric Ozone Characteristics over a Tropical Region. *MSc Thesis*, University of Nairobi.

Njau, L. 1982: Tropospheric Wave Disturbance in East Africa. *MSc Thesis*, University of Nairobi.

Ngara, T. 1977: Some Aspects of the EALLJ. *MSc Thesis*, University of Nairobi.

Ogallo, L.J., 1988: Relationship between seasonal rainfall in East Africa and Southern Oscillation. J. Climatol., **8**, 31-43.

Ohyama, H., S. Kawakami, K. Shiomi, Kei; K. Miyagawa, 2012: Retrievals of Total and Tropospheric Ozone From GOSAT Thermal Infrared Spectral Radiances. *Geoscience and Remote Sensing, IEEE Transactions.* **50,** 1770 - 1784

Okoola, R.E. 1989: Westwards moving disturbances in the Southwest Indian Ocean. *Earth and Environ. Sci. Met. and Atmos. Phys.* **41**, 35-44, DOI: 10.1007/BF01032588.

Okoola, R. E. 2000: The Characteristics of Cold Air Outbreaks over the Eastern Highlands of Kenya. *Earth and Environ. Sci. Met. and Atmos. Phys.* **73**, 177-187, DOI: 10.1007/s007030050072.

Omeny, P., 2006: East African Rainfall Variability Associated with Madden- Julian Oscillation. *MSc Dissertation*, Dept of Met., UoN.

Parrish, D.D., K. C. Aikin, S. J. Oltmans, B. J. Johnson, M. Ives, and C. Sweeny 2010: Impact of transported background ozone inflow on summertime air quality in a California ozone exceedance area. *Atmos. Chem. Phys. Discuss.*, **10**, 16231-16276. www.atmos-chem-phys-discuss.net/10/16231/2010/ doi: 10.5194/ acpd-10-16231-2010.

Rajab, J. M, M. Z. MatJafri, H.S. Lim and K. Abdullah 2010: Daily distribution Map of Ozone (O3) from AIRS over Southeast Asia. *Energy Res. J.* **1,** 158-164.

Rosa L.P., M.A. dos Santos, B. Matvienko, E.O. dos Santos & E. Sikar 2004: Greenhouse gases emissions by hydroelectric reservoirs in tropical regions. *Climatic Change* **66,** 9-21.

Sakwa V.N., 2006: Assessment of the Skill of the High Resolution Regional Model in the Simulation of Air Flow and Rainfall over East African. *MSc Dissertation*, Dept of Met., UoN.

SANCCRS (South African National Climate Change Response Strategy) 2004: http:// www. Climateresponse.co.za/home/gp/1. Last accessed 20th May 2013.

Schlesinger, W.H. 1997: *Biogeochemistry: An analysis of global change*. 2nd edition. Academic Press, California.

Schnell, R. C., 1978: Report on the Mount Kenya Baseline Station Feasibility Study. Rep. no. 12, World Meteorological Organization, 171 pp.

Schuck, T. J., K. Ishijima, P. K. K. Patra, A. K. Baker, T. Machida, H. Matsueda, Y. Sawa, T. Umezawa, C. A. M. A. M. Brenninkmeijer, and J. Lelieveld 2012: Distribution of methane in the tropical upper troposphere measured by CARIBIC and CONTRAIL aircraft, *J. Geophys. Res.*, doi:10.1029/2012JD018199.

Simiyu, G.M., D. D. Adams, J. Ngetich and J. Mundui, 2006: Greenhouse gases, methane and carbon dioxide, and diminishing water resources in Lake Victoria basin, Kenya. *Tech. Report*.

Sinha ,V., J. Williams, P. J. Crutzen and J. Lelieveld 2007: Methane emissions from boreal and tropical forest ecosystems derived from in-situ measurements. *Atmospheric Chemistry and Physics Discussions* **7**, 14011-14039.

Slingo, J., H. Spencer, B. Hoskins, P. Berrisford, and E. Black, 2005: The Meteorology of the Western Indian Ocean, and the influence of the East African highlands. *Philos. Trans. Roy. Soc. London,* **A363,** 25–42.

SRON (Netherlands Institute for Space Research) 2010: Higher temperatures can worsen climate change, methane measurements from space reveal. *ScienceDaily*. Retrieved September 22, 2012, from http://www.sciencedaily.com / releases/ 2010/01/ 100115204416.htm.

Sternad M., M. Knez, B. Rosi 2010: Improving City Transport with the Objective to Reduce CO2 Emissions. *Transport Problems* **5**, 4.

Tathy, J. P., B. Cros, R. A. Delmas, A. Marenco, J. Servant, and M. Labat 1992: Methane Emisssion from Flooded Forest in Central Africa. *J. Geophys. Res.*, **97**, 6159–6168, doi:10.1029/90JD02555.

Thiong'o K.K. 1997: Characteristics of Vertical Profile of Ozone near the Equator. *MSc Thesis*, University of Nairobi.

Tyler, S. C., P. R. Zimmerman, C. Cumberbatch, J. P. Greenberg, C. Westberg, and J. P. E. C. Darlington 1988: Measurements and interpretation of $\delta^{13}C$ of methane from termites, rice paddies, and wetlands in Kenya, *Global Biogeochem. Cycles*, **2**, 341–355, doi:10.1029/GB002i004p00341.

United Nations, 1998: *Kyoto Protocol to the United Nations Framework Convention on Climate Change* (http:/ / unfccc. int/ essential_background/ kyoto_protocol/ items/ 1678. php). Last accessed 27th June 2013.

USDA (United States Department of Agriculture), 2004: U.S. Agriculture and Forestry Greenhouse Gas Inventory: 1990-2001. USDA, *Tech Bull* No. 1907.

Wayne, 1991: *Chemistry of Atmosphere*. Oxford University Press, Oxford.

WDCGG (World Data Center for Greenhouse Gases) 2012: Available online: http://ds.data.jma.go.jp/gmd/wdcgg/ (last accessed on 4 May 2013).

WMO 2010: WCC-Empa Report 10/4, System and Performance Audit of Surface Ozone and Carbon Monoxide at the Global GAW Station Mt. Kenya.

WMO 2008: WCC-Empa Report 08/5, System and Performance Audit of Surface Ozone and Carbon Monoxide at the Global GAW Station Mt. Kenya.

WMO 2005: WCC-Empa Report 05/1, System and Performance Audit of Surface Ozone and Carbon Monoxide at the Global GAW Station Mt. Kenya.

WMO 2002: WCC-Empa Report 02/1, System and Performance Audit of Surface Ozone and Carbon Monoxide at the Global GAW Station Mt. Kenya.

WMO 2012: Greenhouse Gas Bulletin No.8.

World Commission on Dams Report 2000: (Accessed on 4 May 2013) on: http://wwf.panda.org/what_we_do/footprint/water/dams_initiative/dams/wcd/

APPENDICES

These are some of the Figures for the flux of the CO_2 from the biosphere across the country for the months of Decedmber 2009 and March and April 2010.

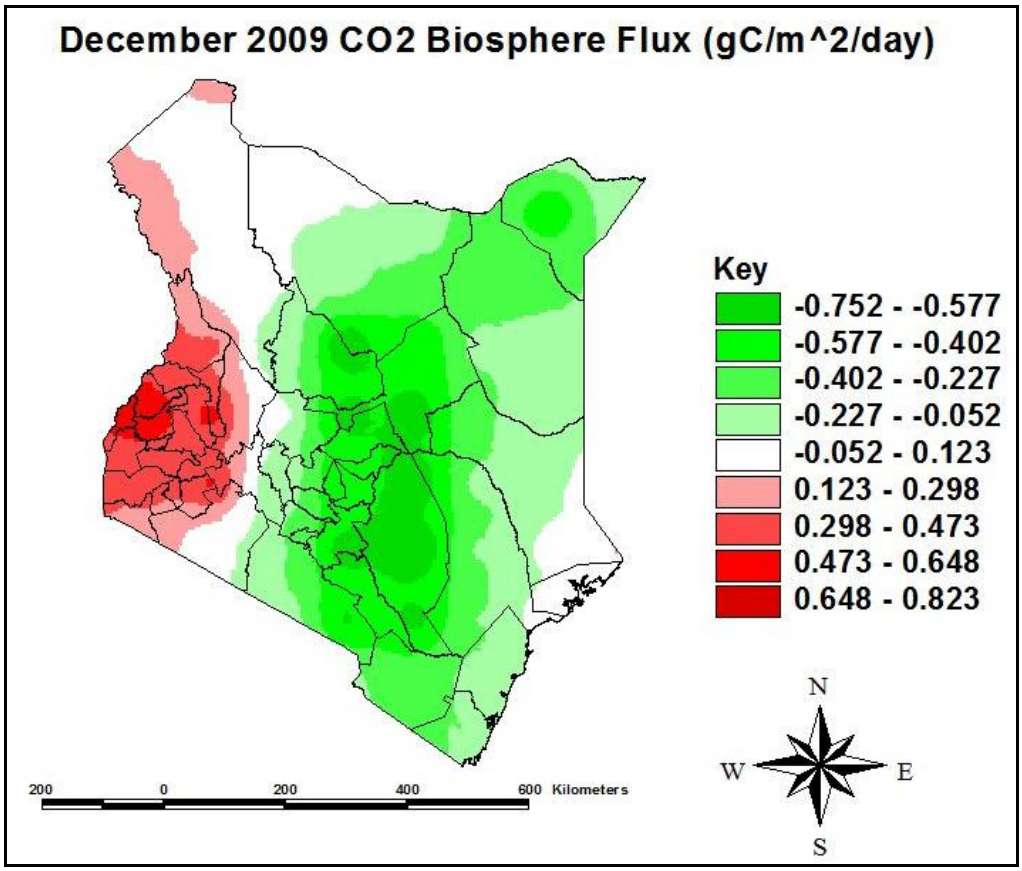

Figure 41: CO_2 Biosphere flux in Kenya for December 2009. (Data from GOSAT)

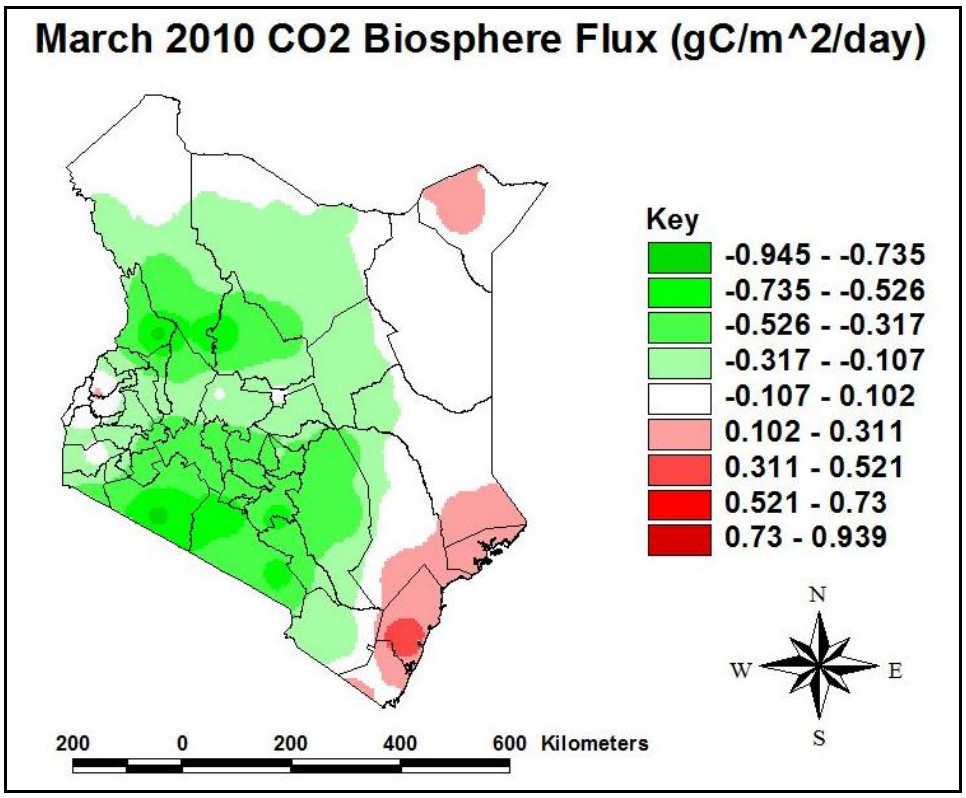

*a)

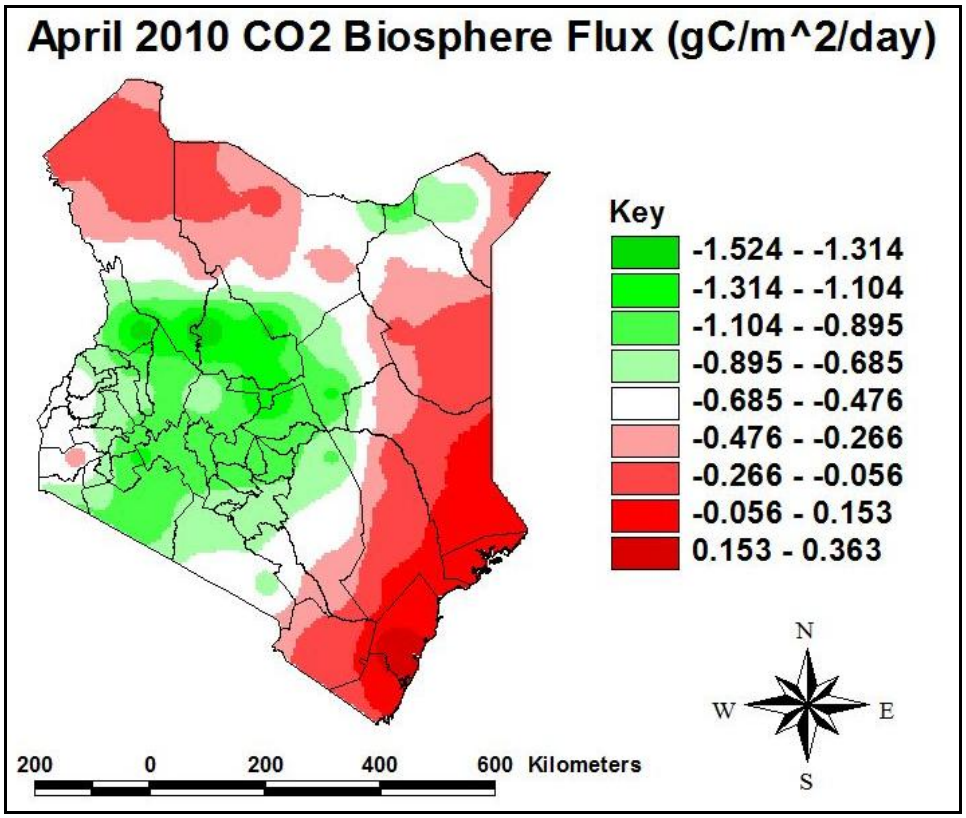

Figure 42: CO_2 Biosphere flux in Kenya for year 2010 (a) March and (b) April.

These are the additional figures of the time series plots for the surface ozone used in the selections of the start/end times of trajectories during the different months used.

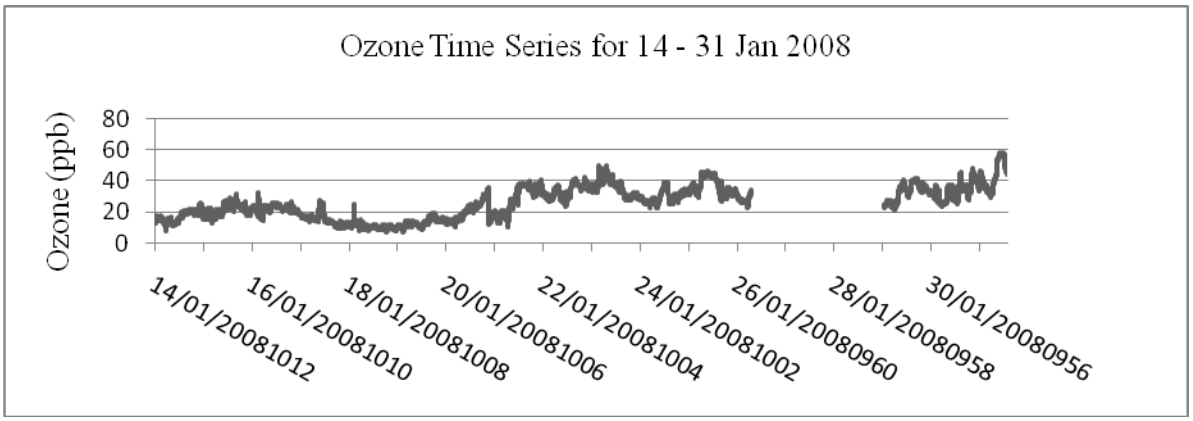

(a)

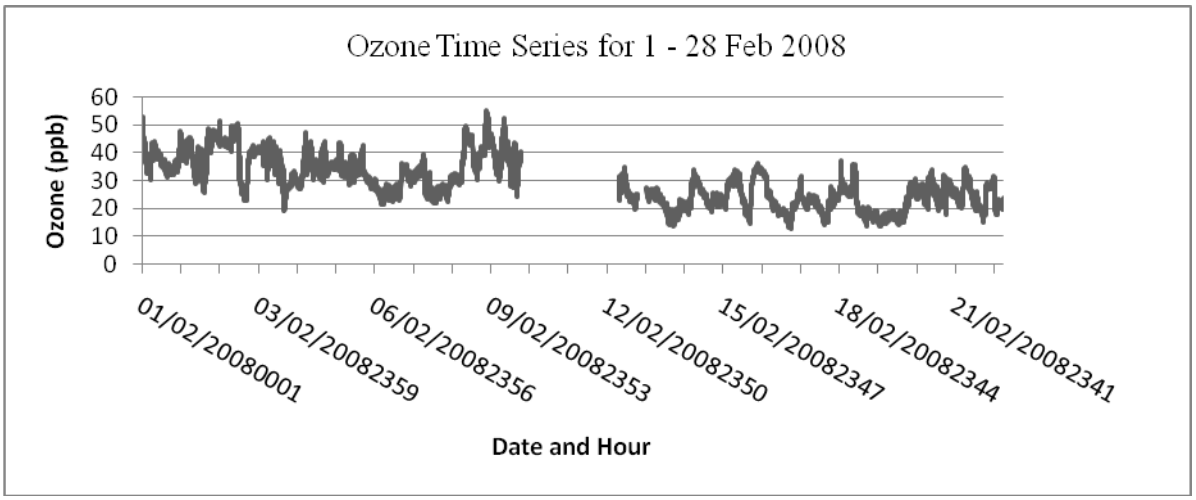

(b)

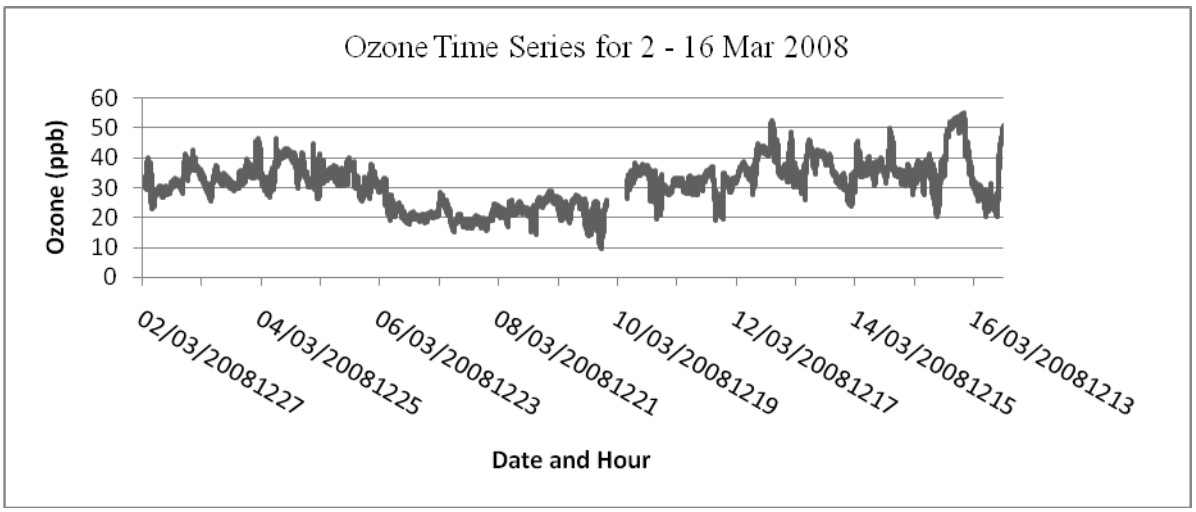

(c)

Figure 43: Surface (Tropospheric) Ozone monthly time series plots for diverse months (a) January, (b) February and (c) March.

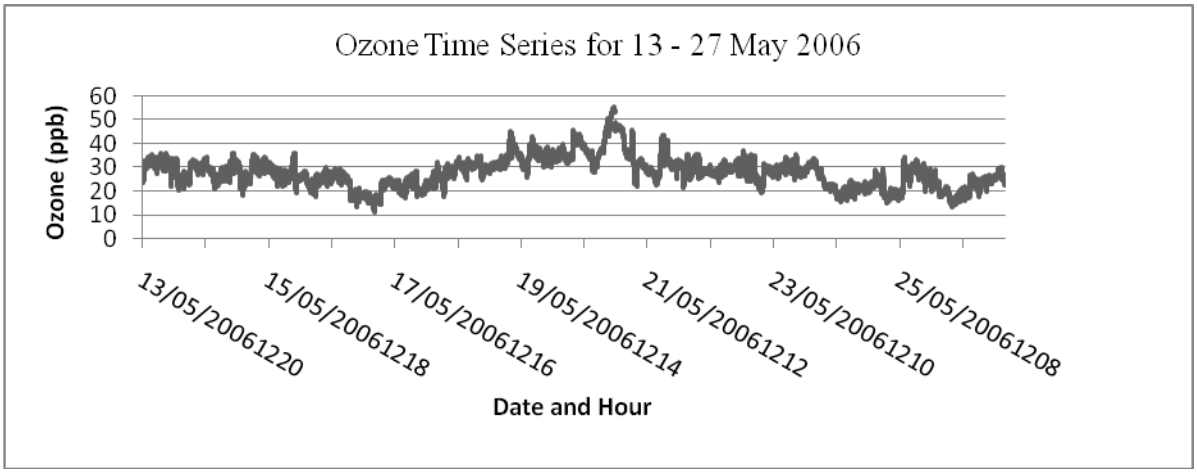

(a)

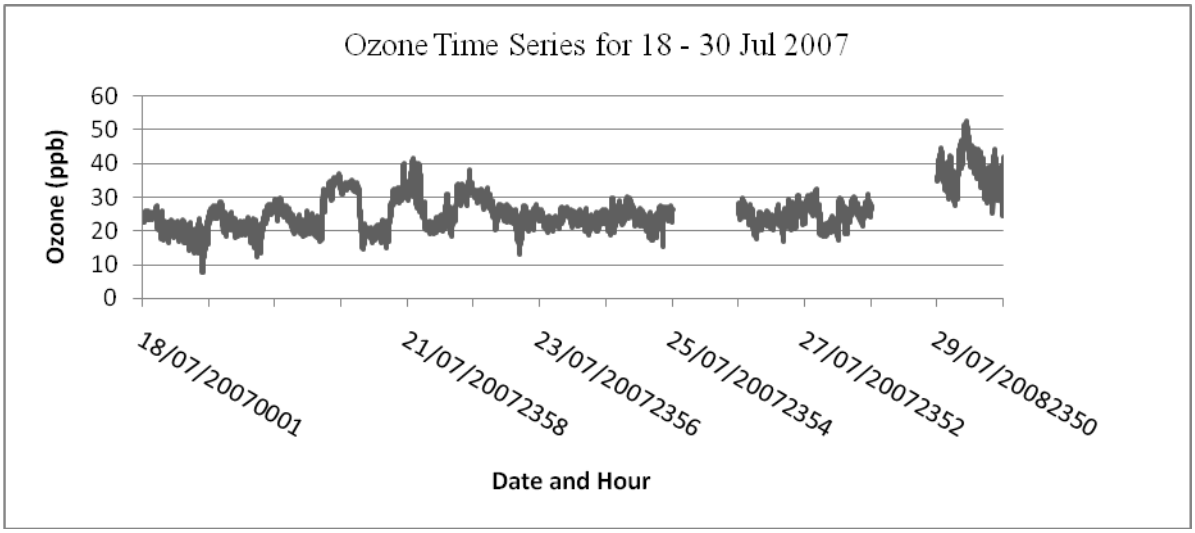

(b)

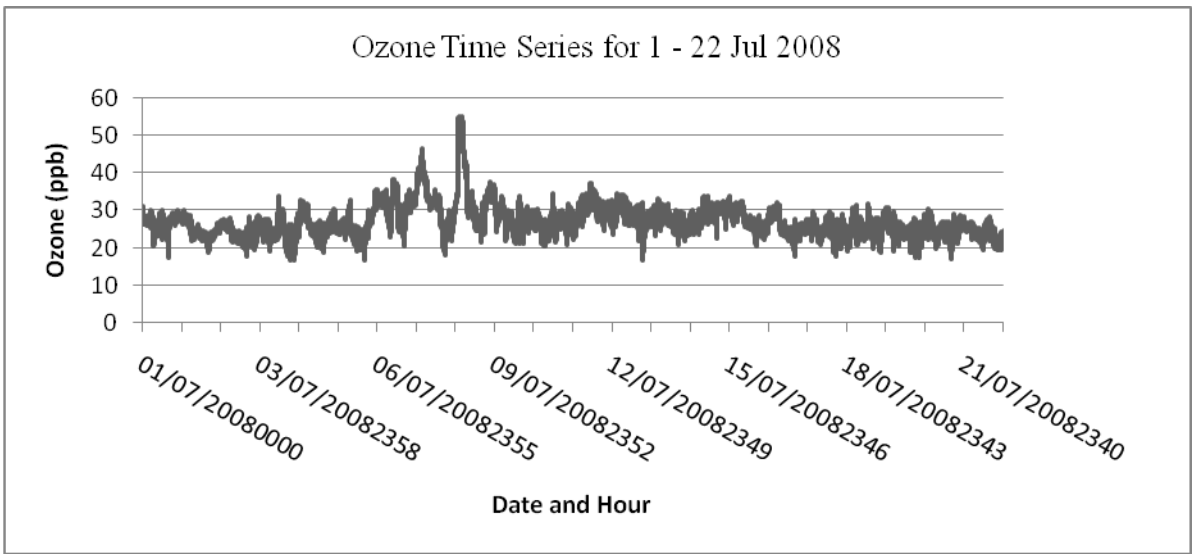

(c)

Figure 44: Surface (Tropospheric) Ozone monthly time series plots for diverse months (a) May, (b) 18 - 30 July 2007 and (c) 1 - 22 July 2008,

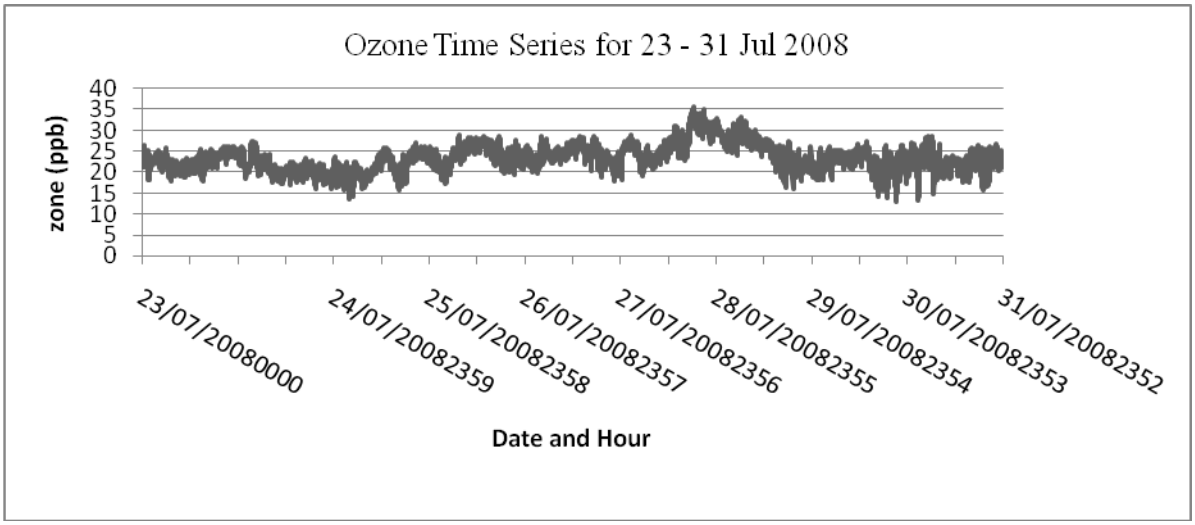

(a)

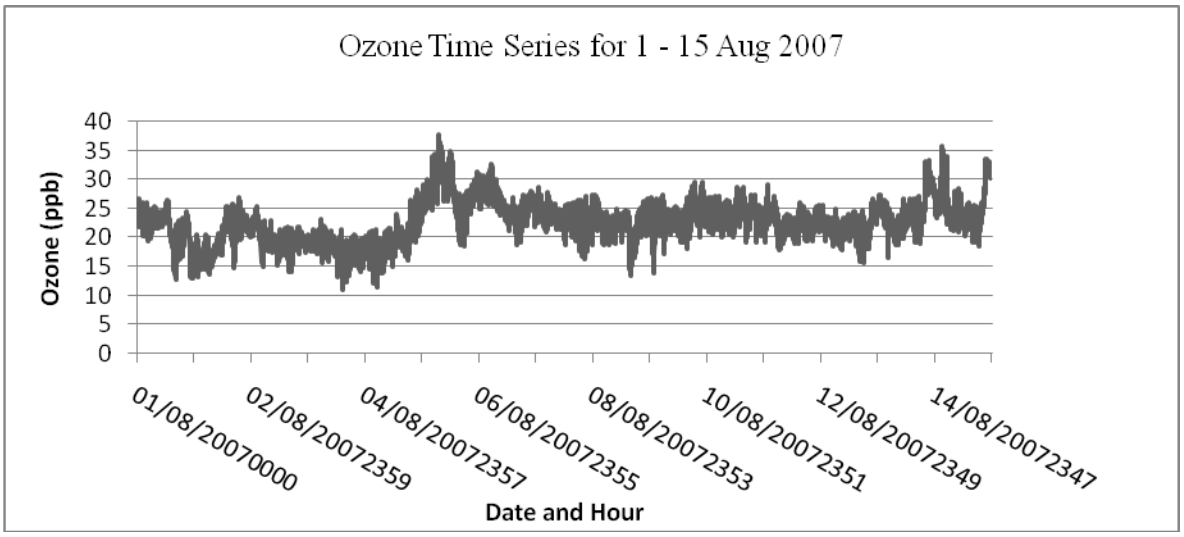

(b)

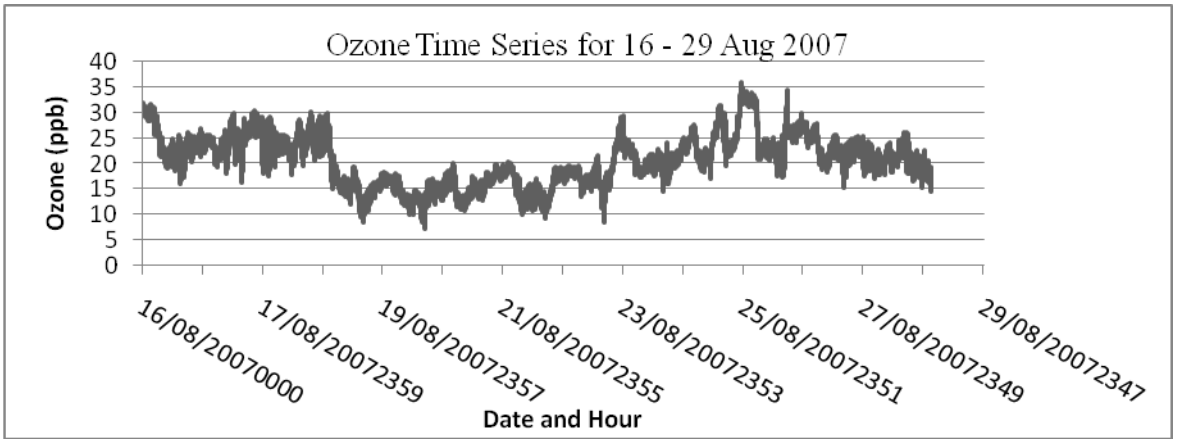

(c)

Figure 45: Surface (Tropospheric) Ozone monthly time series plots for diverse months (a) 23 - 31 July 2008, (b) 1 - 15 August 2007 and (c) 16 - 29 August 2007.

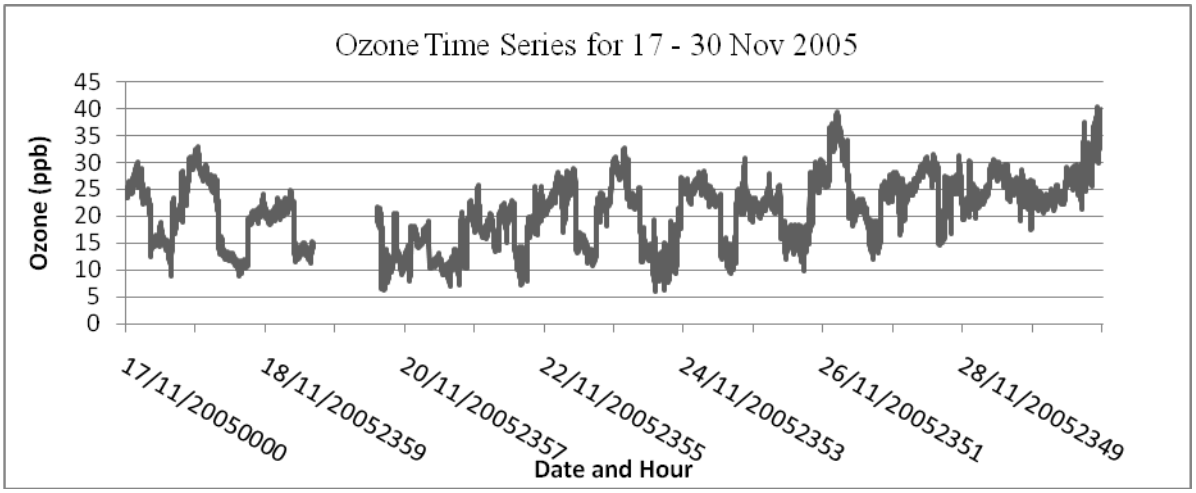

(a)

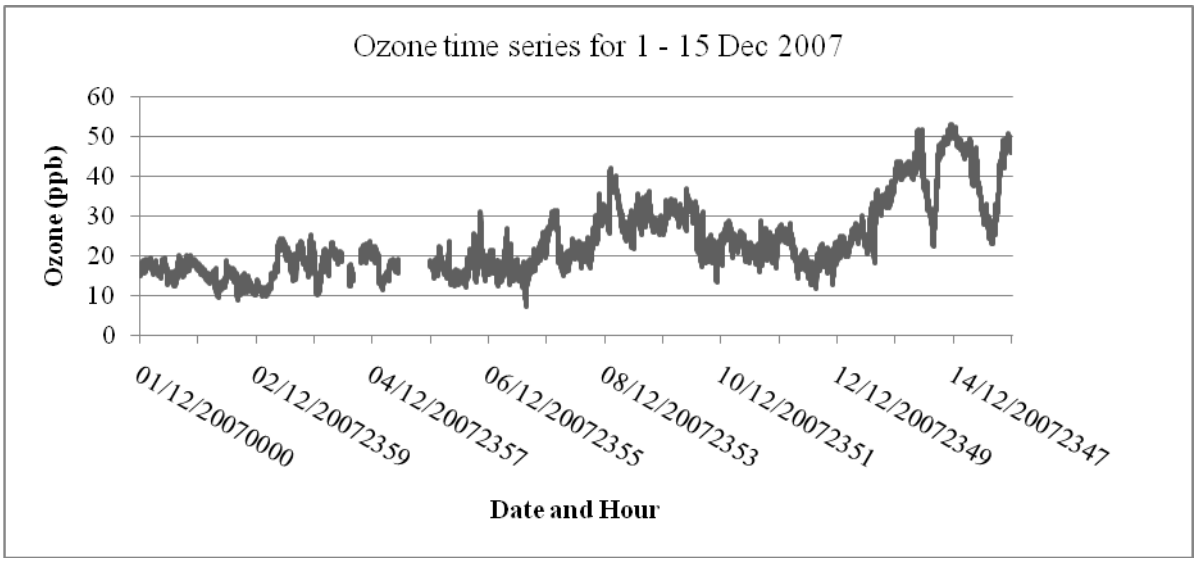

(b)

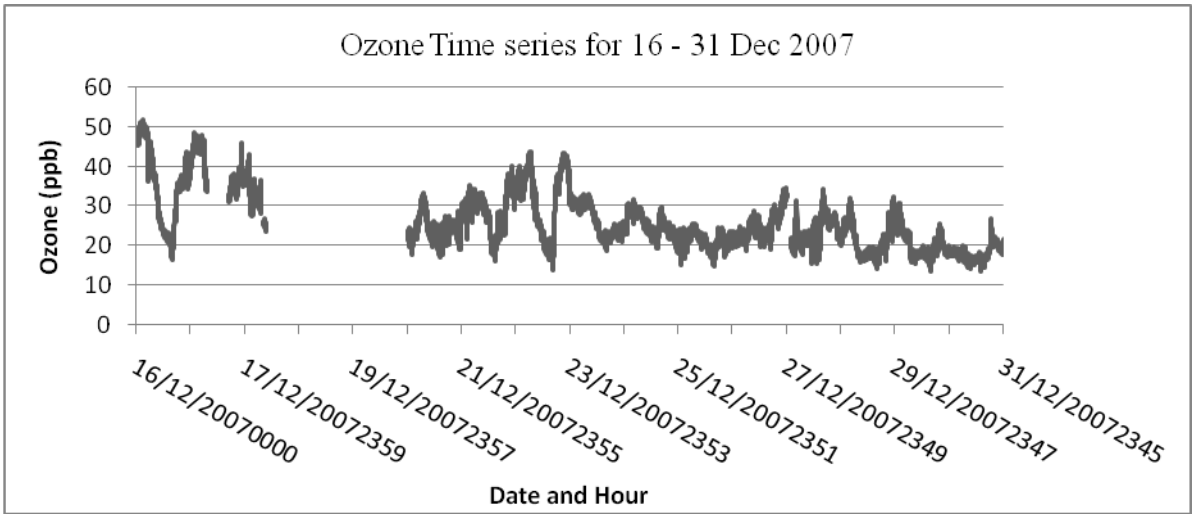

(c)

Figure 46: Surface (Tropospheric) Ozone monthly time series plots for diverse months (a) 17- 30 November 2005, (b) 1- 15 December 2007 and (c) 16- 31 December 2007.